



Herbert Wertheim  
College of Engineering  
UNIVERSITY of FLORIDA

FINAL REPORT

July 2021

---

## **SUNSHINE SKYWAY BRIDGE MONITORING PHASE II: SYSTEM DEPLOYMENT**

**Principal Investigator:**

Jennifer A. Bridge, Ph.D.

**Co-Principal Investigator:**

Justin R. Davis, Ph.D.

---

Department of Civil and Coastal Engineering  
University of Florida  
P.O. Box 116580  
Gainesville, Florida 32611

**Sponsor:**

Florida Department of Transportation  
District 7 Structures Maintenance Office

*Project Manager*

Jim Jacobsen, P.E.

**Contract**

FDOT Contract No. BVD31-977-73

## **Disclaimer**

The opinions, findings, and conclusions expressed in this publication are those of the authors and not necessarily those of the State of Florida Department of Transportation.

SI\* (MODERN METRIC) CONVERSION FACTORS

APPROXIMATE CONVERSIONS TO SI UNITS

SYMBOL	WHEN YOU KNOW	MULTIPLY BY	TO FIND	SYMBOL
<b>LENGTH</b>				
in	inches	25.4	millimeters	mm
ft	feet	0.305	meters	m
yd	yards	0.914	meters	m
mi	miles	1.61	kilometers	km
<b>AREA</b>				
in <sup>2</sup>	square inches	645.2	square	mm <sup>2</sup>
ft <sup>2</sup>	square feet	0.093	square meters	m <sup>2</sup>
yd <sup>2</sup>	square yard	0.836	square meters	m <sup>2</sup>
ac	acres	0.405	hectares	ha
mi <sup>2</sup>	square miles	2.59	square kilometers	km <sup>2</sup>
<b>VOLUME</b>				
fl oz	fluid ounces	29.57	milliliters	mL
gal	gallons	3.785	liters	L
ft <sup>3</sup>	cubic feet	0.028	cubic meters	m <sup>3</sup>
yd <sup>3</sup>	cubic yards	0.765	cubic meters	m <sup>3</sup>
NOTE: volumes greater than 1000 L shall be shown in m <sup>3</sup>				
<b>MASS</b>				
oz	ounces	28.35	grams	g
lb	pounds	0.454	kilograms	kg
T	short tons (2000 lb)	0.907	megagrams	Mg (or "t")
<b>TEMPERATURE (exact degrees)</b>				
°F	Fahrenheit	5(F-32)/9 or (F-32)/1.8	Celsius	°C
<b>ILLUMINATION</b>				
fc	foot-candles	10.76	lux	lx
fl	foot-Lamberts	3.426	candela/m <sup>2</sup>	cd/m <sup>2</sup>
<b>FORCE and PRESSURE or STRESS</b>				
kip	1000 pound force	4.45	kilonewtons	kN
lbf	pound force	4.45	newtons	N
lbf/in <sup>2</sup>	pound force per	6.89	kilopascals	kPa

\*SI is the symbol for the International System of Units. Appropriate rounding should be made to comply with Section 4 of ASTM E380.

SI\* (MODERN METRIC) CONVERSION FACTORS

APPROXIMATE CONVERSIONS **FROM** SI UNITS

SYMBOL	WHEN YOU KNOW	MULTIPLY BY	TO FIND	SYMBOL
<b>LENGTH</b>				
mm	millimeters	0.039	inches	in
m	meters	3.28	feet	ft
m	meters	1.09	yards	yd
km	kilometers	0.621	miles	mi
<b>AREA</b>				
mm <sup>2</sup>	square millimeters	0.0016	square inches	in <sup>2</sup>
m <sup>2</sup>	square meters	10.764	square feet	ft <sup>2</sup>
m <sup>2</sup>	square meters	1.195	square yards	yd <sup>2</sup>
ha	hectares	2.47	acres	ac
km <sup>2</sup>	square kilometers	0.386	square miles	mi <sup>2</sup>
<b>VOLUME</b>				
mL	milliliters	0.034	fluid ounces	fl oz
L	liters	0.264	gallons	gal
m <sup>3</sup>	cubic meters	35.314	cubic feet	ft <sup>3</sup>
m <sup>3</sup>	cubic meters	1.307	cubic yards	yd <sup>3</sup>
<b>MASS</b>				
g	grams	0.035	ounces	oz
kg	kilograms	2.202	pounds	lb
Mg (or "t")	megagrams (or	1.103	short tons (2000 T	T
<b>TEMPERATURE (exact degrees)</b>				
°C	Celsius	1.8C+32	Fahrenheit	°F
<b>ILLUMINATION</b>				
lx	lux	0.0929	foot-candles	fc
cd/m <sup>2</sup>	candela/m <sup>2</sup>	0.2919	foot-Lamberts	fl
<b>FORCE and PRESSURE or STRESS</b>				
kN	kilonewtons	0.225	1000 pound force	kip
N	newtons	0.225	pound force	lbf
kPa	kilopascals	0.145	pound force per square inch	lbf/in <sup>2</sup>

\*SI is the symbol for the International System of Units. Appropriate rounding should be made to comply with Section 4 of ASTM E380.



## Technical Report Documentation Page

1. Report No.	2. Government Accession No.	3. Recipient's Catalog No.	
4. Title and Subtitle Sunshine Skyway Bridge Monitoring Phase II		5. Report Date July 2021	
		6. Performing Organization Code	
7. Author(s) Jennifer A Bridge, Ph.D., Justin R. Davis, Ph.D.		8. Performing Organization Report No.	
9. Performing Organization Name and Address Engineering School of Sustainable Infrastructure & Environment University of Florida 365 Weil Hall / PO Box 116550 Gainesville, FL 32611		10. Work Unit No. (TRAIS)	
		11. Contract or Grant No. BDV31-977-73	
12. Sponsoring Agency Name and Address Florida Department of Transportation 605 Suwannee Street, MS 30 Tallahassee, FL 32399-0450		13. Type of Report and Period Covered Draft Final Report 3/1/2017 – 7/31/2021	
		14. Sponsoring Agency Code	
15. Supplementary Notes			
16. Abstract The District 7 Structures Maintenance Office sought to take the existing monitoring components on the Sunshine Skyway Bridge and create a centralized monitoring system available via a web interface and capable of providing alerts for anomalous bridge response data. This project included the selection of a web development contractor, the design of a web interface, the development of algorithms to produce bridge response information, analysis of long-term data to establish bounds of typical bridge responses, and recommendations for a bridge alert response plan. To centrally capture the ad hoc monitoring hardware installed, a web map and inventory database was upgraded to reflect the newly installed sensors as well as to dynamically link the database and map. BDI, Inc, developed a web portal that provides data archiving, visualization, and alerts. A System Security plan was developed with input from the Information Security Administration Office. Analysis of a year of monitoring data (2020) was carried out to assess the quality/reliability of the data and to determine the bounds of bridge response to temperature-, wind-, and traffic-induced loading. Accelerometer data were correlated with wind and temperature measurements to establish daily and seasonal response patterns. Cable force estimates match well with cable forces determined in previous studies and show the expected variation with temperature. Analysis of the data provided the basis for establishing alert thresholds (encompassed >99% of the data). An alert response plan has been proposed for responding to alerts generated.			
G17. Key Word Cable-stayed bridge, structural health monitoring, bridge management, sensors, data acquisition.		18. Distribution Statement No restrictions.	
19. Security Classif. (of this report) Unclassified	20. Security Classif. (of this page) Unclassified	21. No. of Pages 134	22. Price

## **Acknowledgments**

The authors thankfully acknowledge the support of this research by the Florida Department of Transportation (FDOT).

## Executive Summary

Completed in April 1987, the Sunshine Skyway Bridge has an average traffic volume of over 50,000 vehicles per day. Monitoring of the bridge movement is specified in the extensive maintenance manual provided by the bridge designers, Figg and Mueller. There have been a wide range of past monitoring efforts; however, there had not been a functioning monitoring system integrating data from various sensing systems into a single comprehensive view capable of providing routine or emergency assessment of the bridge response characteristics. The primary roadblock had been the ad hoc approach to the implementation of monitoring hardware without consistent support from a single FDOT office.

The District 7 Structures Maintenance Office (DSMO) sought to take the monitoring components on the bridge and create a single, centralized monitoring system available via a user-friendly web interface capable of providing alerts for anomalous bridge response data. This research project was initiated to achieve this objective and was divided into two phases. *Phase I: System Assessment and Integration Recommendations* sought to assess and document all available data collection systems installed on the bridge and make recommendations for the development of a single bridge monitoring web interface. *Phase II: System Deployment* was carried out to implement the recommendations of Phase I. Phase II included the selection of a web interface development contractor, the design of a web interface to meet the relevant stakeholder needs, the development of data processing algorithms to produce relevant bridge response information, analysis of long-term data to establish bounds of typical bridge responses, and the recommendations for a bridge alert response plan.

To centralize tracking of the monitoring hardware installed on the bridge by different FDOT offices, a web map and inventory database was developed in Phase I. As part of Phase II, these have been upgraded to reflect recently added sensors as well as to dynamically link the map to the database. The interactive web map enables visualization of the location of each component on the bridge while the inventory database provides detailed hardware information. Instructions for editing and using the web map and inventory database are provided so that a dedicated District 7 DSMO personnel can oversee its future enhancement and use.

BDI, Inc, a structural monitoring firm based in Colorado, was selected to develop the web interface for the Sunshine Skyway Monitoring System (SSMS) based on their experience providing monitoring equipment for the bridge and the capability of their monitoring interface, Infrastructure Intelligence (II), to meet monitoring system requirements. As a subcontractor to the Sunshine Skyway Engineering Services Contractor, TY Lin, BDI developed a web portal that provides data archiving, visualization, and alerts. Data from triaxial accelerometers installed on four cable stays and at the top of the North Tower, and weather station data including wind speed, wind direction, and temperature, are currently displayed in the web interface. GPS data to monitor bridge motion has been partially incorporated and the procedure for adding additional sensors or external data has been provided. A user guide to the web interface is provided as well as instructions for downloading raw monitoring data outside of the web portal. A System Security plan for the SSMS was developed with input from the FDOT Information Security (InfoSec) Administration Office to comply with state cybersecurity standards for information technology (IT) resources.

Analysis of one year of monitoring data (2020) was carried out to assess the quality and reliability of the data and to determine the bounds of typical bridge response to temperature-, wind-, and traffic-induced loading. Overall, the quality of data from the working sensors was good with low rates of erroneous data points. However, there were some gaps in data availability as the system was under development and undergoing needed sensor maintenance. Accelerometers on Cables 13 and 18, as well as the North Tower, provided reasonable data that was correlated with wind and temperature measurements to establish daily and seasonal response patterns. In addition to assessing the frequency and amplitude of the vibration, acceleration data from the cables was also used to estimate the cable forces by relating the cable vibration frequencies to the cable tension. The resulting cable force estimates match well with cable forces determined in previous bridge studies and show the expected variation with temperature. The MATLAB data processing source code has been provided in the Appendix.

Statistical analysis of the data over one year provided the basis for establishing alert thresholds. In general, thresholds were set to encompass >99% of the data measured. While the alert thresholds are not meant to represent structural capacity limits, they do provide a good indication of an anomalous response that may require additional investigation. Most of the threshold-exceeding events in 2020 were the result of high wind, though none represented an actual danger to the structural integrity of the bridge.

A bridge alert response plan has been proposed for responding to alerts generated from the SSMS. Four alert levels ranging from 1 (low severity) to 4 (high severity) and corresponding response procedures have been defined based on the nature of the generated alert. When an alert rises to Level 4, emergency response procedures outlined in the Skyway Emergency Response Plan (ERP) would be followed.

## Table of Contents

Disclaimer .....	ii
0B0BTechnical Report Documentation Page .....	v
Acknowledgments.....	vi
Executive Summary .....	vii
List of Figures.....	xii
List of Tables .....	xvi
List of Abbreviations .....	xvii
1 Introduction.....	1
1.1 Project Overview .....	1
1.2 Personnel and Roles.....	1
1.3 Report Overview.....	2
2 Sunshine Skyway Monitoring System Overview .....	4
2.1 Skyway Monitoring History .....	4
2.2 Fiber Network Integration.....	5
2.3 Data Sources .....	6
2.4 Data Availability.....	8
2.5 Data Management .....	9
3 Web Map and Inventory Database .....	10
3.1 Access to the Web Map and Inventory Database .....	10
3.2 Updated Web Map Overview .....	11
3.3 Updated Inventory Database Overview .....	12
4 Web Interface.....	14
4.1 Web Interface Contract.....	14
4.2 Site Location and Access .....	15

4.3	Portal Components.....	15
4.4	Portal Future Development.....	18
4.5	System Configuration.....	19
5	Data Processing.....	23
5.1	Hourly Data Extraction.....	23
5.1.1	Accelerometer Processing.....	23
5.1.2	Force Estimation.....	23
5.2	Processing One Year of Hourly Summary Data.....	26
6	Analysis Results.....	28
6.1	Environmental.....	28
6.2	Acceleration.....	32
6.2.1	Year Summary Plots.....	32
6.2.2	Representative Six-Day Plots.....	35
6.2.3	Examination of High Measurements.....	41
6.2.4	Acceleration Correlation Analysis.....	46
6.3	Cable Force.....	49
6.3.1	Summary Plots.....	49
6.3.2	Statistics and Comparison with Previous Studies.....	51
6.3.3	Cable Force Correlation Analysis.....	52
6.4	High-Wind Events and Bridge Closures.....	55
6.4.1	Bridge Closures.....	55
6.4.2	High Winds, No Closure.....	65
6.4.3	Skyway 10k with Partial Closure.....	68
7	Bridge Alert Response Plan.....	69
7.1	Event Types.....	69

7.2	Alert Levels.....	69
7.2.1	Level 1 .....	70
7.2.2	Level 2 .....	70
7.2.3	Level 3 .....	70
7.2.4	Level 4 .....	70
7.3	Alert Communication and Response .....	70
7.4	Response to Emergency Alerts (Level 4) .....	72
7.5	Reporting.....	72
8	Recommended Alert Thresholds .....	73
9	System Security Plan .....	74
10	Conclusions.....	74
11	References.....	76
12	Appendix A. Editing the Inventory Database and Interactive Web Map .....	77
12.1	Excel Sheet Organization.....	78
12.2	Datasheets Tab .....	81
12.3	Establishing Points to Place Markers.....	81
12.4	Adding Items to the Web Map and Inventory database.....	82
13	Appendix B. BDI PI User Manual.....	84
14	Appendix C. Alternate Approaches to Downloading Data .....	98
15	Appendix D. Data Analysis Code (MATLAB) .....	102
15.1	unzip_process_writetofile.m.....	102
15.2	SummaryPlots.m.....	109

## List of Figures

Figure 1. Location of GPS receivers.....	5
Figure 2. Locations of the sensors and cabinets near the North Tower.....	5
Figure 3. BDI data acquisition cabinet and DSMO maintenance cabinet.....	6
Figure 4. Locations of the six triaxial accelerometers and their axis orientation.....	7
Figure 5. Wind direction measurements relative to bridge orientation.....	7
Figure 6. Screenshot of the web map and inventory database main directory.....	10
Figure 7. Screen captures from the web map.....	12
Figure 8. JavaScript console log as shown using the Chrome web browser.....	13
Figure 9. Landing page with rendered bridge image and sensor status details on the right.....	16
Figure 10. Sensor selection from image marker.....	16
Figure 11. Data plot with sensor selection menu on right.....	17
Figure 12. Map layout.....	17
Figure 13. Sensor status alerts.....	18
Figure 14. The STS Core Monitor application which runs on the data acquisition computer located on the Bridge.....	20
Figure 15. Screen capture of the VPN client and Remote Desktop Connection to the Skyway Bridge computer.....	21
Figure 16. Screen capture of the STS_Core application running on the Skyway Bridge computer, accessed via Remote Desktop Connection.....	21
Figure 17. Acceleration measured in the Z-direction for Cable 13 over a one-hour period on April 27, 2020, at 2pm.....	25
Figure 18. Power spectral density (frequency domain) representation of the Cable 13Z acceleration measurement and identified first 20 peaks (red circles).....	25
Figure 19. Linear regression of the relationship between the frequency peaks, $f_n$ , and their corresponding frequency number, $n$ , for Cable 13Z acceleration.....	26
Figure 20. Hourly mean temperatures during 2020.....	28
Figure 21. Representative hourly mean temperature variation for a six-day period.....	29



Figure 22. Hourly wind speeds (mean and maximum) and wind direction.....	30
Figure 23. Representative hourly mean and maximum wind speeds (top) and hourly mean wind directions (bottom) over six days. ....	31
Figure 24. High wind speed readings on September 11, 2020 (left) with detail (right) showing spikes likely indicating a measurement error. ....	31
Figure 25. Cable 13 hourly maximum and RMS accelerations recorded in 2020 in the Y- and Z-directions (top and bottom, respectively). ....	32
Figure 26. Cable 18 hourly maximum and RMS accelerations recorded in 2020 in the Y- and Z-directions (top and bottom, respectively). ....	33
Figure 27. Tower hourly maximum and RMS accelerations recorded in 2020 in the X- and Y- directions (top and bottom, respectively). ....	34
Figure 28. Tower X- and Y-acceleration, zooming in below data spikes to observe weekly acceleration variations. ....	35
Figure 29. Six days of hourly Cable 13 RMS acceleration measured in the Y- and Z-directions (top and bottom, respectively). ....	36
Figure 30. Six days of hourly Cable 13 maximum acceleration measured in the Y- and Z- directions (top and bottom, respectively). ....	37
Figure 31. Six days of hourly Cable 18 RMS acceleration measured in the Y- and Z-directions (top and bottom, respectively). ....	38
Figure 32. Six days of hourly Cable 18 maximum acceleration measured in the Y- and Z- directions (top and bottom, respectively). ....	39
Figure 33. Six days of hourly North Tower RMS acceleration measured in the X- and Y- directions (top and bottom, respectively). ....	40
Figure 34. Six days of hourly maximum North Tower acceleration measured in the X- and Y- directions (top and bottom, respectively). ....	41
Figure 35. Cable 18 acceleration recorded January 18, 2020, with the record starting at 1:51 pm. ....	42
Figure 36. Cable 18 acceleration recorded January 18, 2020, zoomed in on high value measurement. ....	42
Figure 37. Tower accelerations measured on March 1, with the record starting at 5:54am. ....	43
Figure 38. Zoomed in view of tower acceleration measurements recorded on March 1, with the record starting at 5:54 am: ~3 minutes into record (left) and ~38 minutes into record (right). ....	44

Figure 39. Tower acceleration on August 3, with the record starting at 9:33am.....	44
Figure 40. August 3, 30 minutes into tower vibration record that starts at 9:33am.....	45
Figure 41. Tower acceleration measurements recorded on December 11 for a record starting at 11:50am.....	45
Figure 42. Tower acceleration measurements recorded on December 11 with the record starting at 11:50 am, just after 42 minutes into record.....	46
Figure 43. Hourly RMS acceleration by hour of the day.....	47
Figure 44. Hourly RMS acceleration as function of wind speed perpendicular to the length of the bridge.....	48
Figure 45. Cable force estimates from Y- and Z-axis acceleration on Cables 13 and 18 measured in 2020. ....	50
Figure 46. Six days of cable force estimates in Cables 13 and 18.....	51
Figure 47. Tensions estimated in Cable 13 from Y-axis acceleration measurements. ....	53
Figure 48. Tensions estimated in Cable 13 from Z-axis acceleration measurements.....	54
Figure 49. Tensions estimated in Cable 18 from Y-axis acceleration measurements. ....	54
Figure 50. Tensions estimated in Cable 18 from Z-axis acceleration measurements.....	55
Figure 51. Hourly mean and maximum wind speed from February 4-8, 2020. ....	56
Figure 52. Wind speed measured on February 6 from approximately 6 to 9pm .....	56
Figure 53. Cable 13 acceleration measured on February 6 from approximately 6pm to 9pm. ....	57
Figure 54. Hourly Cable 13 RMS acceleration values from February 4-8, 2020.....	58
Figure 55. Wind speed hourly mean and maximum (top) and hourly direction (bottom) recorded between November 7 and 13, 2020, as Tropical Storm Eta passed nearby. ....	59
Figure 56. Cable 13 hourly RMS acceleration recorded between November 7 and 13, 2020, as Tropical Storm Eta passed nearby.....	60
Figure 57. Cable 13 hourly maximum acceleration recorded between November 7 and 13, 2020, as Tropical Storm Eta passed nearby. ....	61
Figure 58. Cable 18 hourly RMS acceleration recorded between November 7 and 13, 2020, as Tropical Storm Eta passed nearby.....	62

Figure 59. Cable 18 hourly maximum acceleration recorded between November 7 and 13, 2020, as Tropical Storm Eta passed nearby. ....	63
Figure 60. Tower hourly RMS acceleration recorded between November 7 and 13, 2020, as Tropical Storm Eta passed nearby.....	64
Figure 61. Tower hourly maximum acceleration recorded between November 7 and 13, 2020, as Tropical Storm Eta passed nearby. ....	65
Figure 62. Wind speed (top) and wind direction (bottom) recorded from 7:15 to 7:30pm on December 24, 2020. ....	66
Figure 63. Cable 13 acceleration recorded from 7:15 to 7:30pm on December 24, 2020.....	67
Figure 64. Cable 18 acceleration recorded from 7:15 to 7:30pm on December 24, 2020.....	67
Figure 65. Procedure for communication of different alert levels. The responsible entity is shown in square brackets.....	71
Figure 66. Sensor information in Excel worksheet.....	78
Figure 67. Image information in Excel worksheet.....	79
Figure 68. Marker type and location information.....	80
Figure 69. Screen shot of “Mouse Click Event” selection from the control panel (left) and screen shot of example resulting pop-up (right).....	82
Figure 70. Modifications to the Excel Inventory showing how the Car Example would be added.....	82
Figure 71. Saving spreadsheet as a CSV file .....	83
Figure 72. Cars marked on the web map. ....	83
Figure 73. Screenshot of the data acquisition computer via a remote TeamViewer connection showing raw data files which can be downloaded. ....	99
Figure 74. Types of data available for download through the BDI-branded FileCloud web application.....	100
Figure 75. High speed (200 Hz) data files available for download through the BDI-branded FileCloud web application. ....	100
Figure 76. After files to be downloaded have been selected, a “Download” button appears.....	101

## List of Tables

Table 1. SSMS stakeholders .....	2
Table 2. Sensor downtime in 2020. ....	8
Table 4. Cable properties used in analysis (from BES cable analysis reports).....	24
Table 5. Bounds for elimination of measurement errors. ....	26
Table 6. Percent of data points removed for being out of the bounds provided in.....	27
Table 7. Hourly RMS acceleration statistics (mg).....	49
Table 8. Hourly maximum acceleration statistics (mg).....	49
Table 9. Cable tension summary (kips). ....	51
Table 10. Comparison of estimated cable forces (kips).....	52
Table 11. Linear regression coefficients for the relationship between temperature and cable force estimate. ....	52
Table 12. Percent of cable force estimates within the two types of bounds: temperature-dependent linear and constant. ....	55
Table 13. Alert Distribution List.....	72
Table 14. Recommended maximum acceleration thresholds for currently working sensors (mg). ....	73
Table 15. Recommended cable force thresholds (kips).....	74
Table 16. Compatible browsers. ....	78
Table 17. Title and description of each column shown in Figure 66.....	79
Table 18. Title and description of each column shown in Figure 67.....	80
Table 19. Title and description of each column shown in Figure 68.....	81

## **List of Abbreviations**

AMC	Asset Maintenance Contractor
AMTS	Automatic Motorized Total Station
AST	Agency for State Technology
BEMS	Bridge Environmental Monitoring System
BES	Bridge Engineering Solutions
BDI	Bridge Diagnostics, Inc.
CEMP	Comprehensive Emergency Management Plan
D1	FDOT District 1
D7	FDOT District 7
DSMO	District Structures Maintenance Office – District 7
ECO	Emergency Coordination Officer
EOC	Emergency Operations Center
ERP	Emergency Response Plan
ESC	Engineering Services Contractor
FDOT	Florida Department of Transportation
FHP	Florida Highway Patrol
GNSS	Global Navigation Satellite System
GPS	Global Positioning System
II	Infrastructure Intelligence
ITS	Intelligent Transportation Systems
NOAA	National Ocean and Atmospheric Administration
PI	Platform Interactive
PSD	Power Spectral Density
SHM	Structural Health Monitoring

SMO	State Materials Office
SSMS	Sunshine Skyway Monitoring System
SSP	System Security Plan
TTO	FDOT Transportation Technology Office
TWO	Task Work Order
UF	University of Florida
VPN	Virtual Private Network

# 1 Introduction

## 1.1 Project Overview

The overarching goal of this project was to create a Sunshine Skyway Bridge monitoring system that is fully integrated and highly flexible with a user-friendly web interface and full data archiving. The result of this effort is a web portal that combines data from sensors installed on the bridge for data visualization and alerts that can easily expand to include additional sensors and data sources. The larger research effort was divided into two phases: *Phase I: System Assessment and Integration Recommendations* and *Phase II: System Deployment*. This report presents the outcomes of the Phase II research efforts.

The objectives of Phase II were to: (1) integrate sensor / data acquisition systems and oversee the design of a comprehensive web interface, (2) collect and analyze bridge response and environmental data over a one-year period to establish typical bounds of structural behavior, and (3) develop user and training manuals on monitoring system use and maintenance.

The following tasks were carried out to complete the Phase II research objectives:

- **Data integration:** All sensor subsystems on the Skyway were connected to a single fiber network to ensure data access by all Sunshine Skyway Monitoring System users.
- **Inventory and Database Upgrade:** The interactive web map and inventory database that were developed in Phase I were updated.
- **Web Interface Development:** A web interface development contractor was selected, and the web interface was designed to meet anticipated Skyway stakeholder needs.
- **Long-term Data Analysis:** Data processing algorithms were developed and implemented to analyze one year of bridge-collected data to validate system output and to establish bounds of typical bridge response behavior.
- **Alert Thresholds and Response Plan:** Recommended data thresholds were established so that the web portal can automatically generate alerts if responses are not within bounds. A Response Plan based on four alert levels was established to provide response guidance.
- **Training and User Manuals:** User manuals and training documents were developed and compiled, and protocols for adding sensors and data processing technologies in the future were established.
- **System Security Plan:** A system security plan was created with input from the FDOT Transportation Technology Office to ensure that the system adheres to FDOT data security requirements.

## 1.2 Personnel and Roles

This report refers to several groups responsible for monitoring system development and Skyway decision support. These groups are collectively referred to as “stakeholders” and represent individuals and entities that have responsibility for, and an interest in, the safe and effective operation of the Skyway. Those also referred to as “developers” have had direct input on the development and maintenance of the monitoring system and thus generally require low-level access to the networks and raw data from the system. The stakeholders are summarized in Table 1.

The District 7 (D7) Structures Maintenance Office (DSMO) has the responsibility for the monitoring, maintenance, and safe operation of the Sunshine Skyway Bridge. The DSMO has a designated Skyway Project Manager. DSMO works with other D7 FDOT offices and contractors on the various aspects of Skyway operations. BDI is the developer of the Infrastructure Intelligence (II) portal that provides the web interface for the Sunshine Skyway Monitoring System (SSMS). Development includes implementation of alert thresholds and management of alert communication distribution lists. While under contract, BDI staff monitors the data, reviews alerts generated by the system, and ensures system functionality. The Engineering Services Contractor (ESC) on the Skyway, TY Lin, provides structural engineering services to the D7 DSMO. These services include the interpretation of monitoring data to assess the structural performance of the bridge. The Asset Maintenance Contractor (AMC), DBi Services provides all maintenance and repair services for the Sunshine Skyway Bridge. FDOT ITS and ITS contractor, TransCore, maintain and oversee the IT infrastructure on bridge, including a fiber optic communication network and CCTV cameras. In the event of an emergency, the D7 Emergency Coordination Officer (ECO) oversees response operations.

Table 1. SSMS stakeholders

<b>Stakeholder</b>	<b>Point(s) of Contact</b>	<b>Role(s)</b>	<b>Developer</b>
District 7 Structures Maintenance Office (DSMO)	Jim Jacobsen/ Daniel Buidens	Structures Maintenance Engineer/Skyway Project Manager	Yes
District 7 Emergency Coordination Officer (ECO)	Angela Aborizk	Emergency Response Coordinator	No
Intelligent Transportation Systems (ITS)	Andrew Young	Skyway IT Infrastructure Management	Yes
University of Florida (UF)*	Jennifer Bridge	SSMS Research Lead	Yes
Asset Maintenance Contractor (DBi)	Peter Martin	Skyway Maintenance	No
Monitoring System Contractor (BDI)	Jesse Sipple	Web Portal Development and Monitoring	Yes
Engineering Services Contractor (TY Lin, International)	Ivan Gualtero Atiq Alvi	Skyway Structural Assessment	Yes

\*UF involvement and access to the SSMS ends with the current Task Work Order.

### 1.3 Report Overview

This report provides a summary of the work completed to realize the objectives of Phase II. The report is organized as follows: Section 2 provides an overview of the SSMS, including the various data sources, how they were integrated, and how they have performed. Section 3 presents the updates made to the Skyway web map and inventory database since Phase I and Section 4 describes the SSMS web portal. Methods for data extraction and processing are presented in Section 5,



analysis results of one year of data are provided in Section 6, a recommended Response Plan is described in Section 7, and alert thresholds are recommended in Section 8. The System Security Plan is discussed in Section 9. Finally, Section 10 gives the conclusions and recommendations for future work. Appendices A-D consist of user manuals and data processing algorithms/code.

## 2 Sunshine Skyway Monitoring System Overview

Technological advances in the fields of monitoring, cyberinfrastructure, data management, and numerical simulation provide the opportunity to develop real-time decision support systems for bridge operation and maintenance. Central to an effective decision support system is a monitoring system that operates autonomously to collect, store, and archive data as well as provide access to such data in an efficient, reliable, and secure manner (e.g., through user-friendly, interactive web-interfaces). With such a system in place, long-term data records, coupled with accurate and well-calibrated structural / atmospheric / hydrodynamic / transportation / etc. models defining response characteristics (e.g., bridge motion), operational limits of key physical (e.g., vehicular loading) or environmental (e.g., wind speed) parameters can be established. These limits may then be used to automatically generate observed and predicted warning alerts during both routine (e.g., planned maintenance) and extreme loading (e.g., high winds, overload, settlement, and vessel impact) events to assist decision making.

An additional requirement of an effective monitoring system is the ability to integrate and synchronize data from heterogeneous sources. Careful planning to select the most appropriate monitoring intervals is required to ensure the most useful data is collected. The system must be responsive to unexpected loading events, autonomously collecting data at appropriate sampling intervals during periods of interest. All aspects of the system – data collection, communication, processing, visualization, and archiving – should operate with minimal user input while supporting a high level of remote user interaction. To ensure the ongoing usefulness and longevity of the monitoring system, it must possess adequate flexibility so that its operation can be adjusted to support changing bridge conditions and evolving needs of relevant stakeholders. In addition, the system should support the integration, correlation, and visualization of data from external sources, such as atmospheric and coastal condition reporting and forecasting systems operated by NOAA, NCEP, etc.

### 2.1 Skyway Monitoring History

Completed in April 1987, the Sunshine Skyway Bridge has average daily traffic of over 50,000 vehicles. Monitoring of the bridge movement is specified in the extensive maintenance manual provided by the bridge designers, Figg Engineering (Figg, 1988) and the Manual by Parsons Brinckerhoff (PB Americas, 2010). Early in the life of the Bridge, FDOT conducted GNSS (GPS) testing to track structural movement but found the process to be costly and complex and provided limited useful results. In the 1990s, the Surveying and Mapping Office installed five GPS receivers and established a website to track the data (Figure 1). Later, an Automatic Motorized Total Station (AMTS) was installed on one of the dolphins for scanning targets located on the bridge piers and towers. In 2005, an additional AMTS was installed on a second dolphin and two weather stations were added at the locations of two of the existing GPS receivers (Figure 1). In 2011, the five original GPS receivers were upgraded. Due to inconsistent communication and operability, the AMTS units were removed from the dolphins early in Phase II (2017). Weather stations installed and maintained by the State Materials Office (SMO) were mostly operational at the beginning of Phase II with some communication challenges limiting data access. Six triaxial accelerometers and a weather station were installed in 2015 by BDI, contracted by the D7 DSMO, as shown in Figure 2. Even with this wide range of past monitoring efforts, there had not been fully functioning

monitoring system that integrated data from the various sensing systems and had the capability to provide routine or emergency condition assessment of the bridge.

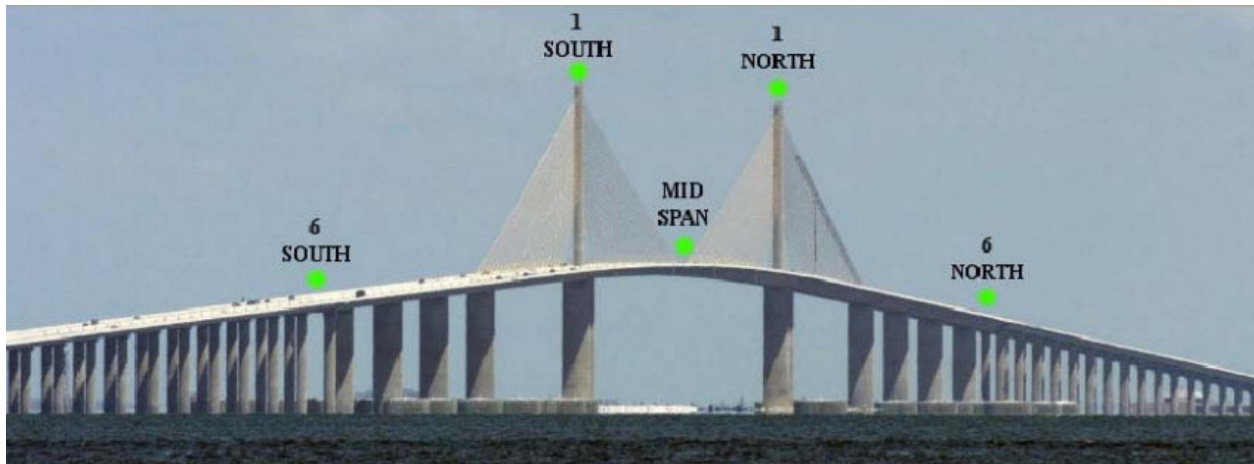


Figure 1. Location of GPS receivers.

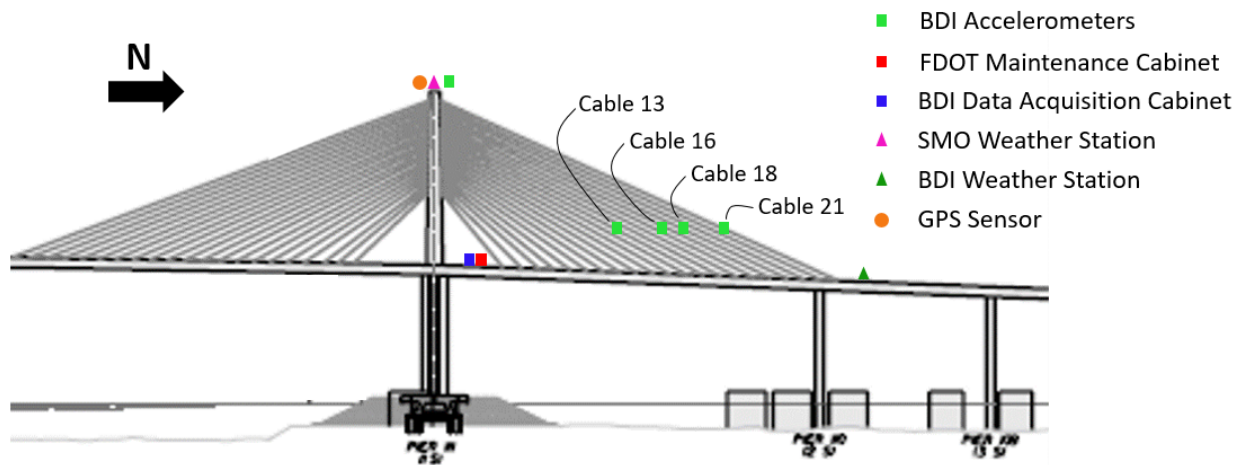


Figure 2. Locations of the sensors and cabinets near the North Tower

Based on the results of Phase I and the available D7 budget and personnel resources, the sensors and data acquisition systems retained for the SSMS developed in Phase II are the BDI triaxial accelerometers / weather station and the GNSS receivers. The AMTS were eliminated due to lack of functionality, communication challenges, and cost of maintenance and/or replacement. A physical connection with the SMO-installed weather station on the top of the North Tower was made; however, the data is not currently accessible.

## 2.2 Fiber Network Integration

The first step in the SSMS development was to integrate the BDI-installed accelerometers and weather station with the existing fiber network on the bridge. The BDI data acquisition cabinet,

located near the base of the North Tower (Figure 3), collects data from these sensors and originally made it available over a cellular connection maintained by BDI. With this original setup, only BDI had remote access to the system (using TeamViewer). As such, to obtain collected accelerometer and weather data, an FDOT employee had to drive out to the bridge and manually save the data to an external hard drive. Additionally, FDOT and UF had had to rely on BDI to make data collection adjustments (e.g., sampling rate and monitoring periods) as they did not have direct access to the system.

To connect the BDI system to the fiber optic communication network on the bridge, a physical connection was made between the BDI cabinet and the FDOT Maintenance cabinet a few feet away (Figure 3). On May 16, 2018, the BDI data acquisition cabinet was connected to the existing DSMO maintenance cabinet via Ethernet cable by a TransCore employee. An ITS employee setup the networking and provided a DHCP entry on the fiber network for the BDI computer. This resulted in the data communication being switched over from the BDI cellular router to the ITS fiber network. With the connection in place and the communication switch made, the data acquired by the BDI system was now directly available for streaming to FDOT servers.



Figure 3. BDI data acquisition cabinet and DSMO maintenance cabinet

### 2.3 Data Sources

Of the six triaxial accelerometers installed on the bridge, four are on cables, one is at the top of the North Tower, and one is at deck level, as shown in Figure 2. The four instrumented cables are Cables 13, 16, 18, and 21. The triaxial accelerations are oriented such that X axis measures vibration along the cable (longitudinal), Y axis measures horizontal/transverse acceleration (out of plane), and Z axis measures vibration perpendicular to the cable and the horizontal plane (Figure 4). The data presented in this report is focused on the vibration measurements perpendicular to the cables, i.e., the Y and Z measurements.

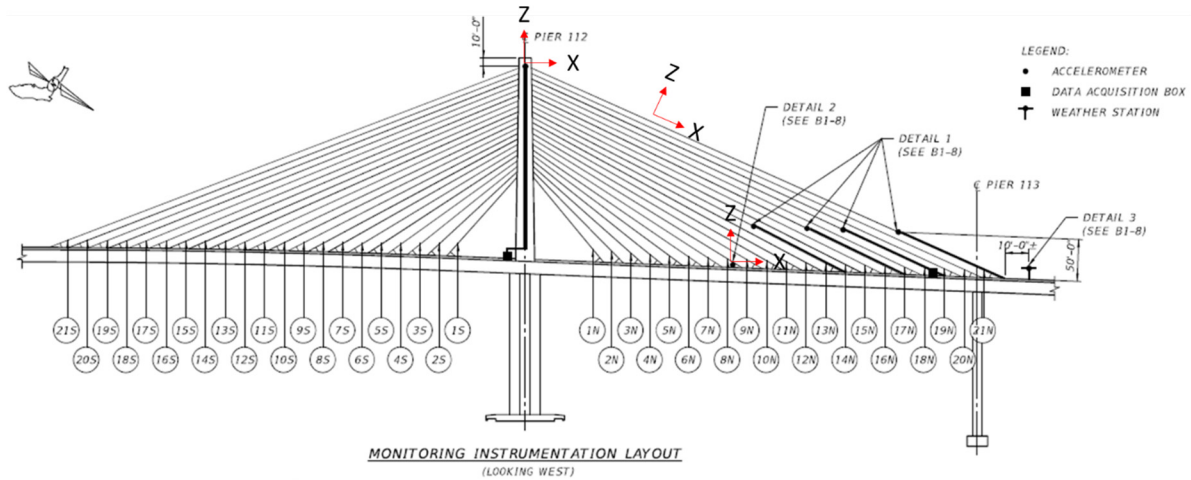


Figure 4. Locations of the six triaxial accelerometers and their axis orientation.

In addition to the accelerometer data, recorded environmental data includes wind speed, wind direction, and temperature. Wind direction is provided in degrees relative North (North = 0°) with the bridge oriented at approximately 33° (Figure 5). In mid-2020, GPS data at several locations on the bridge (as well as an additional weather station) were in the process of being incorporated into the monitoring system. Due to external factors, the completion of this was postponed; however, GPS measurements may be more completely integrated in the future to monitor the motion of the deck and towers.

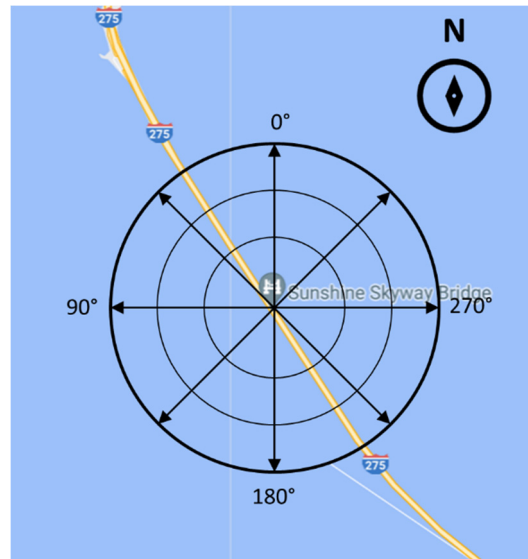


Figure 5. Wind direction measurements relative to bridge orientation.

High frequency data is continuously collected at a rate of 200 Hz, saved in hour-long data files. Note that the sampling rate of the data may be reduced, as discussed in Section 5.1. The data is stored on servers provided by BDI and made available to the relevant stakeholders.

## 2.4 Data Availability

Data was collected almost continuously in 2020 and all available data files from December 30, 2019, to January 3, 2021 (371 days), were analyzed for this report to capture one-year variations in measurements. The expected number of hour-long data files is  $371 \times 24 = 8904$ ; however, due to downtime for maintenance, system outages, or file corruption, 8603 were generated during this period. The difference is equivalent of 301 hours (12.5 days) for a total system downtime of 3.5%. In addition to these missing files, some sensor channels were unavailable or non-functional at different periods of time (Table 2). Note that wind speed and direction come from a single sensor, as do the axes of acceleration measured for each cable; as a result, if one of these channels is down, they are all down, thus they are reported together.

Table 2. Sensor downtime in 2020.

<b>Data Channel</b>	<b>Missing Records</b>	<b>Total Missing (days)</b>	<b>Downtime (%)</b>
Temperature	861	35.9	10%
Wind Speed/ Direction	2391	99.6	27%
Cable 13 Acceleration	354	14.8	4%
Cable 16 Acceleration	4100	170.8	46%
Cable 18 Acceleration	816	34.0	9%
Cable 21 Acceleration	861	35.9	10%
Tower Acceleration	436	18.2	5%
Deck Acceleration	8904	371.0	100%

Some channels did not provide reasonable data during 2020, even when the data was available. The following list summarizes additional data issues.

- Beginning April 15, 2020, wind speed was reported in units of mph. However, wind speed data prior to the date, was negative (not physical) and reported in m/s. When the sign was inverted and units were changed to mph, it was consistent with data collected in the region and from the bridge later in the year. Additionally, between April 15 and July 8, the anemometer was not operational. A new wind sensor came online July 9, 2020.
- Prior to July 9, 2020, at 21:00, the channel labels on Cable 13 and 16 were switched. Tap tests (observation of signals during manual excitation of the cables) were conducted to confirm the mislabel and the labels were corrected. All data presented in this report accounts for the mislabeling.

- Data from Cable 16 did not provide reasonable acceleration levels; the channel was taken offline after the correction of the Cable 13/16 mislabeling on July 9, 2020. As a result, Cable 16 did not provide usable data during 2020.
- Cable 18, wind direction, and the temperature sensors did not provide data between August 18 and September 11.
- No system data was collected between November 13 and 18; the reason for this downtime is unclear.
- Cable 21 sensor did not provide any usable data.
- Data was unavailable from the deck accelerometer.

The levels of sensor downtime experienced in 2020 are the result of a system that was originally installed in 2015 but had very little monitoring and maintenance until 2020. Until it was connected to the web interface, data was not easily observable or accessible by anyone other than BDI; however, BDI did not have an active contract with D7 to oversee the system operation. When a contract with BDI was finally put in place and the web interface was made operational, it became evident that many sensors were no longer operable. Throughout 2020, joint efforts between D7, BDI, the Engineering Services Contract (TY Lin), ITS, and UF researchers, resulted in the repair or replacement of several sensors. Some of the work required to maintain the system resulted in it temporarily being offline. Budget and contract constraints limited additional system repairs and enhancements.

Structural monitoring systems require consistent monitoring and maintenance coupled with maintenance contract structures that allow timely resolution of any system problems that arise. An external contractor is in the best position to provide system oversight to protect the investment of the FDOT. In addition, dedicated personnel within DSMO, such as the Skyway Project Manager, will be required for effective interface with the contractor. With these system management mechanisms in place, it is anticipated (based on UF researcher experience) that any individual data channel would have less than a 3% downtime and that the downtime of the overall system would be closer to 1%.

## **2.5 Data Management**

Approximately 922 GB of data (232 GB compressed) data was collected during 2020; for a year with no data loss, it would be slightly over 1TB. Each hour of data resulted in approximately 110 MB of data from 18 channels (three axes of acceleration on four cables, three axes of tower acceleration, wind speed, wind direction, and temperature) sampling 200 Hz. To make the analysis of the large amount of data manageable on a desktop PC, a three-part procedure was used: 1) weekly during 2020, hourly raw data was downloaded, as described in the Appendix, combined and compressed into zip files each of which contained a week of data, 2) for hourly data file analysis, each zip files was unzipped one at a time with hourly summary results exported to a summary file and 3) the one-year hourly summary results were further analyzed to generate statistics and bounds of typical bridge responses. Each unzipped file was deleted after analysis to minimize local data storage requirements.

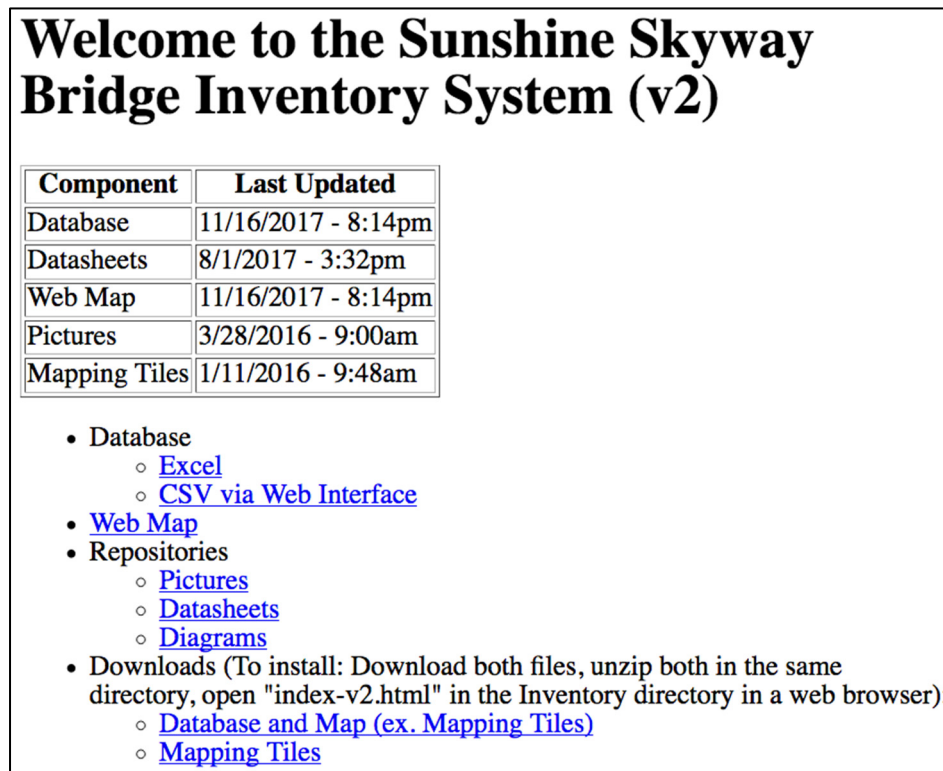


### 3 Web Map and Inventory Database

In addition to the SSMS web portal, a comprehensive database and corresponding interactive web map have been created to inventory equipment and monitoring hardware currently installed on the bridge. The web map and database are described in detail in the Phase I final report. This section describes the upgrades that have been made to the web map and inventory database since Phase I. The map and database are now dynamically linked so that the information entered in the database automatically populates the web map. This change makes the system easily expandable as additional monitoring system components are added to the bridge. Furthermore, a protocol for the addition and tracking of all monitoring items on the Skyway has been developed. Appendix A gives detailed instructions on editing map and database.

#### 3.1 Access to the Web Map and Inventory Database

The updated web map and inventory database source files have been provided to the DSMO. Currently, the files for the web map and inventory database must be stored locally on the computer from which it is being accessed. However, in the future, these files could be placed on the same webserver as the SSMS ensuring access and availability of the most up-to-date information about the sensors on the Skyway to users with appropriate access. The contents of the main directory, including the links from which the web map and inventory database, as well as the aerial image tiles that serve as the basemap of the web map, that can be downloaded are shown in Figure 6.



**Welcome to the Sunshine Skyway  
Bridge Inventory System (v2)**

Component	Last Updated
Database	11/16/2017 - 8:14pm
Datasheets	8/1/2017 - 3:32pm
Web Map	11/16/2017 - 8:14pm
Pictures	3/28/2016 - 9:00am
Mapping Tiles	1/11/2016 - 9:48am

- Database
  - [Excel](#)
  - [CSV via Web Interface](#)
- [Web Map](#)
- Repositories
  - [Pictures](#)
  - [Datasheets](#)
  - [Diagrams](#)
- Downloads (To install: Download both files, unzip both in the same directory, open "index-v2.html" in the Inventory directory in a web browser):
  - [Database and Map \(ex. Mapping Tiles\)](#)
  - [Mapping Tiles](#)

Figure 6. Screenshot of the web map and inventory database main directory.



## 3.2 Updated Web Map Overview

While the fundamental design and function of the Phase II version of the map is essentially the same as the Phase I map, the mechanism by which point and line feature data is populated from the database is now automated and all of the relevant JavaScript libraries have been updated to their latest versions. The result is that the process of adding new items to the inventory database and to the web map has been greatly simplified and it no longer requires any JavaScript programming knowledge. Leaflet, an open-source JavaScript library for making interactive maps, was upgraded to v1.2.0, the Leaflet Styled Layer Control plugin was also upgraded to the latest version, and a package containing color variations of the standard leaflet marker has been added. To facilitate parsing of the database file, the Papa Parse JavaScript library is now being used. The W3C Markup Validation service was used to validate the web pages. The necessary libraries are already incorporated into the program and the original download locations can be found below:

- **Leaflet** - A JavaScript library for interactive maps: <http://leafletjs.com/>
- **leaflet-color-markers** - Color variables of the standard Leaflet markers: <https://github.com/pointhi/leaflet-color-markers>
- **Leaflet.StyledLayerControl** - Leaflet plugin that supports organization of layers into groups: <https://github.com/davicustodio/Leaflet.StyledLayerControl>
- **Papa Parse** - A JavaScript CSV parser: <http://papaparse.com/>
- **jQuery** - A JavaScript library that makes document manipulation simpler: <https://jquery.com/>

Updates to these libraries may be released in the future, however they do not necessarily need to be updated unless the DSMO would like to incorporate newly added features, which may be available in a future release of the libraries, into the web map. Upgrading will, however, potentially require some knowledge of programming in HTML and/or JavaScript. Another major enhancement to the web map view is that now, the pop-ups display all database fields for each item on the bridge (Figure 7).

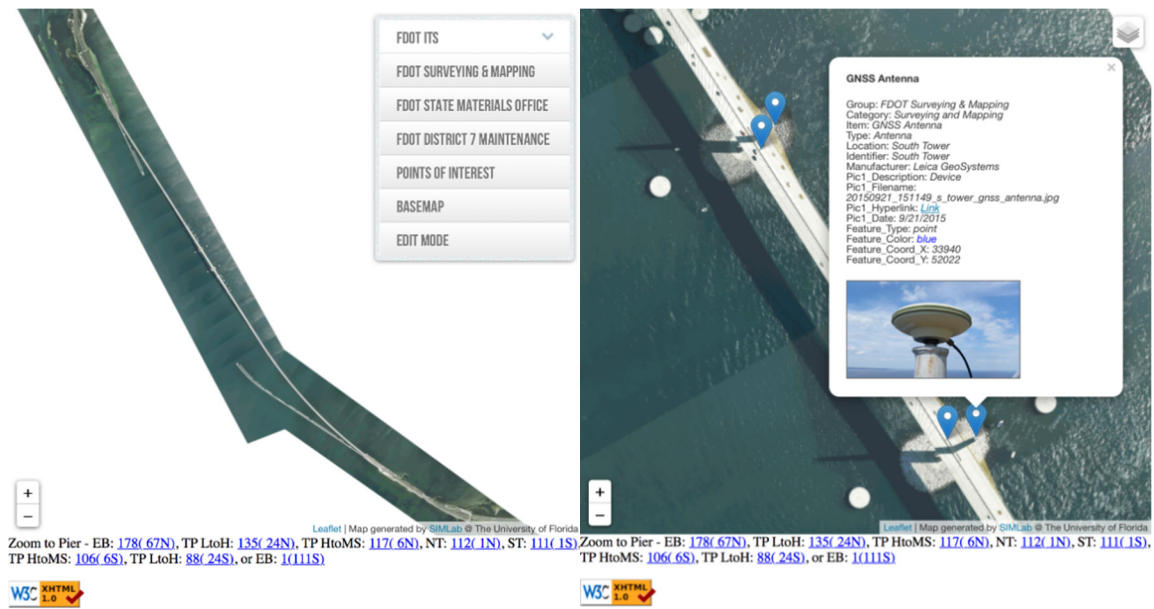


Figure 7. Screen captures from the web map

### 3.3 Updated Inventory Database Overview

The foundation of the Phase II web map is a reorganized and updated version of the Phase I Excel database. Some of the columns have been renamed or moved, and the database, which was originally comprised of separate worksheets for each FDOT department, has now been condensed into a single worksheet of point and line features. This file structure allows users to easily add or update the information that appears on the map by saving the updated database as a CSV file, which contains all of the point and line descriptions, coordinates, and colors. The capability of adding line features, which are markers that depict an item or feature that exists linearly along the length of the bridge, has also been added, and this will allow the DSMO to depict things such as visual site lines or a main bridge span. Furthermore, other minor updates, such as the ability to update the ITS traffic camera links, have also been added. Finally, in addition to the web map view of the database, a new table view has also been created. This enables browser-based viewing of the worksheet containing all of the point and line features, which can be particularly helpful when searching for a specific database entry. A few of the major highlights of the new table view of the database include clickable hyperlinks to images / web links (e.g., traffic camera feeds) and the feature colors that are used.

Map features in the database are organized by the "Group" (formerly "Agency") and "Item" fields. Dropdowns in the legend are shown in the order that the items appear in the database. Features are defined by the use of the "point" or "line" keyword in the "Feature\_Type" column. Point features are indicated by a single-colored marker. The color of the marker is defined in the "Feature\_Color" column. Possible choices are blue, red, green, orange, yellow, violet, grey and black. The location of the marker is based on its map coordinates, which is its pixel location on the basemap, and it is specified in the "Feature\_Coord\_X" and "Feature\_Coord\_Y" column. All markers and Line segments for a given "Group → Item" combination must be the same color, however, only line segments for a given "Group → Item → Location" combination will be connected.

The Phase II web interface also includes improved JavaScript console logging, which can be accessed through browser developer tools, as seen in Figure 8. The console logging can aid the user in the debugging process. For example, in instances where an issue is preventing the web map from being displayed correctly, the JavaScript console log can be used to determine if the issue is being caused by a security feature of the browser, or by a problem with the program or the CSV file. Both the table and console log display the name of the database CSV file, the number of database entries, and the first record in the file. The web map control log also displays the size of the basemap image, the view center, and the color of the mouse click event icon, all of which are defined in the database file. The console log then displays a list of the groups and items within each group as they are read from the CSV file. JavaScript alerts for common errors have been added including error conditions such as: Papa Parse library could not be found; Unsupported point/line color; Items to plot are tagged as both points and lines; Items to plot are tagged with multiple colors; Missing/undefined/Out-of-range map coordinate values. Finally, the W3C Markup Validation service was used to ensure the document conformed to HTML rules and grammar requirements.

More detailed instructions on the use of the interactive database are provided in Appendix A.

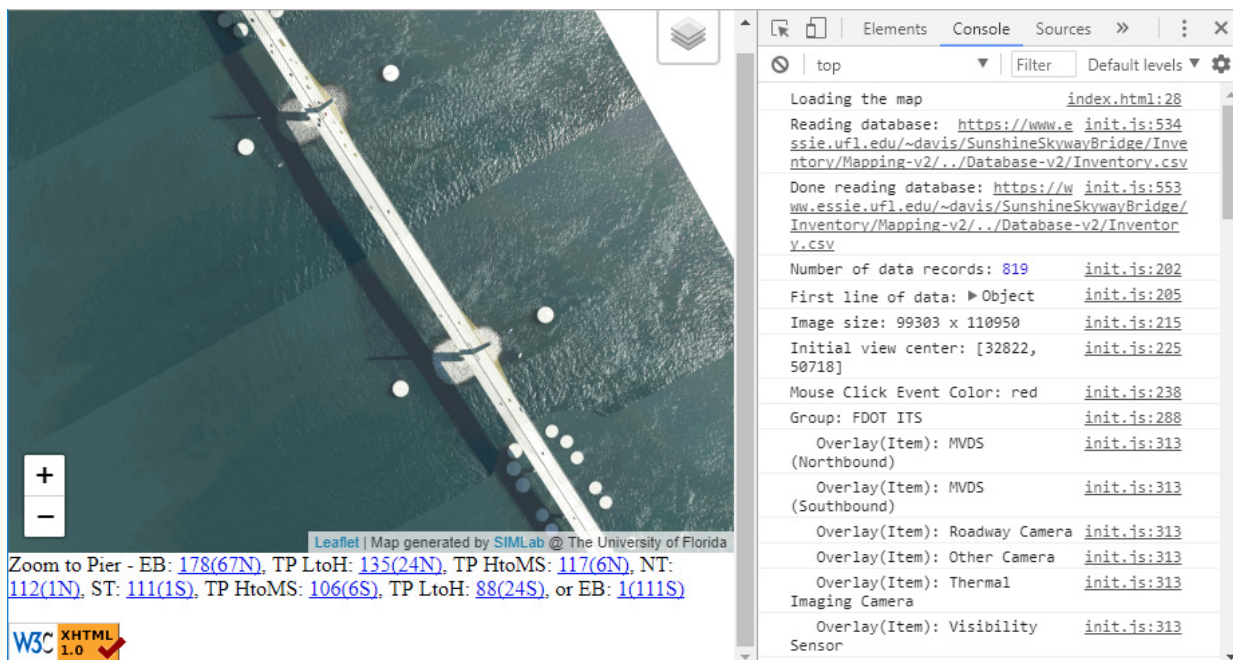


Figure 8. JavaScript console log as shown using the Chrome web browser

## 4 Web Interface

A web portal is an internet-based interface that provides end users access to interrogate and visualize data from different data sources. A key component of an effective monitoring system web interface is the visualization of all environmental and structural monitoring data installed on the Skyway in near real-time. In addition to providing real time plots of observed data, the interface must also have the ability to display processed data that may have more utility for safety and maintenance decision support. Processed data displays may be as simple as basic statistics of measured data (e.g., minimums/maximums, means, and standard deviations) or may require more involved processing (e.g., frequency domain analysis to estimate stay cable forces from vibration data).

When displaying data or processed response information, the web interface should indicate the location on the bridge where the data was generated. An interactive visualization interface can use three-dimensional renderings and/or pictures of the bridge to provide a means of viewing data or results from various locations on the bridge. This may be effectively achieved by placing appropriately placed markers for each data channel's physical location. As the user clicks on each marker, the data or results from that location can be shown.

Beyond the visualization of time varying data and bridge response values, the web interface should also allow for the setting of threshold values for evaluating whether the measured/calculated response values are within normal or safe bounds. When these thresholds are exceeded, the system should provide alerts, both in the interface dashboard and via a push communication method (email, text messages, RSS, etc.), to the relevant stakeholders. To ensure the highest levels of system security, the web interface should also be able to support customized access roles (view only, view and threshold setting, etc.) to designated stakeholders.

### 4.1 Web Interface Contract

A number of companies provide portals specifically designed for structural health monitoring, such as the Infrastructure Intelligence (II) web application used by BDI, or the Intelligent Decision Support (IDS) platform developed by CAMGIAN microsystems. Contractors with existing instrumentation and/or experience on the Skyway were considered for selection as the web portal development contractor. The assessment of the contractors was based on their ability to achieve the desired system functionalities, as described above. In addition to being able to provide these features, a history of providing systems for bridges and working with state departments of transportation was prioritized. The two primary sensor systems currently installed on the bridge are the GPS sensors by Leica Geosystems, and the accelerometers by BDI. As such, web portals offered by both Leica and BDI were considered.

Leica's web portal service, GeoMoS Now!, has many of the features required for the SSMS. However, at the time it was considered, it did not easily integrate data from non-Leica instrumentation or enable the integration of user-developed data processing code to display specialized processed data (e.g., derived cable tensions). In contrast, II can integrate data from multiple sensors and sources and has the ability to display "virtual" data channels resulting from integrated data processing algorithms. Based on a review of these vendors by UF and DSMO, it was determined that the II web application used by BDI would be the best fit for the SSMS.

BDI (<https://bditest.com>) is a structural instrumentation and monitoring company based in Colorado. They provide sensors, data acquisition equipment, monitoring software, data analysis/diagnostics, and data management services. Since the late 1980s they have contracted with local and state governments as well as private contractors and firms on many monitoring projects, both short- and long-term. In addition, the DSMO has prior experience working with BDI as they installed accelerometers on several Sunshine Skyway Bridge stay cables and a weather station in 2015. In August 2019, BDI presented a scope of work for developing the SSMS, including the development of the web portal using II. After a review by UF and the DSMO, later in 2019, BDI was brought on as a subcontractor to TY Lin, the engineering services contractor for the Sunshine Skyway Bridge, to carry out their scope of work.

Development and initial operation of the SSMS web interface was done under the branding of Platform Interactive (PI). PI was a product developed by Datum which is a part of DYWIDAG-Systems International which in turn is owned by Triton, an International Investment firm. In Fall 2020, PI was rebranded as Infrastructure Intelligence (II). As such, weblinks were also rebranded from <https://PI.DatumPlatformInteractive.com> to <https://DYWIDAG.cloud>. In addition, other related DNS names, IP numbers, email addresses related to the system (e.g., alert email addresses) changed as well. As such, going forward, references to the web interface will be referred to as II. Unfortunately, due to the previously mentioned suspension of work by the contractor BDI, a functional version of the rebranded monitoring system has not yet been made available (in addition, the PI-brand interface is also currently unavailable). Some features contained herein contain the legacy PI branding but may be referred to as II in the text. Notwithstanding the name change, it is important to note, that the rebranding effort in no way affects the back-end functionality, operation, or capabilities of the system.

## 4.2 Site Location and Access

The web address for the original PI developmental portal is: <https://pi.datumplatforminteractive.com/>. Site authentication is managed by Microsoft Azure AD (Active Directory). Access to the site is limited to those who have been authorized access by the DSMO and who have been provided credentials by BDI. Upon initial login, the user is directed to create their own password. A guide to the generic PI interface is provided in Appendix B, while a guide to the Sunshine Skyway Bridge-specific system follows.

## 4.3 Portal Components

Once credentials have been entered, users land on the Image Layout page. This page has a 3D rendering of the bridge, with markers indicating the general location of the various sensors (Figure 9). The status of each sensor is summarized to the right of the image, with the latest average, maximum and minimum value for each sensor displayed. An indicator in the upper left of each sensor summary box indicates the status of the sensor. If the sensor measurements are within the expected range and the sensor is outputting data as expected, the indicator will be a green circle. Other colors (yellow and red) indicate an issue with the sensor output.



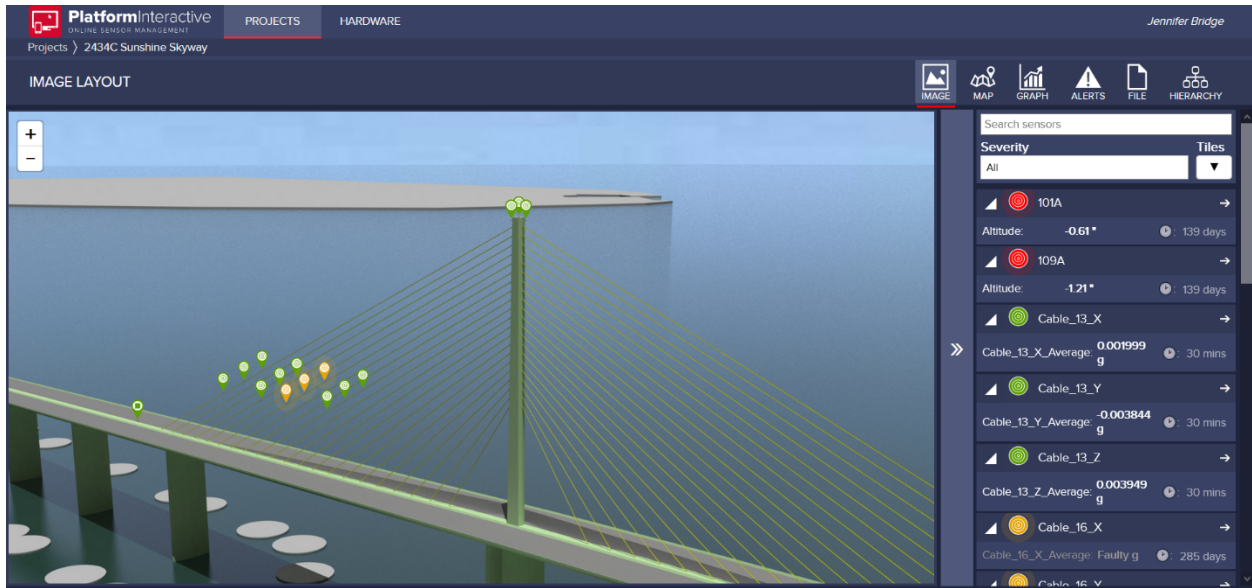


Figure 9. Landing page with rendered bridge image and sensor status details on the right.



Figure 10. Sensor selection from image marker.

When the user clicks on an image marker, the sensor label appears and the corresponding sensor information is highlighted to the right. Clicking on the left arrow of the sensor summary box brings up a small graph of the last 24 hours of the mean, maximum, and minimum values measured by the sensor (Figure 10). The status of the sensor is displayed above the small graph, indicating whether there is a potential issue with the sensor or if it has exceeded a set threshold value.

Clicking on the right arrow at the top of the sensor summary box takes the user to the Chart/Graph Layout page. This page provides a large graph of the last 24 hours of the mean sensor reading. A double arrow to the right of the graph takes the user to check boxes for all sensors mean, minimum, and maximum values (Figure 11). Once a box is checked, the corresponding data is added to the plot.



Figure 11. Data plot with sensor selection menu on right.

In addition to the Image Layout and Graph Layout pages, the user may view the sensors on a map of the structure (Figure 12), or view a listing of the sensor alert statuses (Figure 13).



Figure 12. Map Layout.

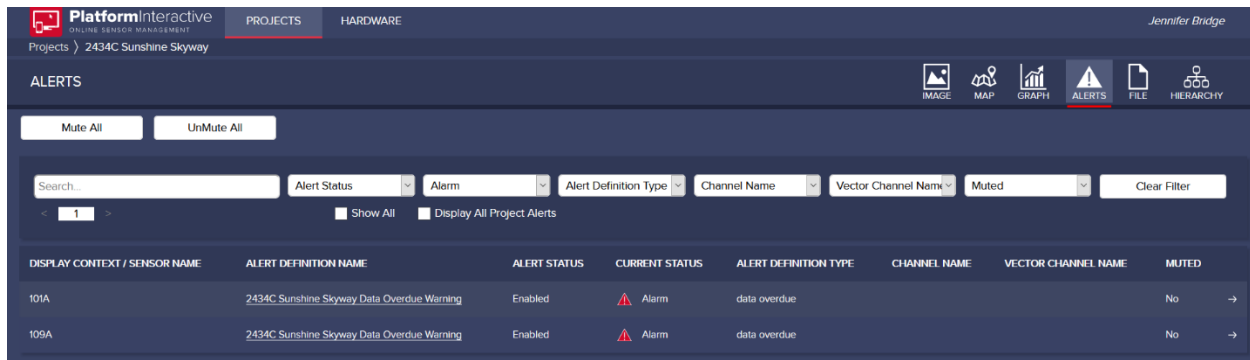


Figure 13. Sensor status alerts.

In addition to the accelerometer and environmental data, GPS data channels are also included in the portal display:

- Locations:
  - 101A: South end of the main span
  - 109A: North end of the main span
  - MS: Middle of the main span
- Three dimensions of movement are reported:
  - Altitude (vertical)
  - Northing (N-S)
  - Easting (E-W)

GPS outputs are time-averaged (currently set to 24-hours) to suppress error and improve movement estimates; this can likely be reduced to 12-hours with additional calibration. The result is that GPS measurements do not support dynamic analysis but are appropriate for monitoring slower moving processes such as motion due to seasonal temperature changes or settlement.

#### 4.4 Portal Future Development

Budget and contract challenges during this project led to some incomplete site development. It is expected that when BDI resumes their contract, these items will be addressed (outside of the scope of this task work order):

- GPS Data
  - Missing data markers for GPS sensors on Image Layout
  - Data from GPS sensors has not been available since middle of December 2020.
  - GPS data from North and South Towers is not integrated with the portal; this is likely a hardware issue with the GPS receivers.
- Reporting processed results – adding virtual channels
  - Current data reporting is limited to basic statistics (minimum, maximum, and average)
  - Cable force estimates can be calculated and reported every hour as virtual channels
  - Cable force thresholds can also be implemented
- Alert implementation



- Current alerts are only set for data availability
- Set minimum and maximum values for cable vibration, bridge movement and cable forces, based on values provided in Section 8.

## 4.5 System Configuration

At a low level, the operation of the monitoring system is handled by the data acquisition hardware located on the Bridge. Through its configuration and setup, the data acquisition computer (STS\_Core) is responsible for communicating with sensors (e.g., accelerometers) on the bridge and relaying those values to II through its fiber-based Internet connection. As such, to change or update the system configuration (change sampling, rates, adding a new sensor in the future, etc.), a system administrator must login via TeamViewer to the computer and updates settings of the STS\_Core Monitor program (Figure 14). TeamViewer facilitates connections through a broker service. A TeamViewer client installed on a computer to be accessed (e.g., the data acquisition computer) contacts a broker and registers itself. Then, if a user wishes to connect to the computer, the user contacts the broker and requests a connection to the remote computer. If the user-supplied credentials are authenticated successfully and the user authorized, then a remote display of the remote computer is provided. This approach allows access to systems which are not otherwise reachable (e.g., firewalls) through the Internet. Currently, through DSMO, BDI handles the authorization of individuals to login to this system via TeamViewer as well the role of updating the configuration settings of the Monitor. As it is not anticipated that FDOT personnel will be involved at this low-level of configuration, detailed guidelines for the using of Monitor are outside the scope of this report. If there is a need to delve into low-level operation of the system, a more detailed manual on the operation of Monitor can be obtained directly from BDI.

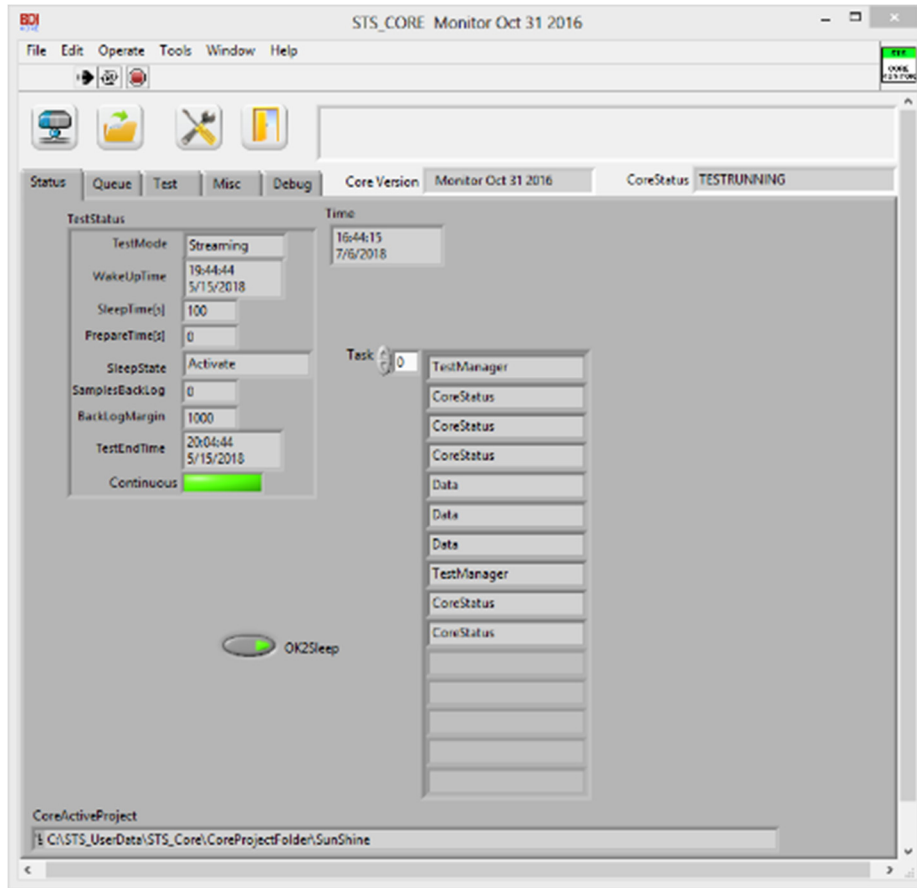


Figure 14 The STS Core Monitor application which runs on the data acquisition computer located on the Bridge.

While the current approach to connect to the data acquisition computer is through TeamViewer, it is also possible to connect via the Remote Desktop Protocol (RDP). Due to security concerns, this is not the recommend approach; however, it is an option worth documenting in case there are issues with the recommended TeamViewer application.

To establish an RDP connection, it is necessary to be connected to a network which is allowed to communicate with the data acquisition computer. To this end, a Virtual Private Network (VPN) has been setup by ITS and Lucent (as part of a maintenance contract) to allow connections to the Bridge network. After authorization is provided by DSMO, ITS provides login credentials to permitted individuals. With credentials in hand, a VPN client (e.g., SonicWall Mobile Connect or NetExtender Client) is then started on a user's local computer and the credentials supplied. At this point, the user can then open a remote desktop session to the server by entering the IP address of the data acquisition computer on the Bridge fiber network (Figure 15). Once connected to the VPN and logged into the computer on the bridge, the user will see the STS\_Core application, which is the BDI software used to collect the data (Figure 16), in which system modifications may be made. Login credentials to the data acquisition computer itself are supplied by BDI after authorization by the DSMO.

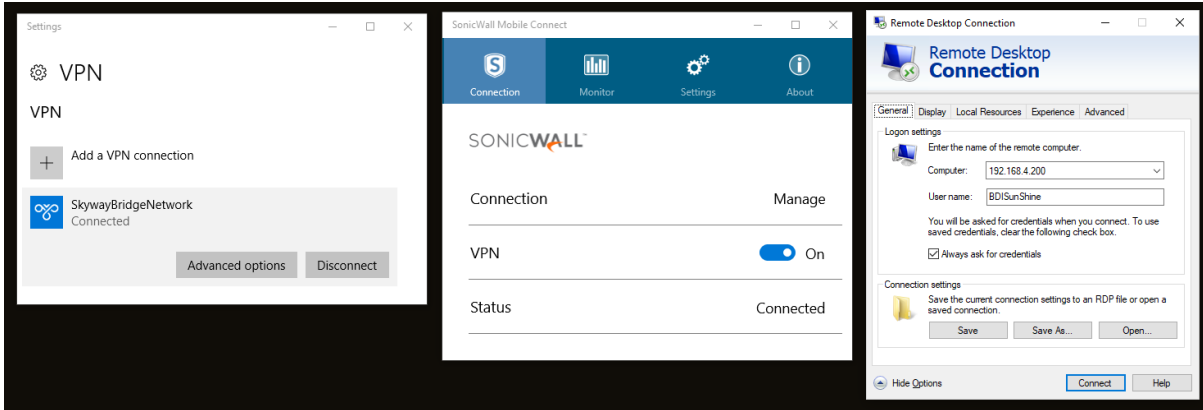


Figure 15. Screen capture of the VPN client and Remote Desktop Connection to the Skyway Bridge computer.

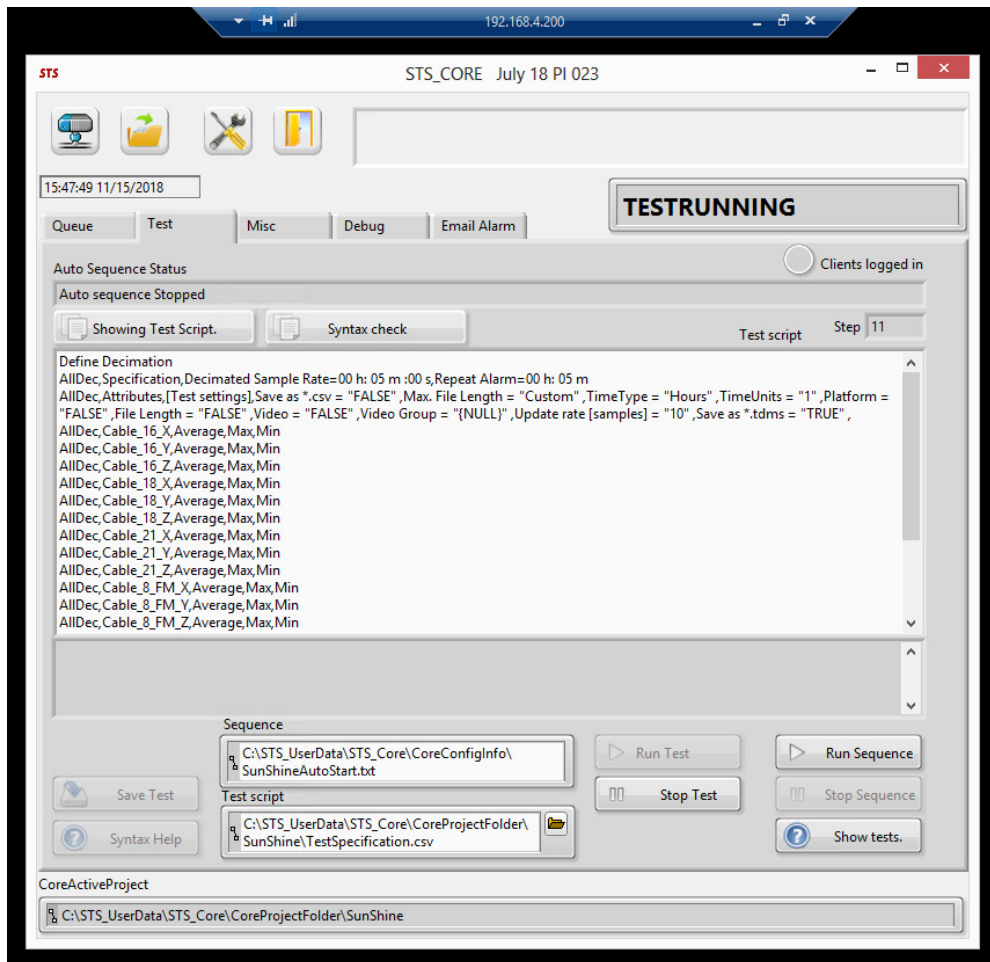


Figure 16. Screen capture of the STS\_Core application running on the Skyway Bridge computer, accessed via Remote Desktop Connection

The operating system installed on the Core is Microsoft Windows Embedded 8 (Version 6.2 – Build 9200) and it is licensed to BDI (although ownership of the computer itself belongs to FDOT). This version of Windows is vulnerable to the CredSSP “Remote Code Execution” vulnerability (CVE-2018-0886 <https://cve.mitre.org/cgi-bin/cvename.cgi?name=CVE-2018-0886>). As this version of Windows is used by all BDI’s monitoring sites, it has gone through numerous compatibility checks and testing, as such, upgrading or updating the BDI data acquisition computer would not be a simple process (but is possible). The CredSSP vulnerability affects all recent versions of Windows and, as such, has been remediated through patches provided by Microsoft (<https://portal.msrc.microsoft.com/en-US/security-guidance/advisory/CVE-2018-0886>).

Unfortunately, due to the nature of the patch, any Windows computer which has been patched for this vulnerability is prohibited from connecting via RDP to an un-patched computer. If necessary, several workarounds are available to circumvent these restrictions and access the computer via RDP. As these workarounds require Windows registry changes which can compromise the security of the local machine, they are outside the scope of this report.

As described previously, low-level configuration (individual sensor configuration, sample rates, etc.) is achieved through modification of systems running on the data acquisition computer that the FDOT physically owns and has direct access to. Medium- (e.g., backend services and analysis scripts) and high-level (e.g., web interface) configuration takes place on cloud-based systems owned or managed solely by the contractor, BDI. It is not anticipated the FDOT will ever have a need to directly interface with configuration-related functionality that II provides. As such documentation on these systems use and operation is not provided in this report. Should there ever be a need to, for example, add new data processing technologies, a contract with BDI would need to be established. Although the current system architecture is not expected to change, should the cloud-based resources ownership ever be transferred back to the FDOT, BDI would be able to provide necessary manuals and instruction in their use at that time.

## 5 Data Processing

This section describes how the bridge-collected data is stored, extracted, and analyzed to assess the system functionality and determine bounds of typical bridge responses.

### 5.1 Hourly Data Extraction

All data processing was done in MATLAB (see Appendix D for source code). MATLAB code (`unzip_process_writetofile.m`) was created to automatically extract and process all weekly data files in a specific directory (or within specific date ranges as needed) and generate the data summary file for the period of data analyzed. A weekly zip file is approximately 5GB and contains approximately 168 hourly tdms data files. The data extracted to the summary file for each hour of data includes:

- All channels:
  - Mean
  - Standard deviation
  - Root mean square (RMS)
  - Maximum (absolute)
- For all acceleration channels:
  - First natural frequency
- For cable accelerometer channels (X, Y, and Z axis per location):
  - Cable tension estimate
  - Slope of the linear fit of the cable frequencies for estimating tension
  - $R^2$  (measure of how well the linear fit matches the frequencies plotted vs. frequency number for estimating tension [0,1]).

If any channel was empty for a given data record, zeros were inserted to provide uniform output in the summary file.

#### 5.1.1 Accelerometer Processing

All acceleration values are detrended. Detrending subtracts a best-fit straight line from the one-hour data record to eliminate the mean and any drift, which cause errors in natural frequency and tension estimation. Natural frequencies were determined by picking peaks in the power spectral density (PSD) of each hour-long acceleration record.

#### 5.1.2 Force Estimation

Cable tensions may be estimated from frequency analysis of the cable vibration data (Kim and Park, 2007). Assuming the cables act as a flat, taut string and neglecting sag and bending stiffness, tension,  $T$ , can be calculated as:

$$T = 4mL^2 \left( \frac{f_n}{n} \right)^2 \quad (1)$$

where  $m$  = cable mass density

$L$  = effective cable length

$f_n = n^{\text{th}}$  natural frequency

Accounting for bending stiffness results in the following relationship (Kim and Park, 2007):

$$\left(\frac{f_n}{n}\right)^2 = \left(\frac{1}{4mL^2}\right)T + \left(\frac{n^2\pi^2}{4mL^4}\right)EI \quad (2)$$

where  $EI$  = flexural rigidity of the cable

This equation (2) results in a linear relationship between  $\left(\frac{f_n}{n}\right)^2$  and  $n^2$  where the intercept is proportional to  $T$ . Linear regression is used to estimate the intercept,  $b$ , and  $T = 4mL^2b$ .

The values used for cable lengths and mass densities (Table 3) were taken from Bridge Engineering Solutions (BES) cable testing reports provided to D7 (BES, 2010; BES, 2012; BES, 2015). Note that BES used a single frequency for their analysis but did not provide specific equations in their reporting. In estimating mass density, previous studies used two different grout densities: 110 lb/ft<sup>3</sup> based on a 1999 estimation and 124 lb/ft<sup>3</sup> based on 2003 material sampling. The results calculated in the current study use 110 lb/ft<sup>3</sup>. to be consistent with the majority of the previous studies (comparison results are presented in Section 6.3).

Table 3. Cable properties used in analysis (from BES cable analysis reports).

	<b>Cable 13</b>	<b>Cable 16</b>	<b>Cable 18</b>	<b>Cable 21</b>
Mass Density (kg/m)	145.631	145.162	146.229	143.651
Length (m)	128.661	152.349	167.530	190.398

Data collected on April 27, 2020, at 2pm EDT is used to illustrate the data processing approach to estimate the force in Cable 13 using the Z-axis acceleration measurements. The detrended acceleration record (Figure 17) is converted to a frequency domain PSD (Figure 18). Fundamental frequencies are determined by the locations of the peaks in the PSD plots, indicated with red circles (Figure 18) and are found using a MATLAB peak picking algorithm. The algorithm uses two user-specified parameters to ensure accurate peak selection: 1) minimum peak distance that specifies the minimum distance between peaks and 2) minimum peak prominence that specifies the minimum value that may be considered a peak. The two parameters were set to different values for different cables and optimized for accurate peak detection.

Note that the frequency peaks used in force estimation are all less than 30 Hz, indicating that a lower sampling rate than 200 Hz may be used. A rule of thumb is to sample at least 2.5 times the highest frequency of interest. In this case, a sampling rate of  $25 \text{ Hz} \times 2.5 = 62.5 \text{ Hz}$ . This reduction in sampling rate would result in 69% reduction in the amount of data stored.

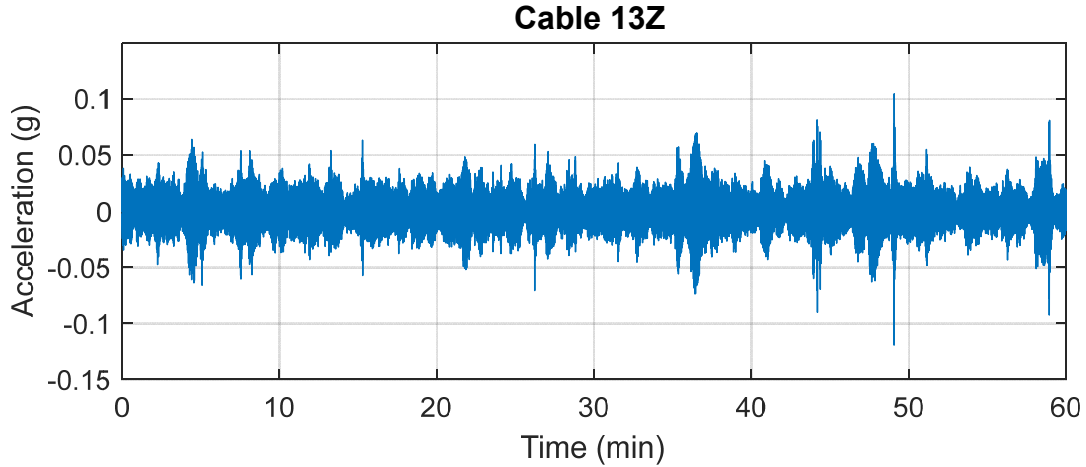


Figure 17. Acceleration measured in the Z-direction for Cable 13 over a one-hour period on April 27, 2020, at 2pm.

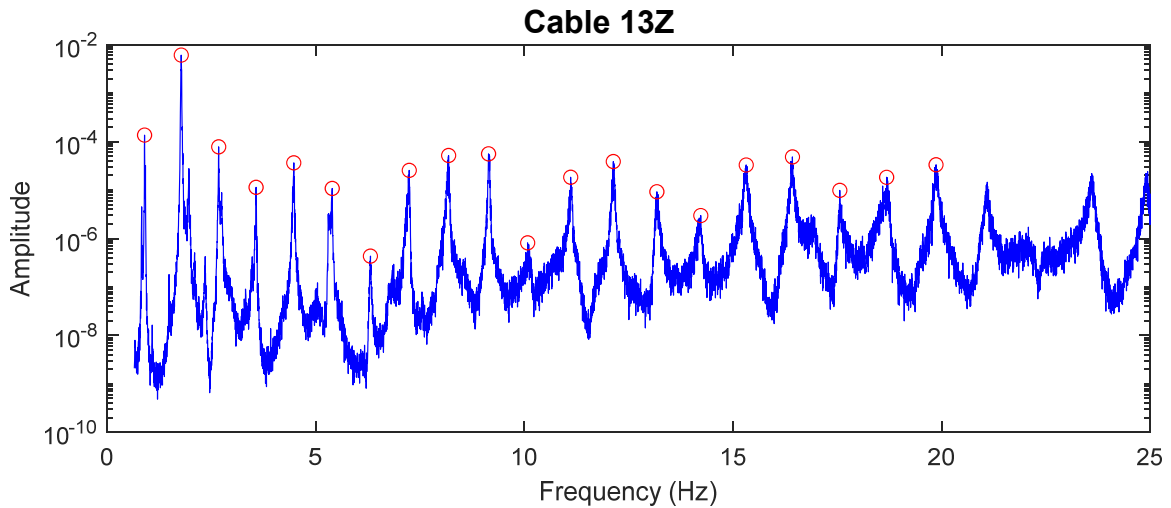


Figure 18. Power spectral density (frequency domain) representation of the Cable 13Z acceleration measurement and identified first 20 peaks (red circles).

For each of the first 12 peaks,  $\left(\frac{f_n}{n}\right)^2$  is plotted versus  $n^2$  (Figure 19). A matrix approach to linear regression was used to calculate a first order best-fit approximation. The intercept of the linear regression provides a value proportional to the tension estimate according to Equation 2. The corresponding  $R^2$  value was also calculated to provide a measure of how well the linear regression fit the frequency data.

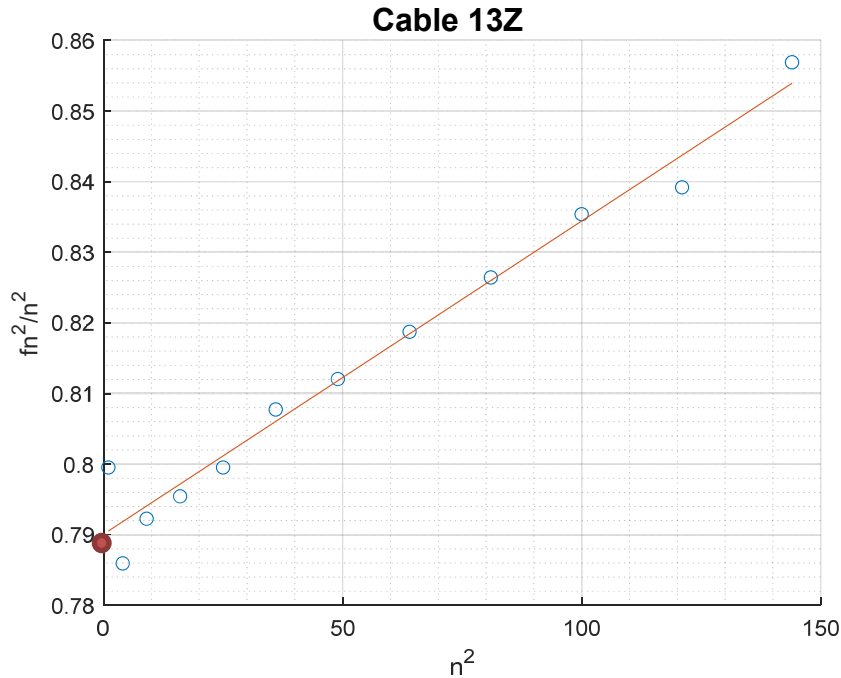


Figure 19. Linear regression of the relationship between the frequency peaks,  $f_n$ , and their corresponding frequency number,  $n$ , for Cable 13Z acceleration.

## 5.2 Processing One Year of Hourly Summary Data

MATLAB code (`SummaryPlots.m`) was created to read the summary file and generate plots, statistics, and thresholds for a full year of data.

Erroneous data, usually in the form of outliers in the measurements, are values that are not representative of a physical event. The source of the errors/outliers is typically a fault in the measurement system and will often be obviously incorrect (e.g., a physically impossible value or unreasonable shift in values). However, some outliers may represent a physically possible response due to an anomalous event on the structure. Cleaning measurement errors from the data should not eliminate possible responses to real, extreme events.

Non-physical outliers were removed from the data by setting response bounds indicated in Table 4.

Table 4. Bounds for elimination of measurement errors.

Measurement Value	Units	Minimum	Maximum
Hourly mean temperature	°F	15	120
Hourly mean and hourly maximum wind speed	mph	0	250
Hourly mean wind direction	degrees	0	360
Hourly RMS and hourly maximum acceleration	g	0	1
Cable force	kip	0	5000
Cable force $R^2$ fit	--	0	1
Cable and tower first natural frequency	Hz	0	100



For most hourly summary values, no data was removed. For the working sensors, the percentage of data eliminated due to being out of bounds is shown in Table 5. Excluding wind direction, these percentages amount to only one or two data points removed over the one-year analysis period.

Table 5. Percent of data points removed for being out of the bounds provided in Table 4.

<b>Hourly Summary Value</b>	<b>Percent Out of Bounds</b>
Mean temperature	0.01
Wind direction	1.6
Mean wind speed	0.01
Maximum wind speed	0.0
Cable 13Y force	0.01
Cable 13Z force	0.03
Cable 18Y force	0.03
Cable 18Z force	0.03
Tower Y maximum acceleration	0.01

The accuracy of the cable force estimates is highly dependent on the regression fit. Vibration amplitudes that are too low or measurements with too much noise or mean-value drift result in poor regression fits indicated by lower  $R^2$  values. As a result, cable tension estimates were eliminated (not reported) if the corresponding  $R^2$  values were below thresholds established by analysis of one year of data. The minimum  $R^2$  thresholds set for the working cable accelerometers are 0.89 for both Cable 13 and 0.79 for Cable 18. For the 2020 data, the percent of cable tension estimates that were eliminated from the remaining data due to low  $R^2$  values were:

- Cable 13Y: 21.9%
- Cable 13Z: 15.6%
- Cable 18Y: 6.0%
- Cable 18Z: 14.6%

The Cable 13 tensions have a higher  $R^2$  threshold, resulting in fewer retained tension values; however, lowering the Cable 13  $R^2$  threshold resulted in a high number of erroneous tension estimates. The reason for the higher incident of errors in the Cable 13 force estimates is not clear as there is no evident correlation with acceleration levels, wind speeds, calculated natural frequency, time of day, or temperature.

Even with non-physical or obviously erroneous data removed, a very small number of data points remain in some channels that appear to be incorrect when compared with adjacent measurements in the same data channel (i.e., they are physically unlikely while being physically possible). During routine monitoring, these data will be assessed by the engineer reviewing the response data and a judgement on the data validity will be made (as discussed in the Alert Response Plan).

## 6 Analysis Results

### 6.1 Environmental

The mean hourly temperature recorded on the bridge during 2020 follows an expected seasonal variation (Figure 20). The minimum recorded hourly mean temperature was 34.3°F early in the morning on January 22, 2020, and the maximum mean hourly temperature was 87.1°F on the afternoon of June 26, 2020. Figure 21 illustrates the expected daily fluctuations in temperature in the data from a representative six days between July 27 and August 2, 2020.

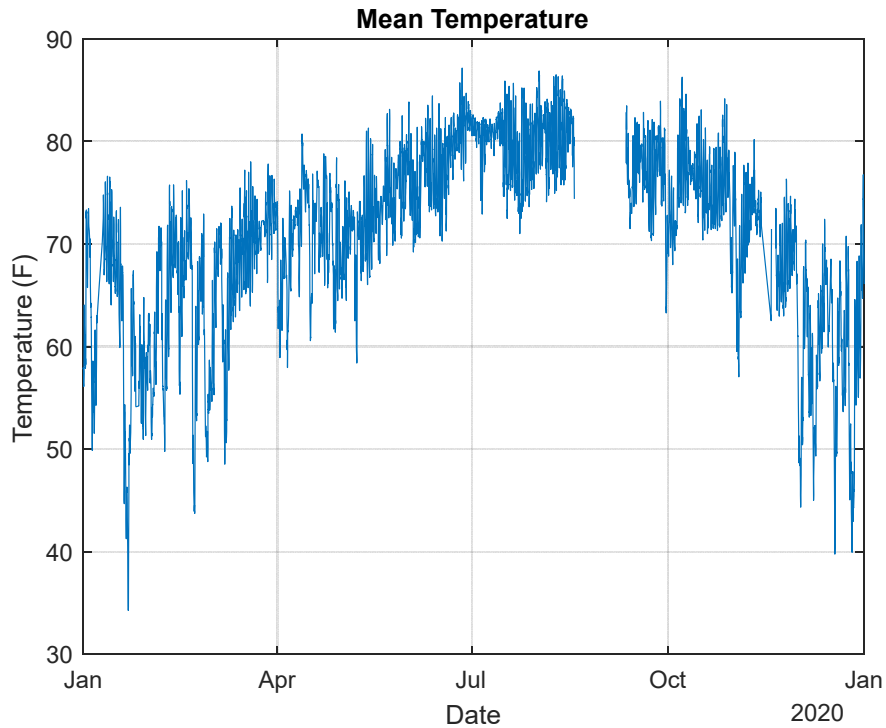


Figure 20. Hourly mean temperatures during 2020.

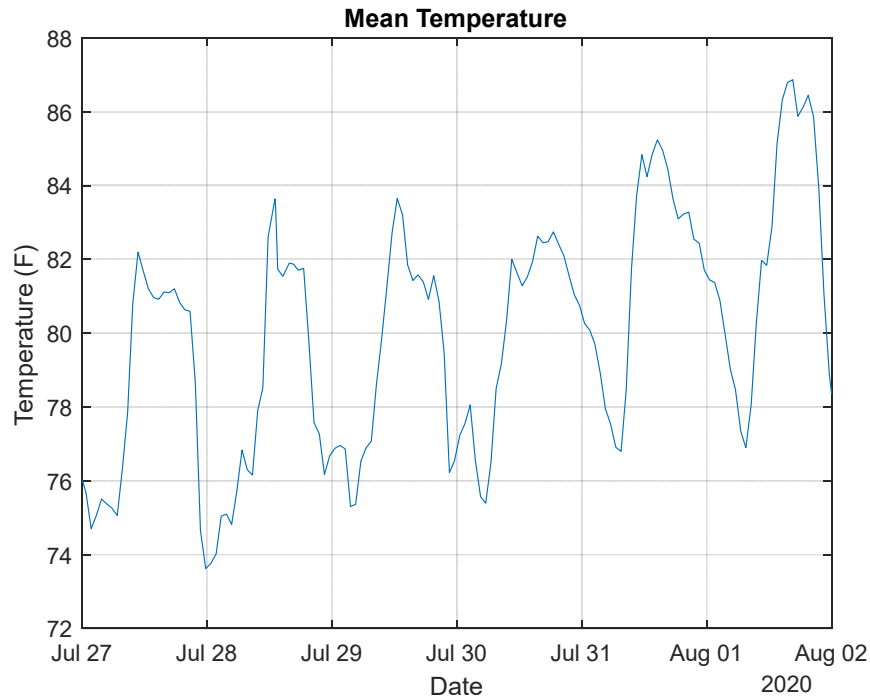


Figure 21. Representative hourly mean temperature variation for a six-day period.

The hourly mean wind speed, hourly maximum wind speed, and hourly mean wind direction recorded in 2020 are shown in Figure 22. The wind direction varies from 0 to 360°; however, the values indicated in Figure 23 do not quite reach the extreme values as each data point represents a mean of an hour of wind direction measurements. Figure 23 shows the variation of the wind speed and direction over six days.

The maximum hourly mean wind speed was 50.9 mph on November 11, 2020, when Tropical Storm Eta passed nearby. The same day the maximum wind speed reached 72 mph. A maximum wind speed of 82.7 mph was recorded during the 9am hour of September 11, 2020. There was no weather event at that time to explain this high reading. Upon review of the full hour data record for that day, several spikes in the measurements are observed that are clearly measurement error (Figure 24). TransCore was performing maintenance on the system, and it was restarted shortly after this data was observed. This maintenance is the likely source of the measurement errors. This instance provides an example of measurement outliers that were not removed by automated bounding but can be subsequently removed upon review. The likely true maximum recorded wind speed on the bridge in 2020 was 76 mph on the evening of December 24, 2020, during a strong thunderstorm.

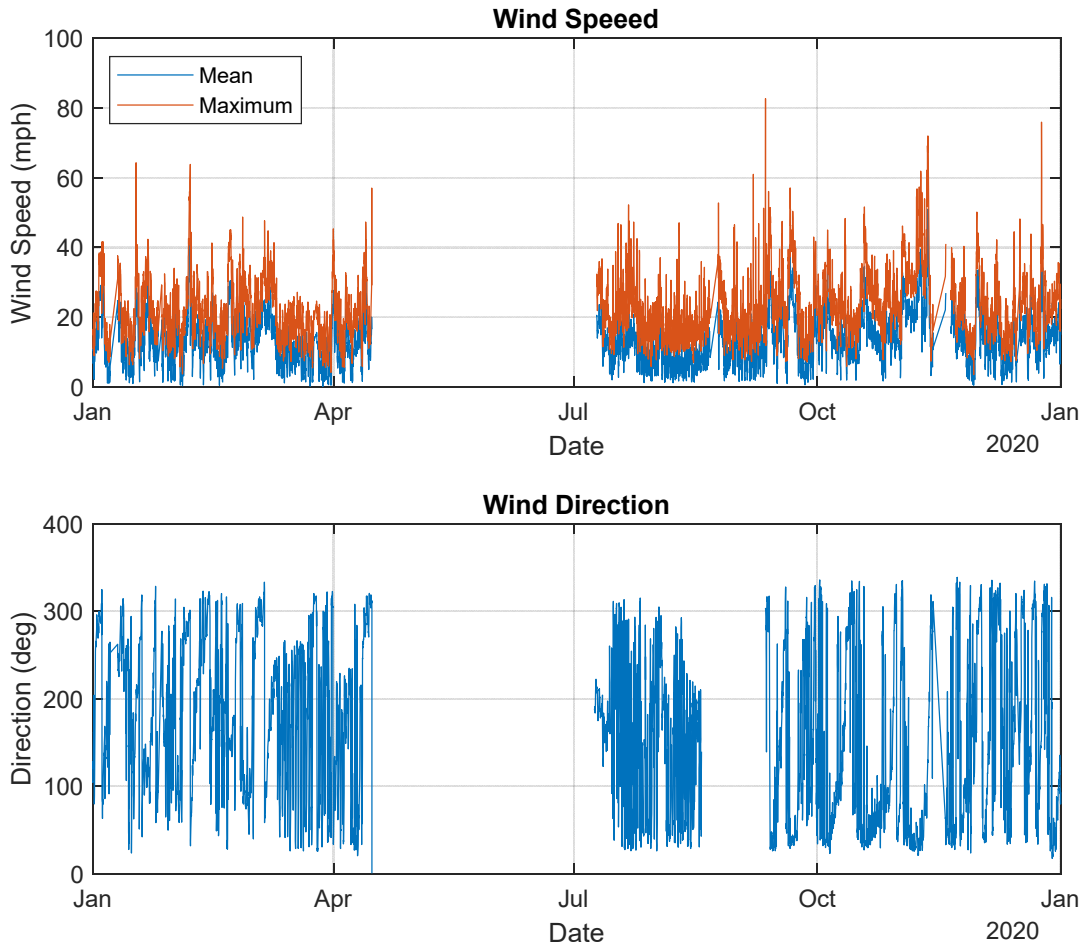


Figure 22. Hourly wind speeds (mean and maximum) and wind direction.

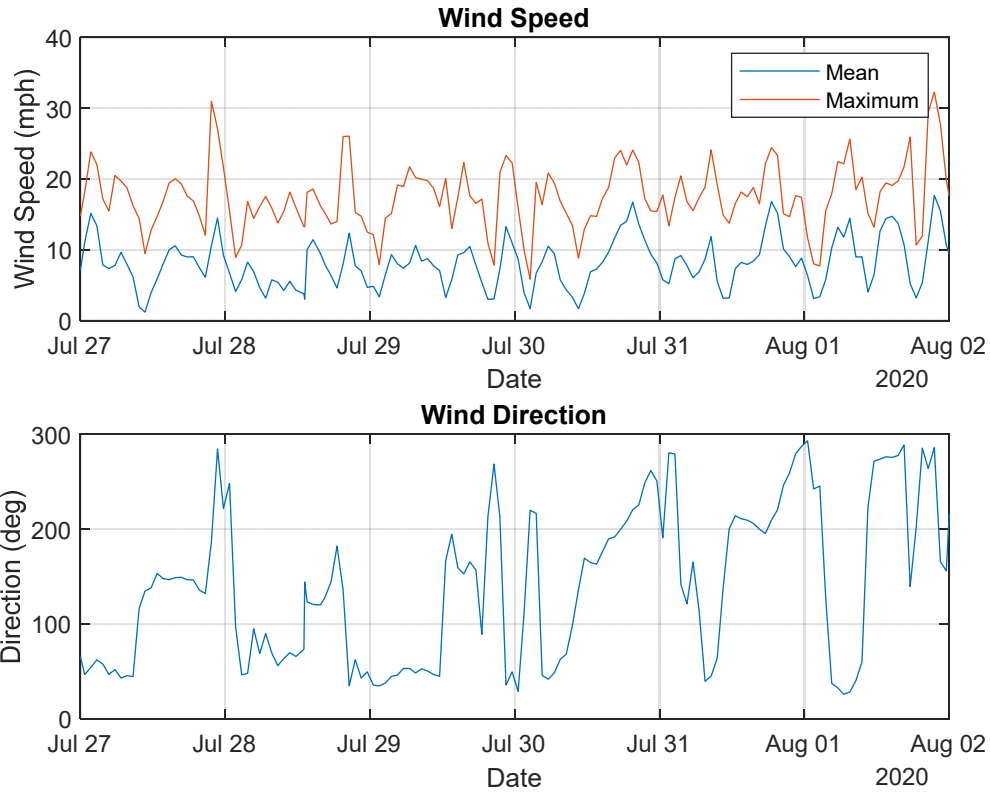


Figure 23. Representative hourly mean and maximum wind speeds (top) and hourly mean wind directions (bottom) over six days.

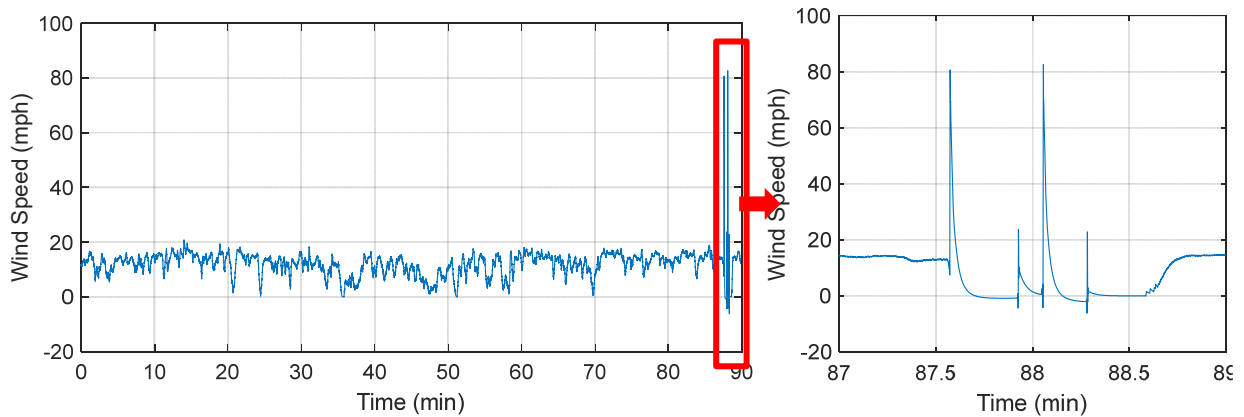


Figure 24. High wind speed readings on September 11, 2020 (left) with detail (right) showing spikes likely indicating a measurement error.

## 6.2 Acceleration

### 6.2.1 Year Summary Plots

The one-year maximum acceleration record represents the maximum value recorded during each one-hour measurement period. The root mean square, or RMS, acceleration provides a measure of the amplitude of the acceleration over a given hour of data. Figure 25 and Figure 26 show the hourly RMS and maximum acceleration measured in the Y and Z directions on Cables 13 and 18, respectively. Besides rare outliers (see discussion in subsequent section), peak cable accelerations did not exceed 0.3g while RMS accelerations stayed below 0.035g throughout the year. Accelerations at the top of the North Tower are shown in Figure 27. Figure 28 shows the same data but is truncated in the Y axis to better illustrate the variation in the acceleration. In general, the tower accelerations are an order or magnitude lower than the cable accelerations, with maximum values rarely exceeding 0.04g.

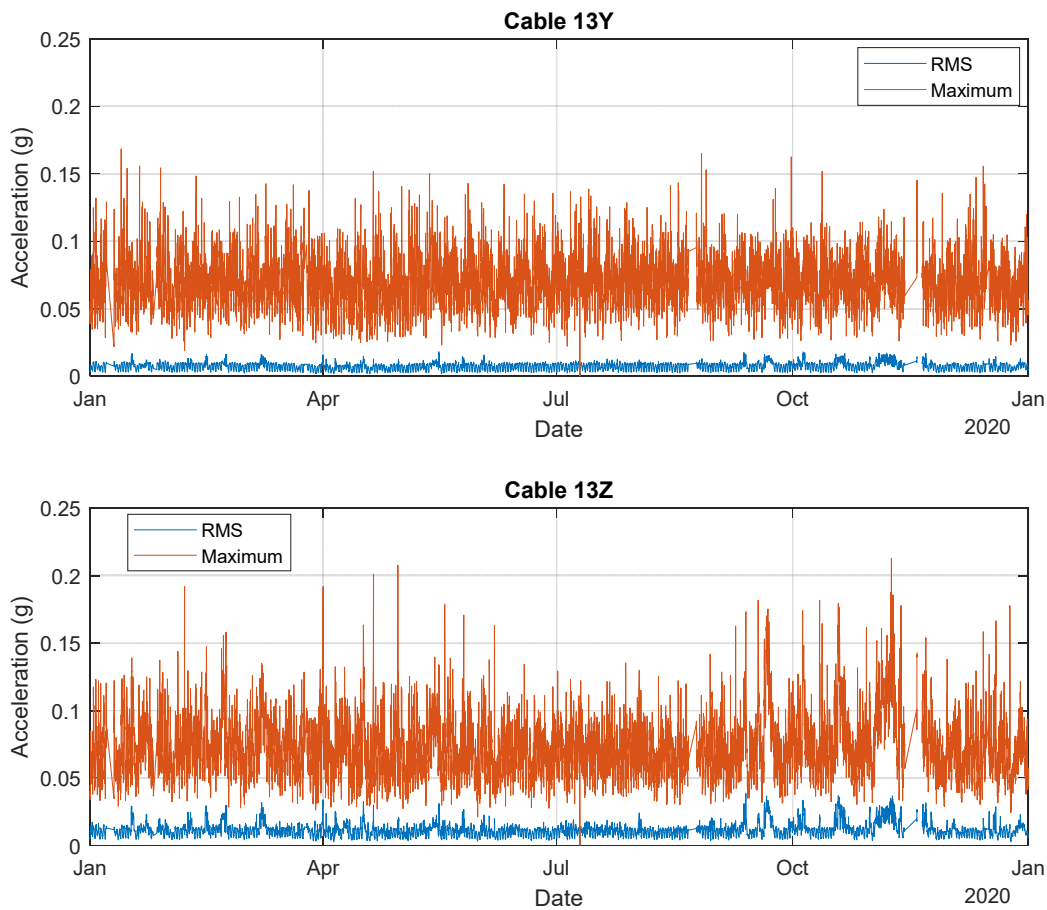


Figure 25. Cable 13 hourly maximum and RMS accelerations recorded in 2020 in the Y- and Z-directions (top and bottom, respectively).

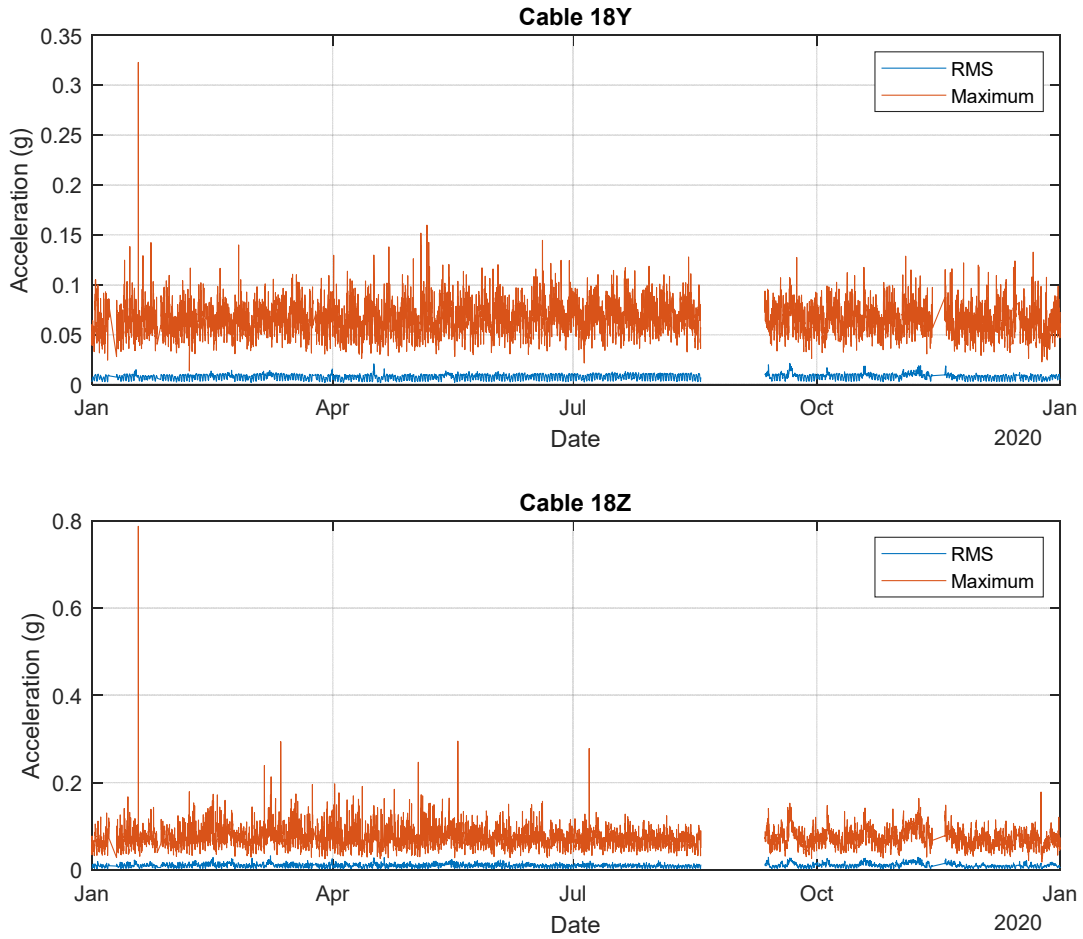


Figure 26. Cable 18 hourly maximum and RMS accelerations recorded in 2020 in the Y- and Z-directions (top and bottom, respectively).

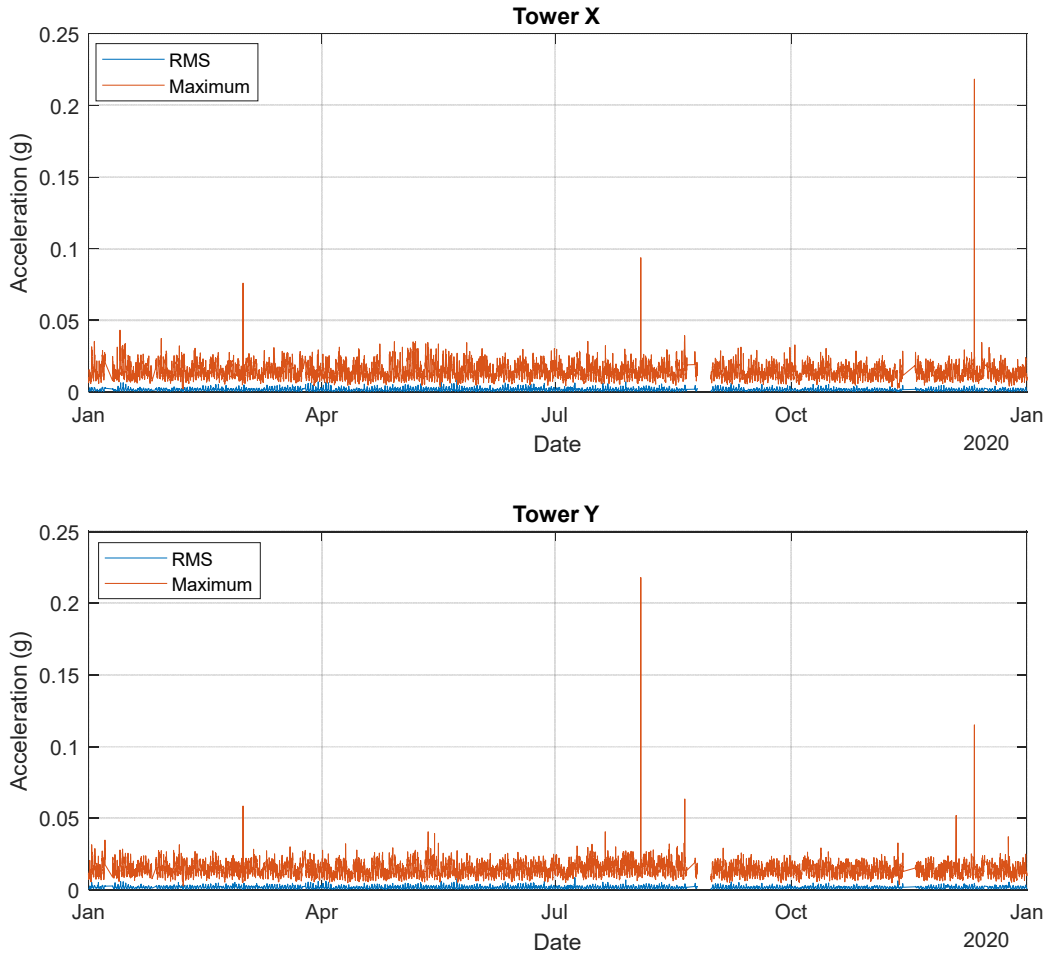


Figure 27. Tower hourly maximum and RMS accelerations recorded in 2020 in the X- and Y-directions (top and bottom, respectively).



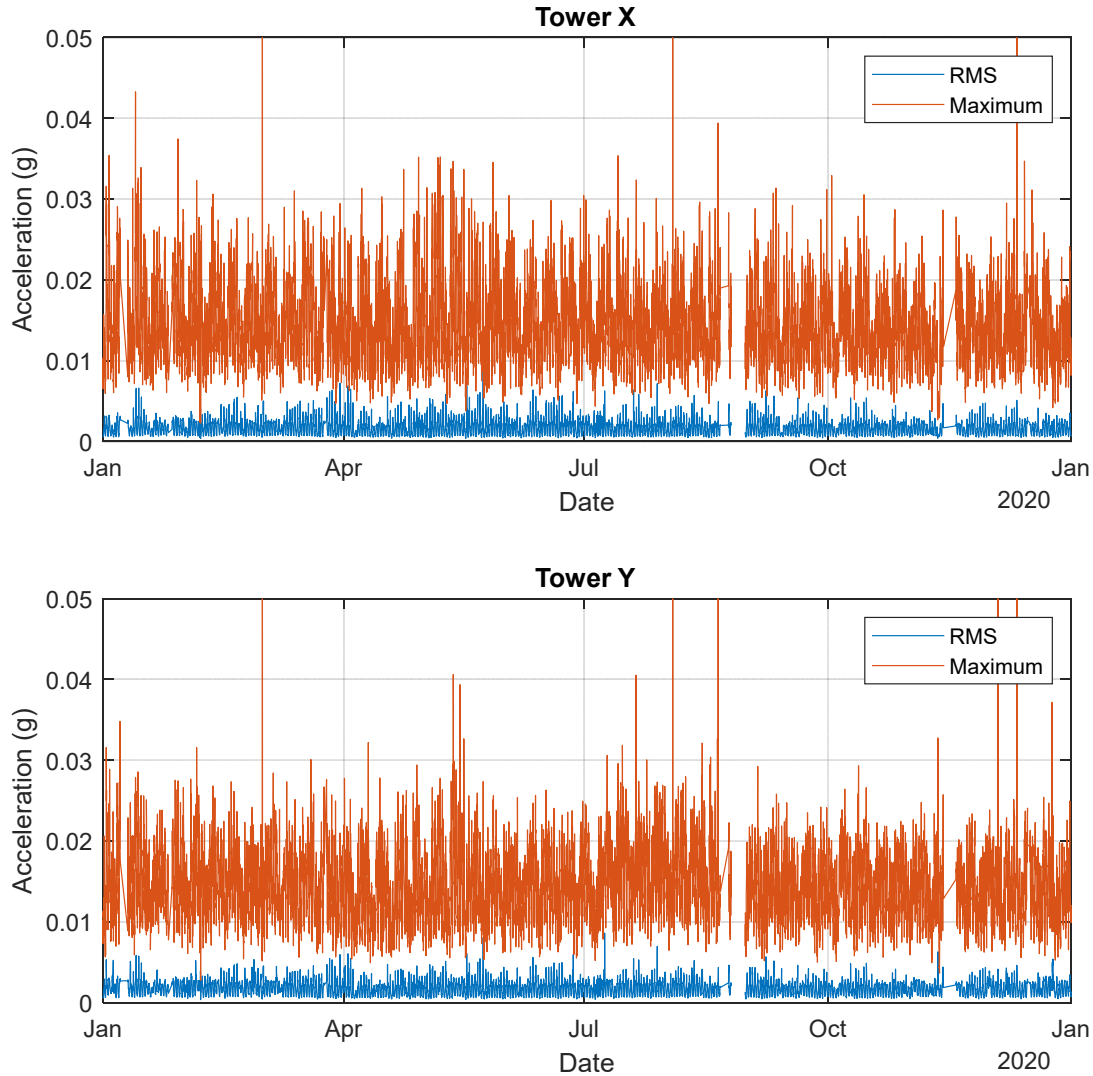


Figure 28. Tower X- and Y-acceleration, zooming in below data spikes to observe weekly acceleration variations.

### 6.2.2 Representative Six-Day Plots

Due to the influence of traffic on cable accelerations, clear trends can be observed in six-day snapshots of the hourly acceleration data. Figure 29 through Figure 34 show the hourly RMS and maximum acceleration on Cables 13 and 18 and the North Tower from Monday, July 27 to Sunday, August 2, 2020. A clear pattern of lower values during the night and higher values during the day can be observed. One exception to this pattern is a higher-than-expected cable RMS values late on July 28 and August 2 when the wind speed increases (as seen in Figure 23). The tower accelerations also increase to higher levels between noon and 2pm – more pronounced on some days than others. The reason for this increase may be attributed to sensitivity of the tower motion to temperature changes.

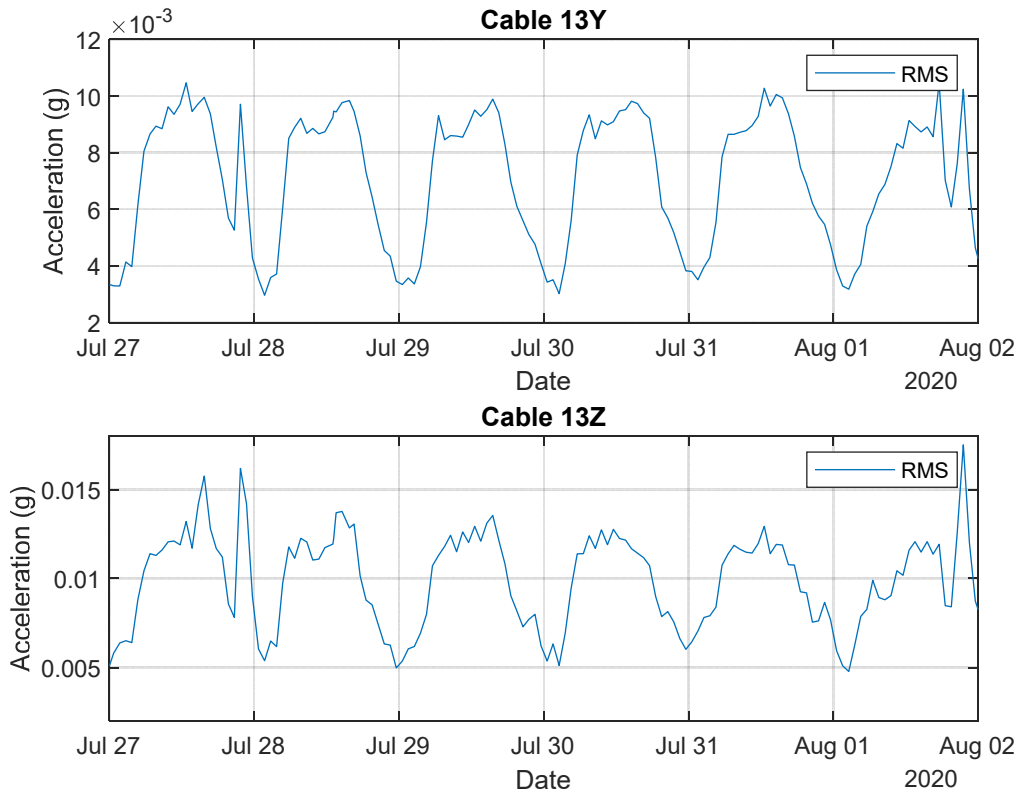


Figure 29. Six days of hourly Cable 13 RMS acceleration measured in the Y- and Z-directions (top and bottom, respectively).

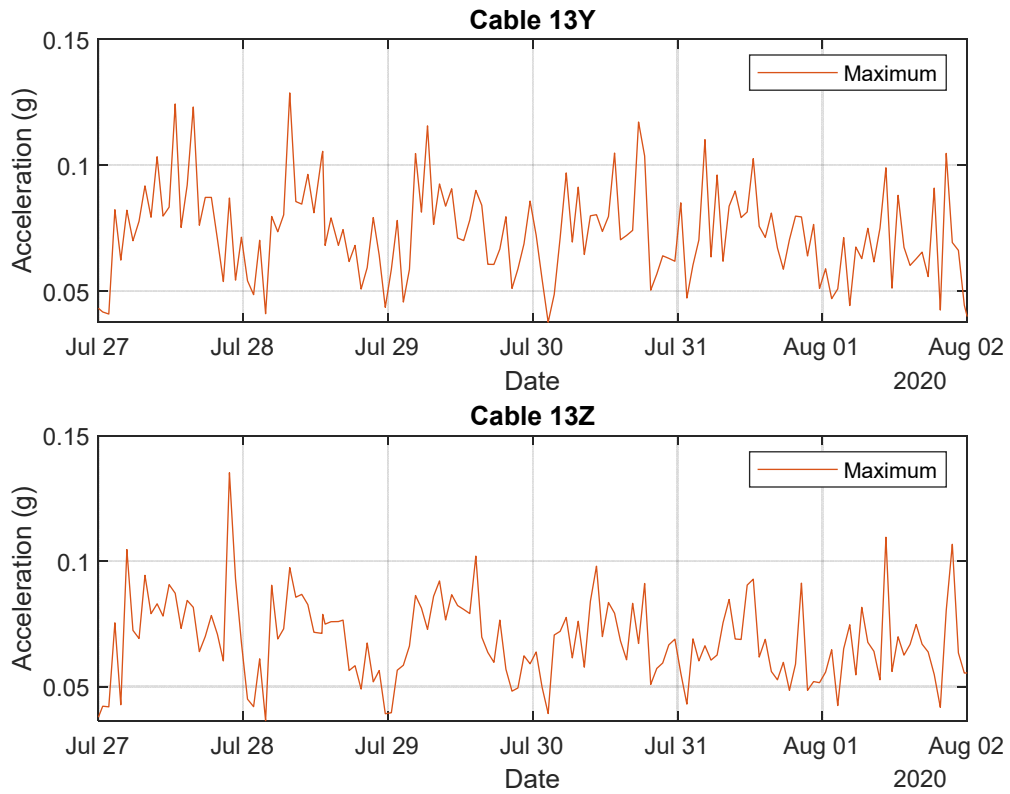


Figure 30. Six days of hourly Cable 13 maximum acceleration measured in the Y- and Z- directions (top and bottom, respectively).

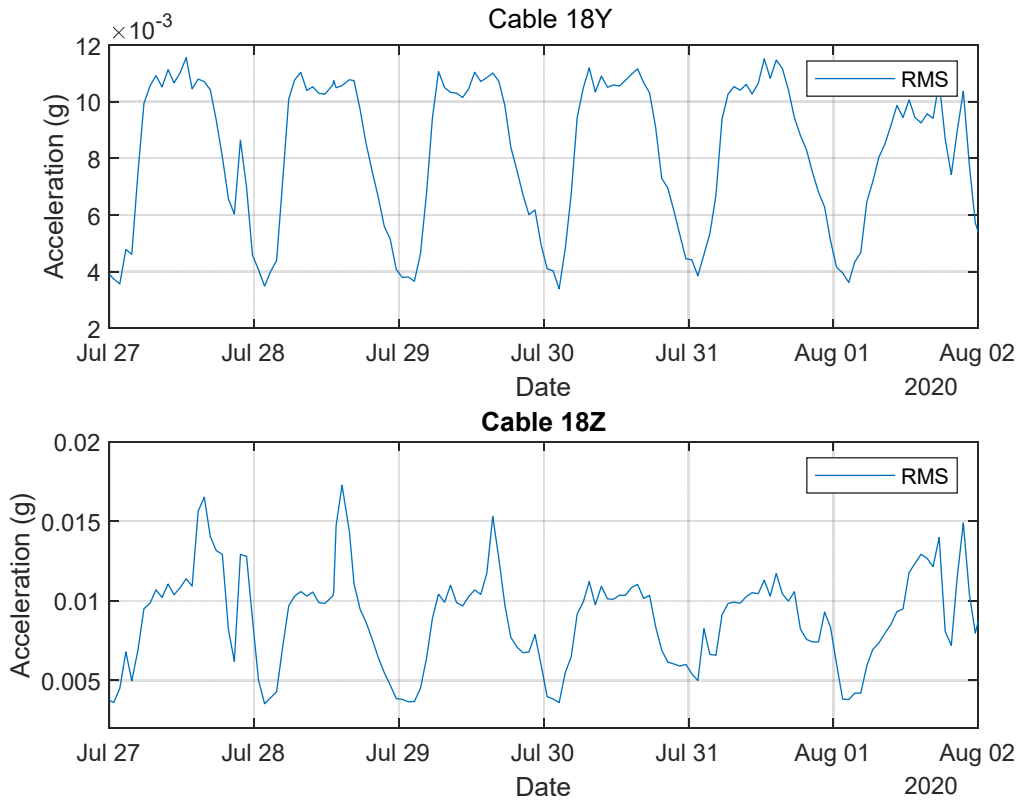


Figure 31. Six days of hourly Cable 18 RMS acceleration measured in the Y- and Z-directions (top and bottom, respectively).

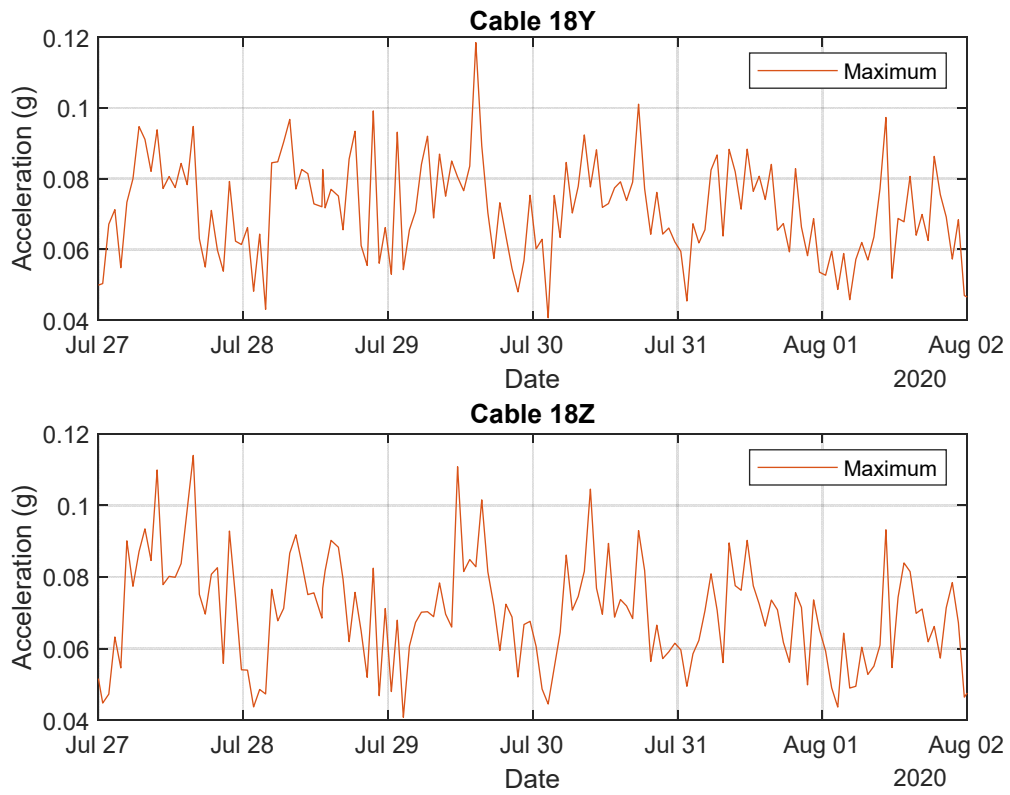


Figure 32 Six days of hourly Cable 18 maximum acceleration measured in the Y- and Z- directions (top and bottom, respectively).

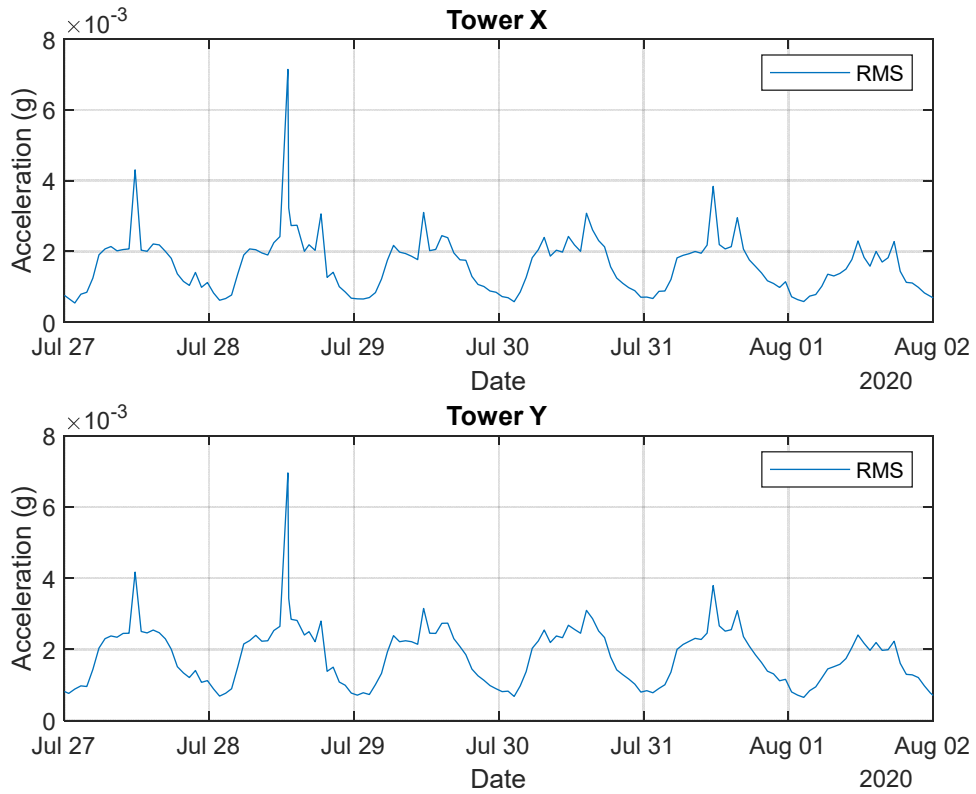


Figure 33. Six days of hourly North Tower RMS acceleration measured in the X- and Y-directions (top and bottom, respectively).

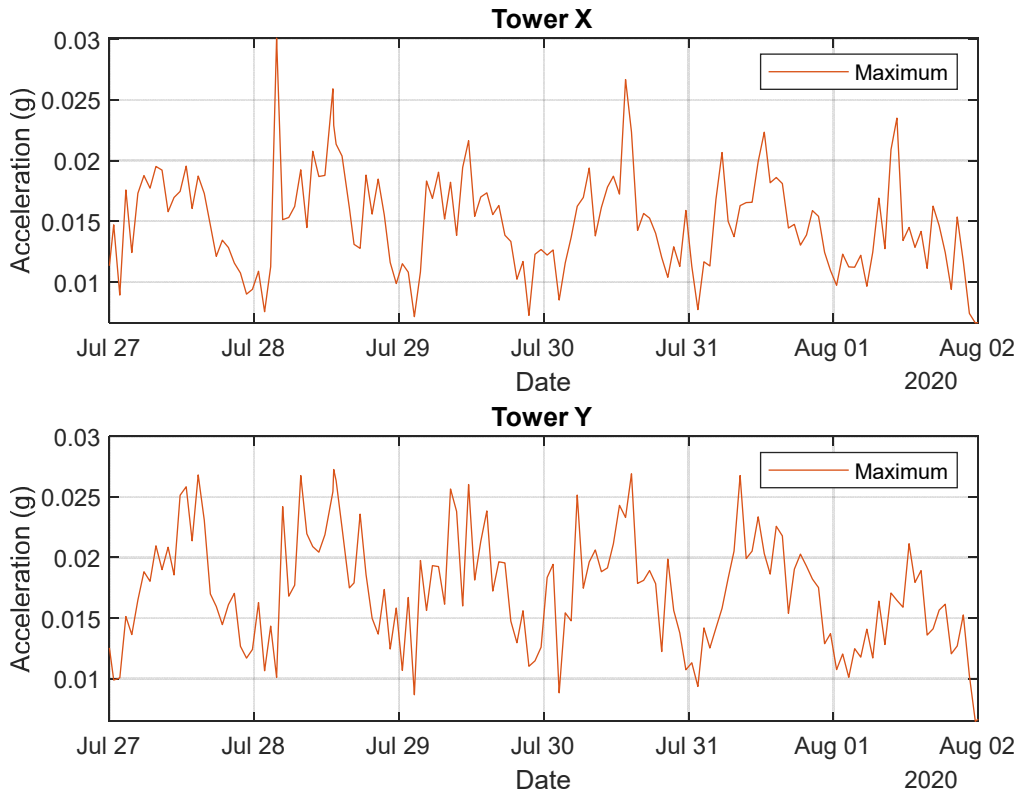


Figure 34. Six days of hourly maximum North Tower acceleration measured in the X- and Y-directions (top and bottom, respectively).

### 6.2.3 Examination of High Measurements

While non-physical outliers in the data have been removed according to the procedure outlined in Section 5.2, some additional high values remain that warrant further attention. High hourly maximum values are examined by looking at plots of the full high-speed data record for the hour.

For Cable 18, high maximum accelerations ( $\sim 0.8g$  in the Z-direction) were recorded in the hour-long dataset recorded starting at 1:51pm on January 18. Figure 35 shows clearly shows the high acceleration measurement during the hour-long record, while Figure 36 provides a zoomed in view. The maximum values are one or two data points and do not exhibit the decaying, periodic vibration expected when the cable is subject to an external impulse excitation. These results may indicate a measurement error but there is not enough information to conclusively determine the source of the measurement spikes. At only a few data points ( $<10$  ms), this type of acceleration is not a danger to the structure, should it be a real measurement result.

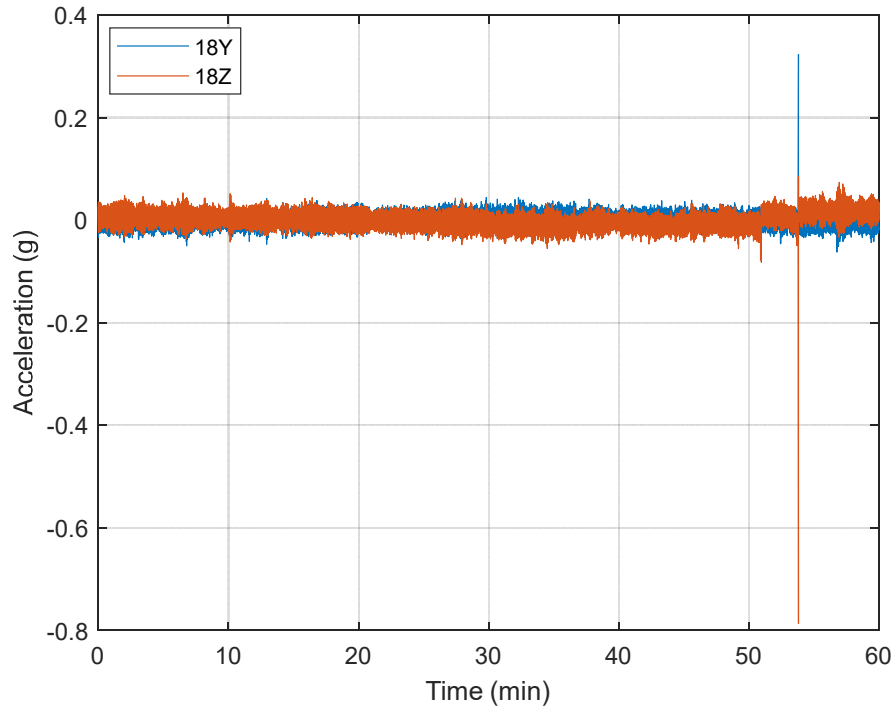


Figure 35. Cable 18 acceleration recorded January 18, 2020, with the record starting at 1:51 pm.

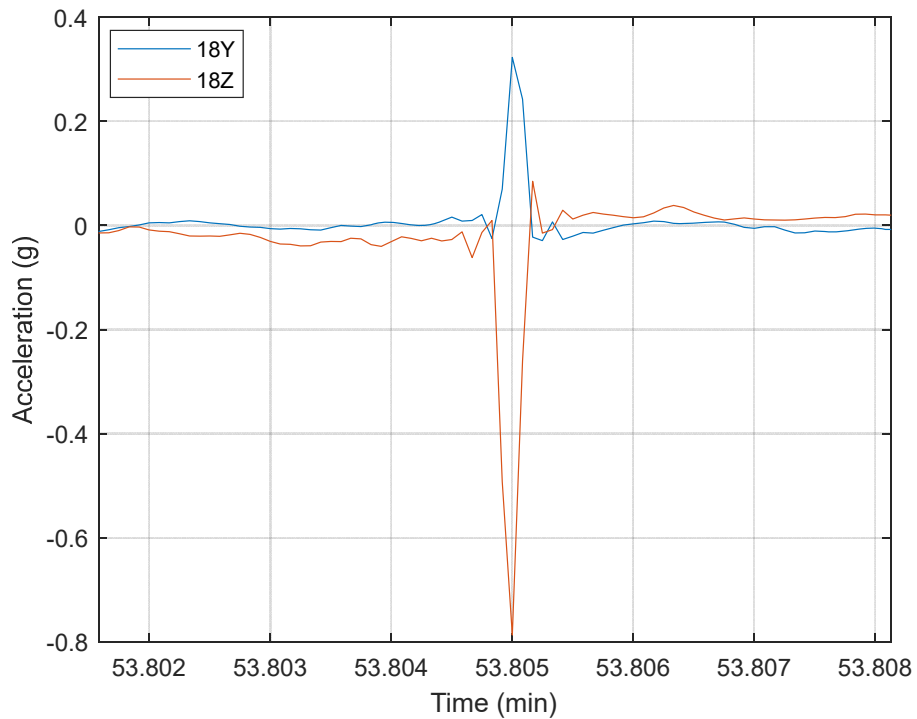


Figure 36. Cable 18 acceleration recorded January 18, 2020, zoomed in on high value measurement.



Figure 27 shows several data spikes in the maximum tower acceleration. The high-speed data record for March 1 starting at 5:54am EST is shown in Figure 37 with zoomed in regions shown in Figure 38. The data spikes are followed by periodic, decaying amplitude vibration, indicating a real physical event and response. The Skyway 10k race occurred during this time so activities on the bridge, including reports of maintenance personnel on the tower, seem to have caused a disturbance of the accelerometers (e.g., a person tapping the structure nearby or AC interference). The frequency of the rapid vibration is approximately 50 Hz – much higher than the fundamental frequencies of the tower – indicating a very localized excitation. Similar behavior is observed in data spikes recorded on August 3 (Figure 39 and Figure 40) and December 11 (Figure 41 and Figure 42). These events highlight the importance of communication between maintenance personnel and the Skyway Project Manager. If these events generate alerts in the future (see Section 7), the Skyway Project manager will likely be able to rule them out as a concern based on knowledge of maintenance activities. While the exact cause of the higher than usual accelerations is not known in all cases, none of the instances lasted beyond a few milliseconds nor do they appear to indicate any damage or detriment to the structure.

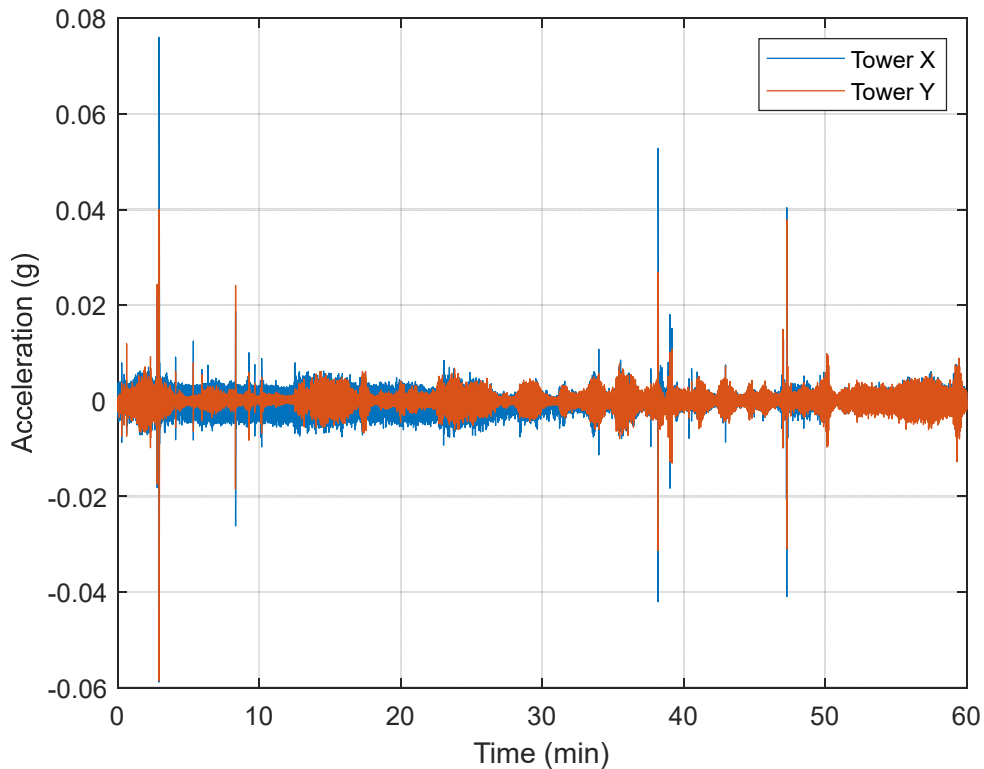


Figure 37. Tower accelerations measured on March 1, with the record starting at 5:54am.

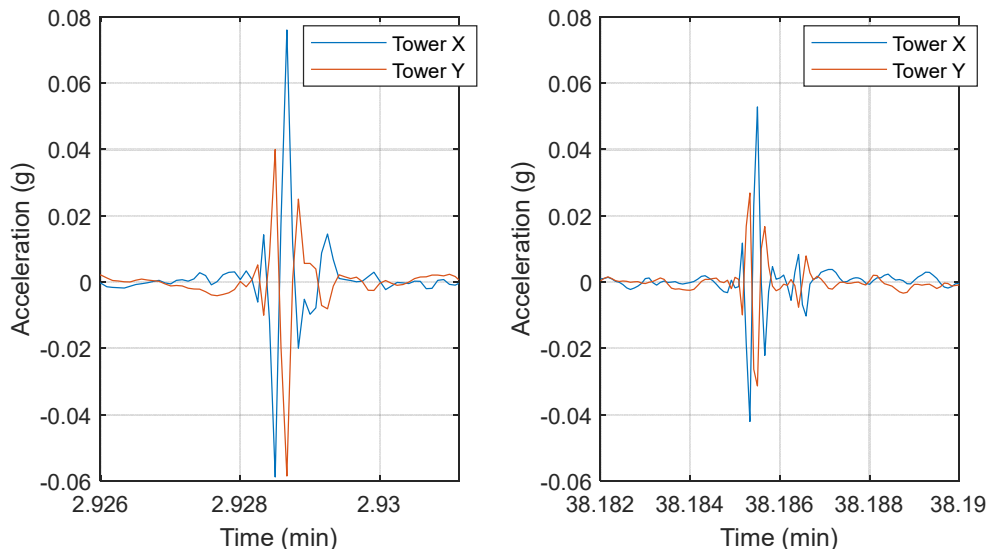


Figure 38. Zoomed in view of tower acceleration measurements recorded on March 1, with the record starting at 5:54 am: ~3 minutes into record (left) and ~38 minutes into record (right).

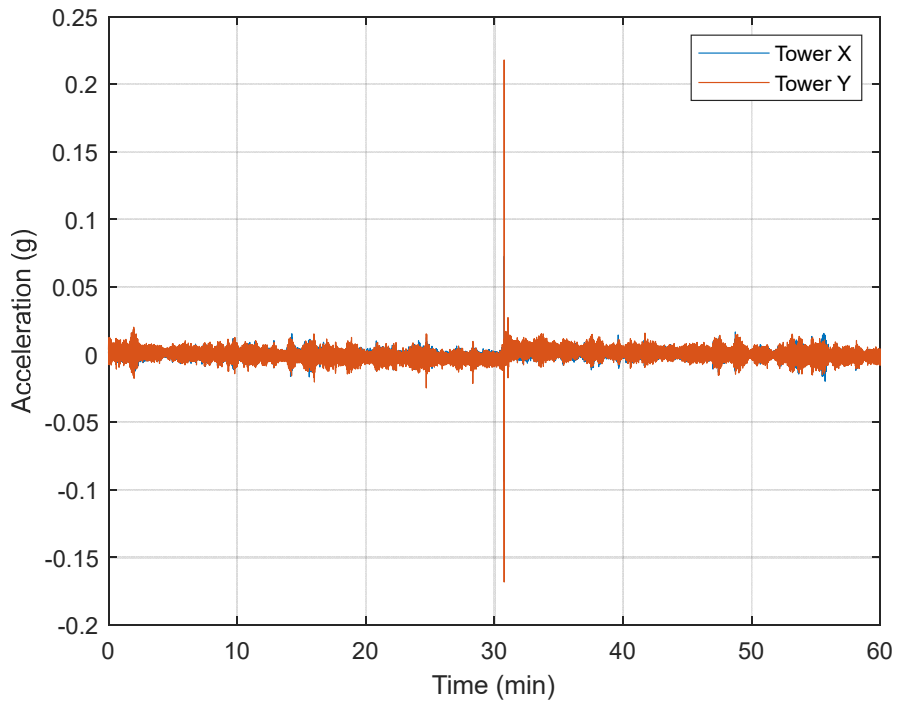


Figure 39. Tower acceleration on August 3, with the record starting at 9:33am.

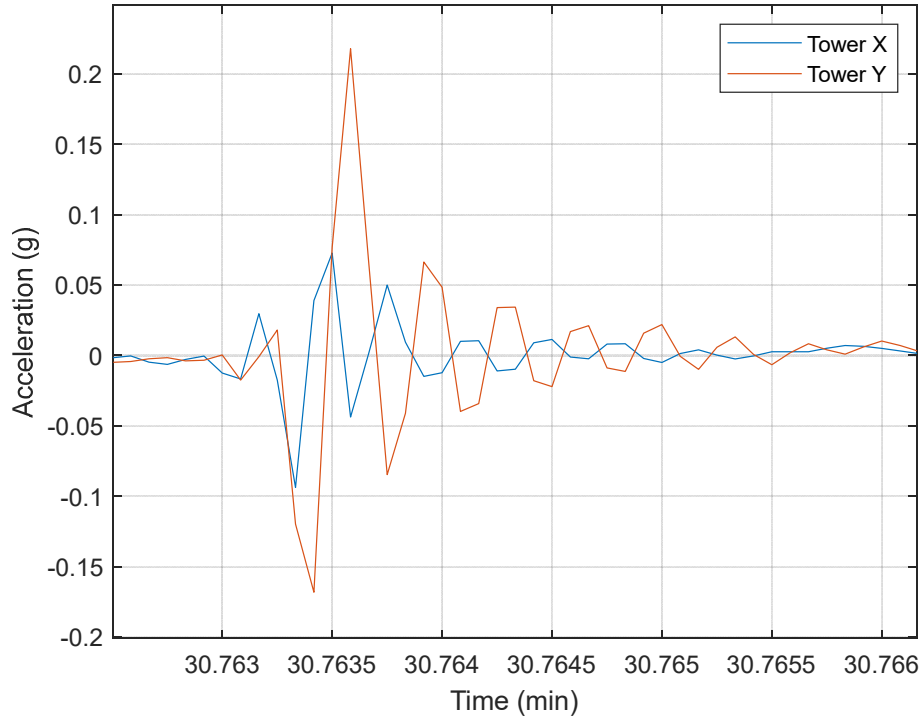


Figure 40. August 3, 30 minutes into tower vibration record that starts at 9:33am.

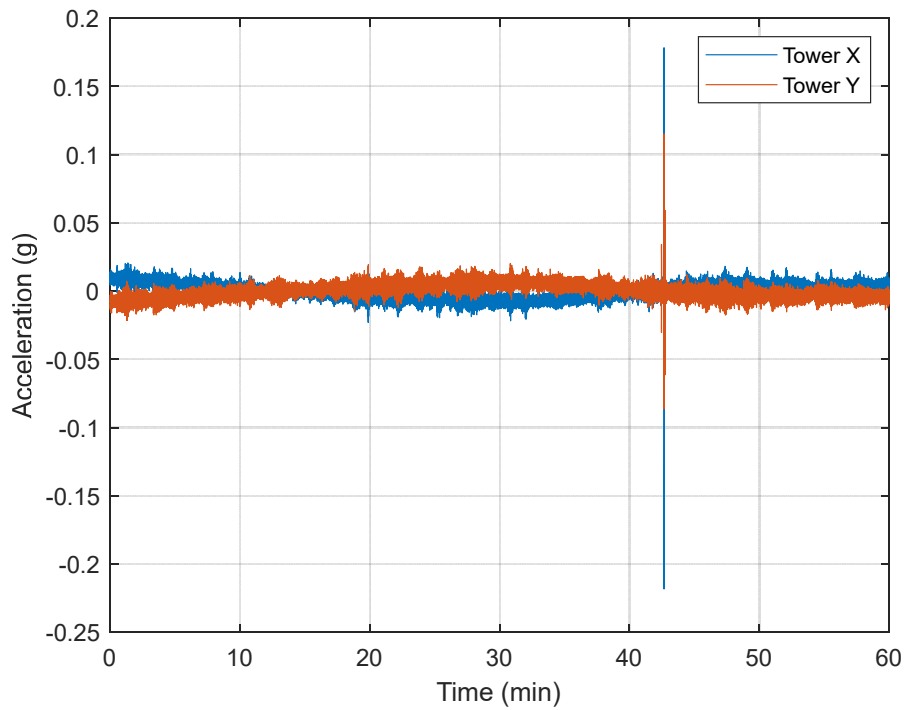


Figure 41. Tower acceleration measurements recorded on December 11 for a record starting at 11:50am.

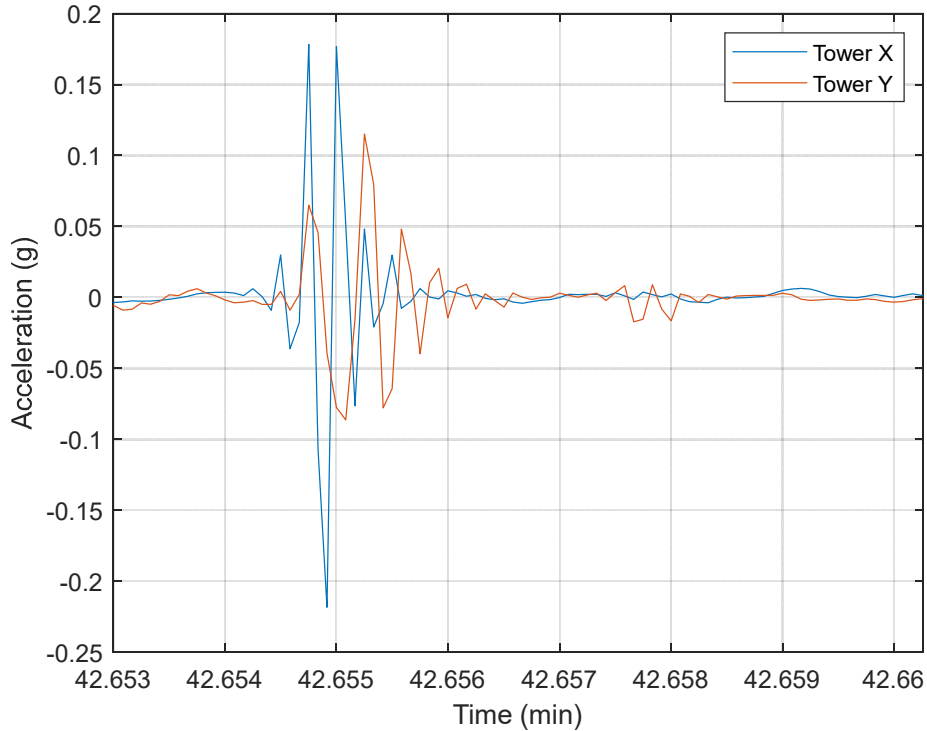


Figure 42. Tower acceleration measurements recorded on December 11 with the record starting at 11:50 am, just after 42 minutes into record.

#### 6.2.4 Acceleration Correlation Analysis

The two primary causes of cable excitation are wind and traffic loading. As shown in the six-day representative data plots, higher acceleration levels occur during higher levels of traffic during the day. Figure 43 shows the RMS acceleration level recorded on Cables 13 and 18 and the North Tower throughout 2020 versus the time of day. Acceleration levels are highest between 6am and 5pm and lowest between midnight and 3am. Tower accelerations exhibit some additional increase between noon and 4pm, a phenomenon that was also observed in the weekly representative plots (Figure 33). Note that the tower accelerations are very well correlated with the time of day relative to the cable accelerations, which exhibit more spread in the motion amplitude relative to the time of day. This indicates that the tower motion is driven primarily by traffic excitation. This result is expected since the cables are much more flexible and more susceptible to wind excitation.

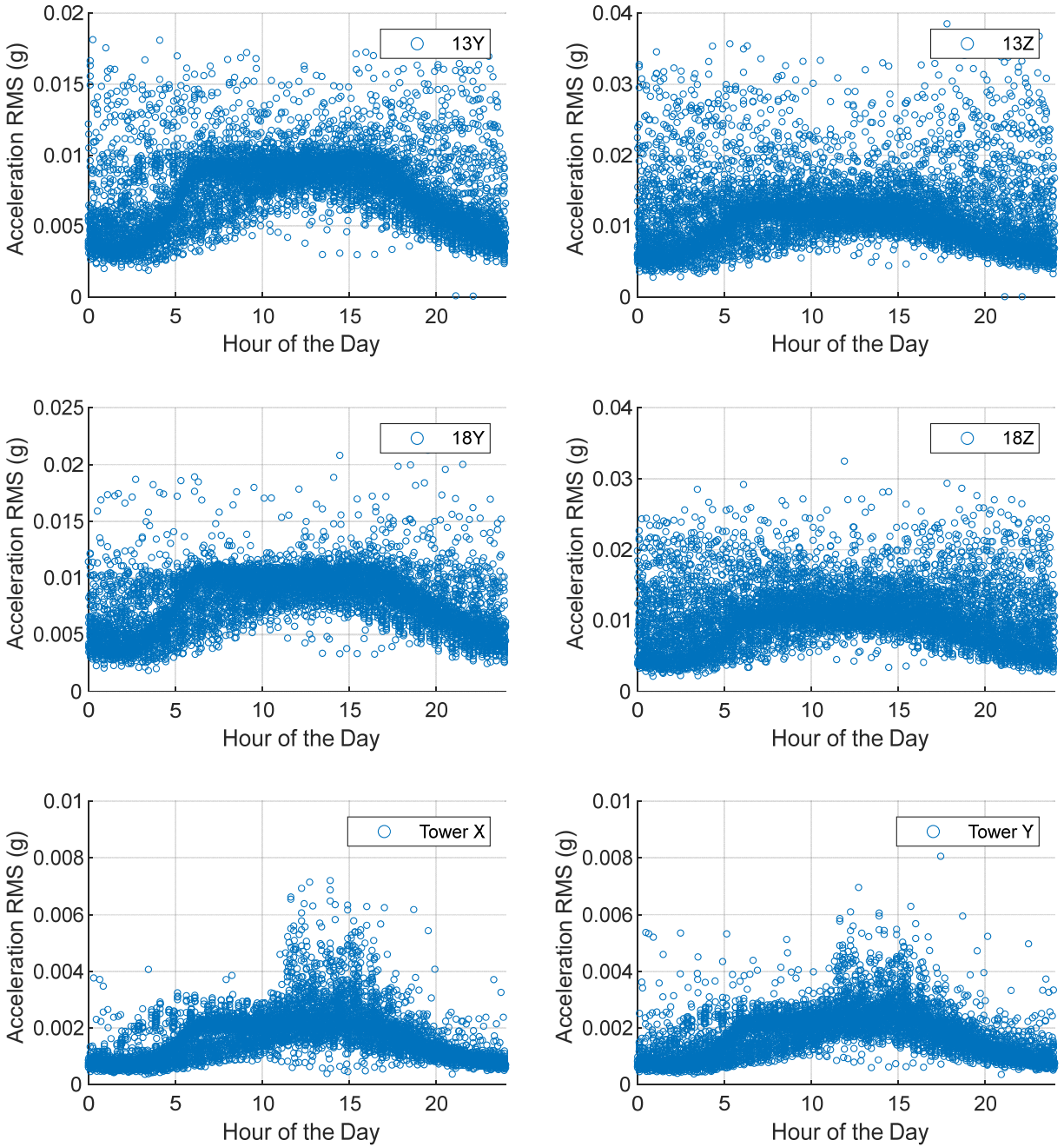


Figure 43. Hourly RMS acceleration by hour of the day.

The force imposed by wind loading is proportional to the square of the wind velocity. As a result, the amplitude of wind-induced vibration is expected to increase with the velocity squared. This response pattern is observed in the cable vibrations in both directions as seen in Figure 44, where the wind speed perpendicular to the length of the bridge (mean wind speed times the cosine of the wind direction) is plotted vs RMS acceleration levels. The tower is less susceptible to wind loading and its motion does not vary with the square of the wind speed.

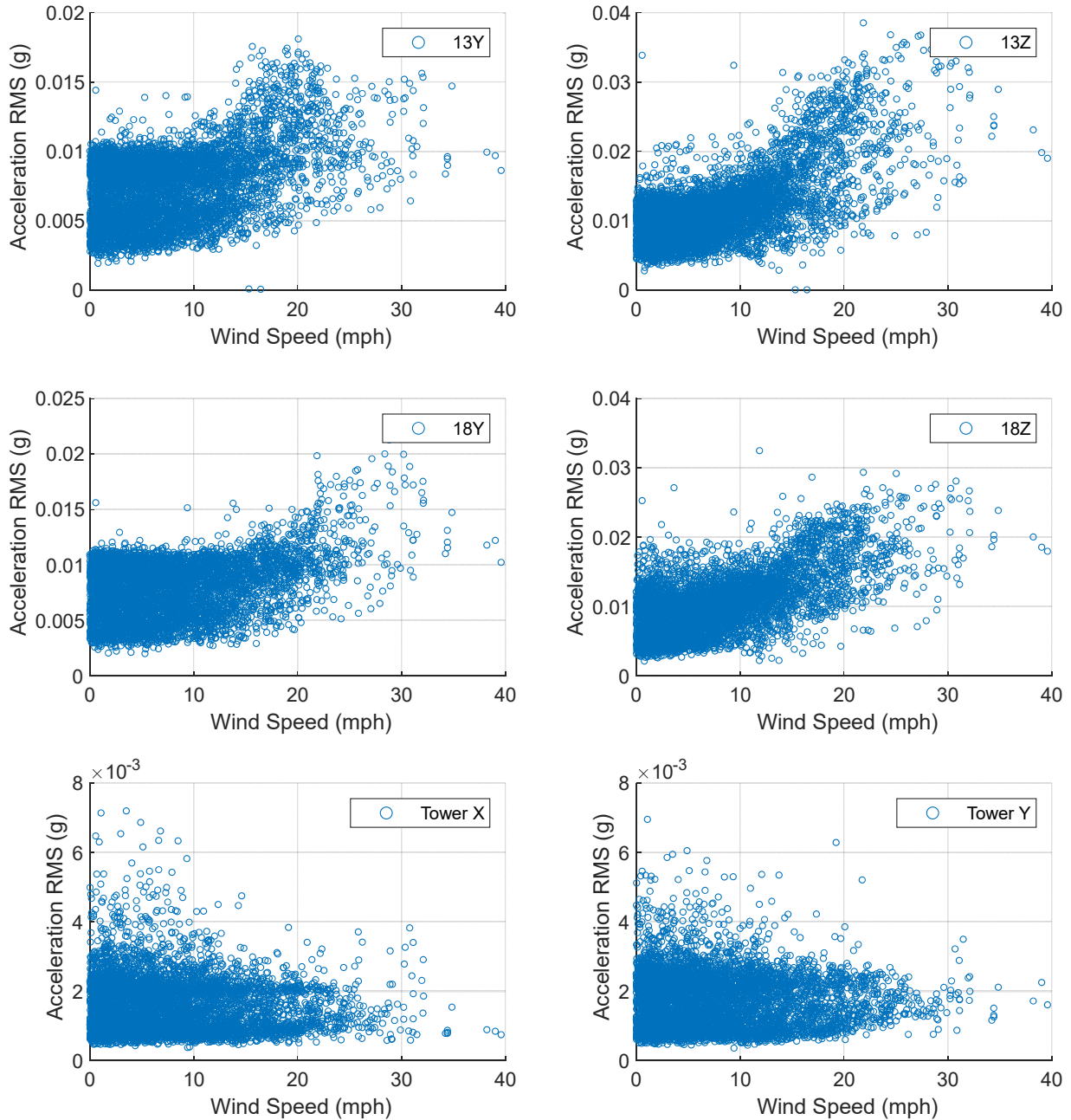


Figure 44. Hourly RMS acceleration as function of wind speed perpendicular to the length of the bridge.

#### Statistics

Table 6 provides the statistics (minimum, maximum, mean, and standard deviation) of the hourly RMS accelerometer measurements for the X- and Z-axis measurement of Cable 13 and 18 and the X- and Y-direction measurements for the North Tower.

Table 6. Hourly RMS acceleration statistics (mg).

	<b>Cable 13X</b>	<b>Cable 13Z</b>	<b>Cable 18X</b>	<b>Cable 18Z</b>	<b>Tower X</b>	<b>Tower Y</b>
Mean, $\mu$	7.41	11.38	7.90	10.44	1.62	1.72
Minimum	0.065	0.060	1.84	2.16	0.369	0.363
Maximum	18.15	38.54	21.27	32.49	8.91	8.60
Standard Deviation, $\sigma$	2.60	4.77	2.56	4.20	0.847	0.822

The statistics for the maximum accelerations are shown in Table 7. The standard deviation of the maximum acceleration measurements is used to establish bounds for accelerations measurements expected during typical bridge operation. For each acceleration location/direction, an upper acceleration limit of the mean hourly maximum plus 3.2 standard deviations encompasses at least 99% of all measurements in 2020. Table 7 shows the percent of measurements within this bound for each data channel.

Table 7. Hourly maximum acceleration statistics (mg).

	<b>Cable 13X</b>	<b>Cable 13Z</b>	<b>Cable 18X</b>	<b>Cable 18Z</b>	<b>Tower X</b>	<b>Tower Y</b>
Mean, $\mu$	68.96	72.00	65.11	73.33	14.35	14.39
Minimum	0.31	0.31	13.55	18.37	2.28	2.76
Maximum	168.54	212.73	322.72	811.09	218.29	217.91
Standard Deviation, $\sigma$	19.11	23.15	15.69	24.56	5.52	5.12
Upper bound: $\mu + 3.2\sigma$	130.13	146.07	115.31	151.93	32.00	30.78
Percent of data within bounds	99.5	99.0	99.5	99.4	99.7	99.8

## 6.3 Cable Force

### 6.3.1 Summary Plots

The cable force estimates calculated in 2020 using the procedures outlined in Section 5.1 are shown in Figure 45. Z-axis tension estimates are consistently higher than Y-axis, likely due to slight differences in boundary conditions for each vibration direction. For both cables, Z-axis tension variation is smaller than Y-axis. Without a direct measurement of the cable force or additional finite element analyses, it is not possible to say which axes provides a more accurate force estimate. Both values can be used to track relative changes and for comparison with one another to rule out erroneous force estimates or confirm unexpected force variations. Figure 46 shows a representative six days of cable force estimates. The gaps in data are where estimates have been eliminated due to low  $R^2$  values, indicating that the vibration levels are too low and/or noise levels are too high to achieve a regression fit adequate for accurate force estimation. The cable forces change throughout each day in response to temperature changes, as quantified in a subsequent section. The forces estimated from Cable 13 Y acceleration are the least consistent; however, a reason for this result is not yet established.

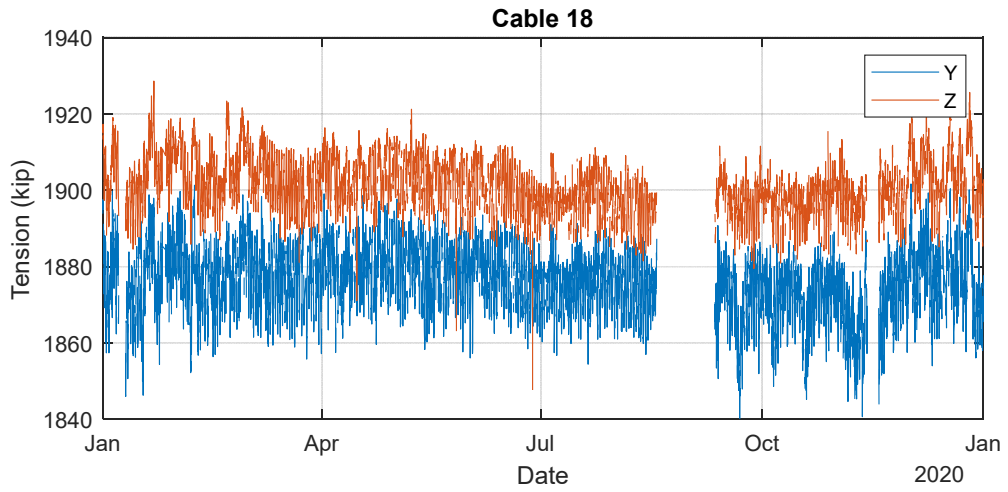
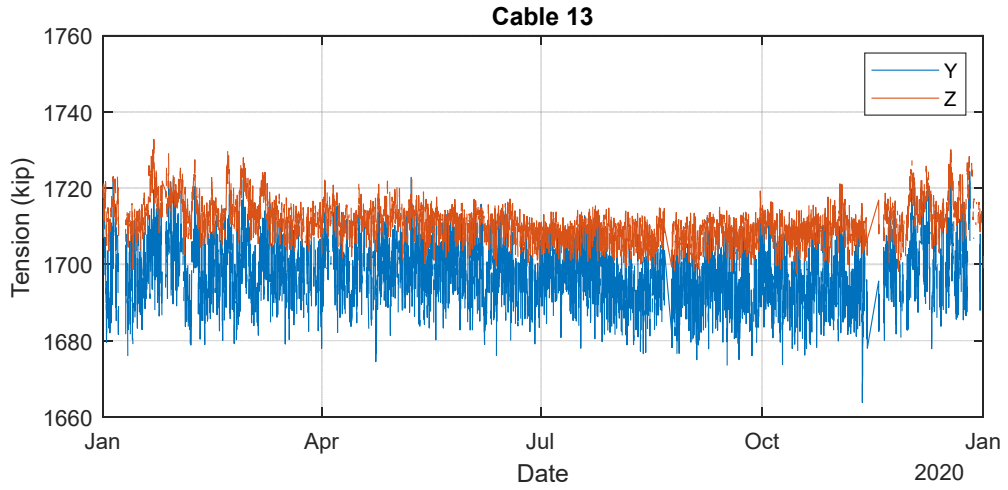


Figure 45. Cable force estimates from Y- and Z-axis acceleration on Cables 13 and 18 measured in 2020.



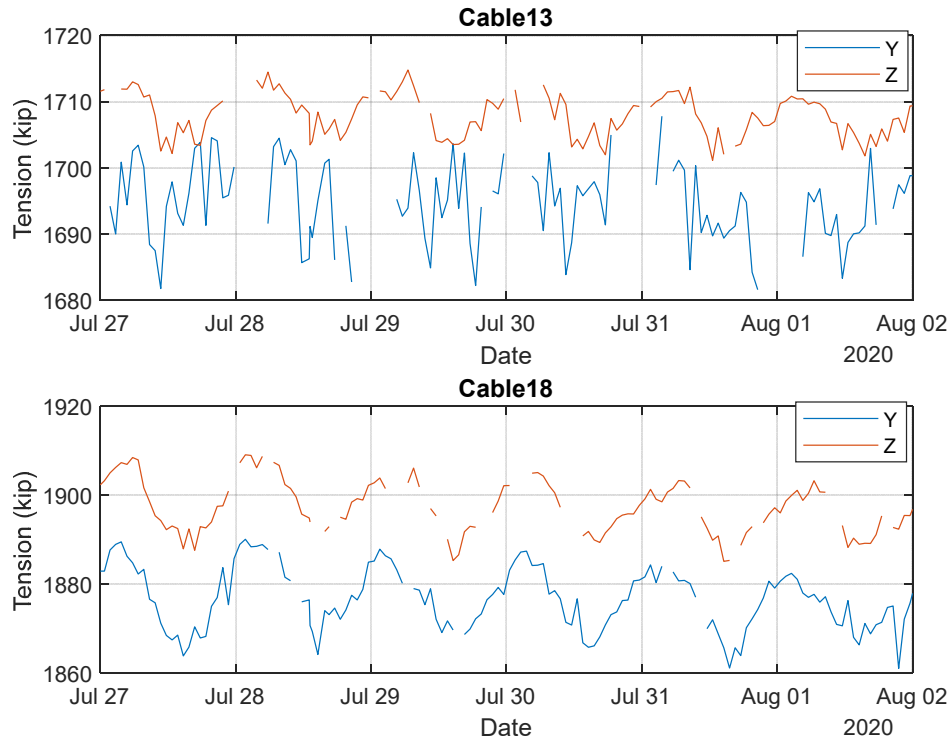


Figure 46. Six days of cable force estimates in Cables 13 and 18.

Table 8 provides the statistics for the cable forces estimated in 2020. The standard deviations for the forces (6.4 kip and 8.16 kip for Cables 13 and 18, respectively) are reasonable for seasonal and diurnal temperature changes and provide a basis for establishing the bounds of expected forces, as discussed in a subsequent section.

### 6.3.2 Statistics and Comparison with Previous Studies

Table 8. Cable tension summary (kips).

	Cable 13			Cable 18		
	Y	Z	Average	Y	Z	Average
Mean, $\mu$	1697	1711	1704	1876	1901	1889
Minimum	1664	1698	1681	1839	1848	1843
Maximum	1748	1733	1740	1902	1929	1915
Standard Deviation, $\sigma$	7.82	4.97	6.40	8.95	7.36	8.16

Table 9 compares the average cable force estimated during 2020 for Cables 13 and 18 (Y- and Z-directions averaged) to estimates obtained in previous studies. In addition to the results of this study, Table 9 includes CTL, RWDI and BES force estimates, the design-predicted forces due to dead load, and the forces measured after construction (after grout was fully hardened). The values estimated in this study are on the higher end of the range of forces measured or predicted by other methods. Differences in the predicted or measured forces between studies may have to do with how boundary conditions are modeled and the conditions when the measurements were conducted.

Cables forces decrease with temperature increase; if the previous measurements were all conducted during the day, it is expected that those results will be lower than the average values resulting from this study, which are based on an entire day (24 hours).

Table 9. Comparison of estimated cable forces (kips)

<b>Estimate Condition</b>	<b>Estimate Grout Density</b>	<b>Cable 13</b>	<b>Cable 18</b>
Design prediction under dead load	--	1638.4	1888.8
VSL measured after grout hardened	--	1552.8	1824.9
CTL 1999	110 lb/ft <sup>3</sup>	1692.4	1831.3
RWDI 2004	124 lb/ft <sup>3</sup>	1751	1934
BES 2010	110 lb/ft <sup>3</sup>	1622.4	1823.9
BES 2010	124 lb/ft <sup>3</sup>	1679.1	1887.7
BES 2015	110 lb/ft <sup>3</sup>	1662.6	1823.9
UF/BDI 2020 (this study)	110 lb/ft <sup>3</sup>	1704	1889

### 6.3.3 Cable Force Correlation Analysis

The primary source of variation in cable tension is ambient temperature causing thermal material expansion and contraction. Figure 47 to Figure 50 illustrate the linear relationship between temperature estimated cable forces. Linear regression for each cable results in the following relationship between cable force,  $F$  (kips), and temperature,  $T$  (°F):

$$F = p_1 \cdot T + p_2 \quad (3)$$

where the coefficients  $p_1$  and  $p_2$  are given in Table 10 for each cable and measurement direction pair. The units of  $p_1$  and  $p_2$  are °F/kip and kip, respectively

Table 10. Linear regression coefficients for the relationship between temperature and cable force estimate.

<b>Coefficient</b>	<b>Cable 13X</b>	<b>Cable 13Z</b>	<b>Cable 18Y</b>	<b>Cable 18Z</b>
$p_1$	-0.356	-0.493	-0.399	-0.621
$p_2$	1722.8	1746.5	1904.9	1944.8

Standard deviation was used to establish bounds that encompass expected cable forces. The bounds can be set to vary with temperature or remain constant with temperature. In both cases, the goal is to set the bounds so that >99% of all retained force estimates are within the bounds. The temperature dependent bounds are set to +/- 2.6 standard deviations from the linear regression fit for each cable/direction pair, while the constant bounds are set to +/- 3.2 standard deviations from the mean for each cable/direction pair. These bounds are indicated in Figure 47 to Figure 50. The percent of cable estimates that are within these bounds from the 2020 measurements are presented in Table 11.

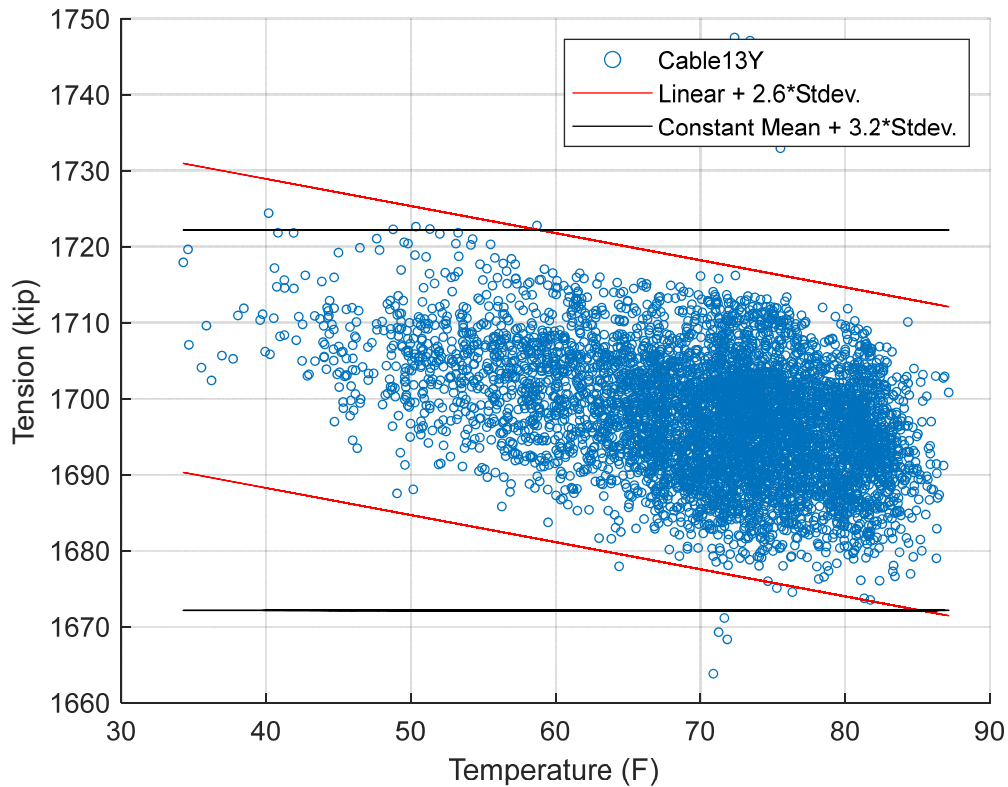


Figure 47. Tensions estimated in Cable 13 from Y-axis acceleration measurements.

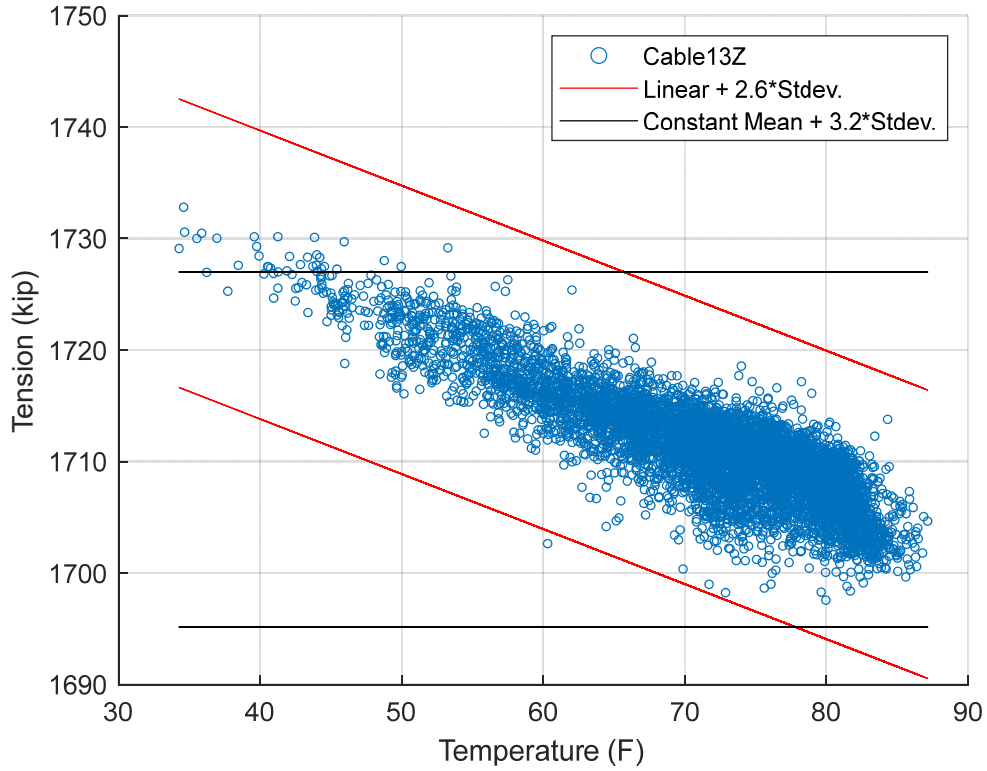


Figure 48. Tensions estimated in Cable 13 from Z-axis acceleration measurements.

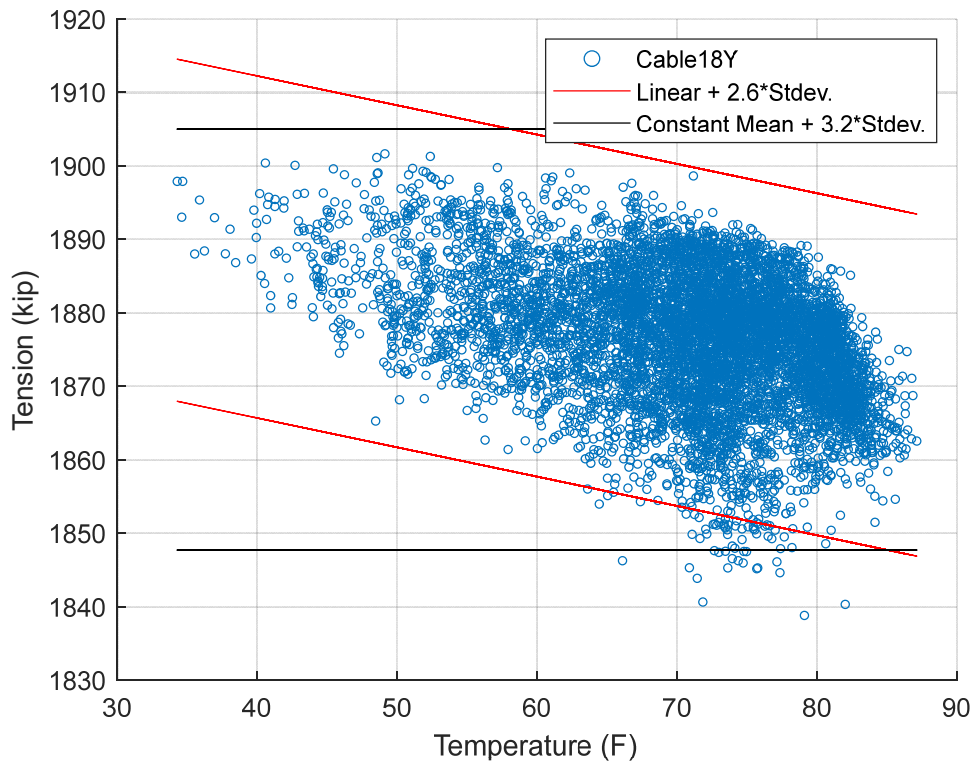


Figure 49. Tensions estimated in Cable 18 from Y-axis acceleration measurements.

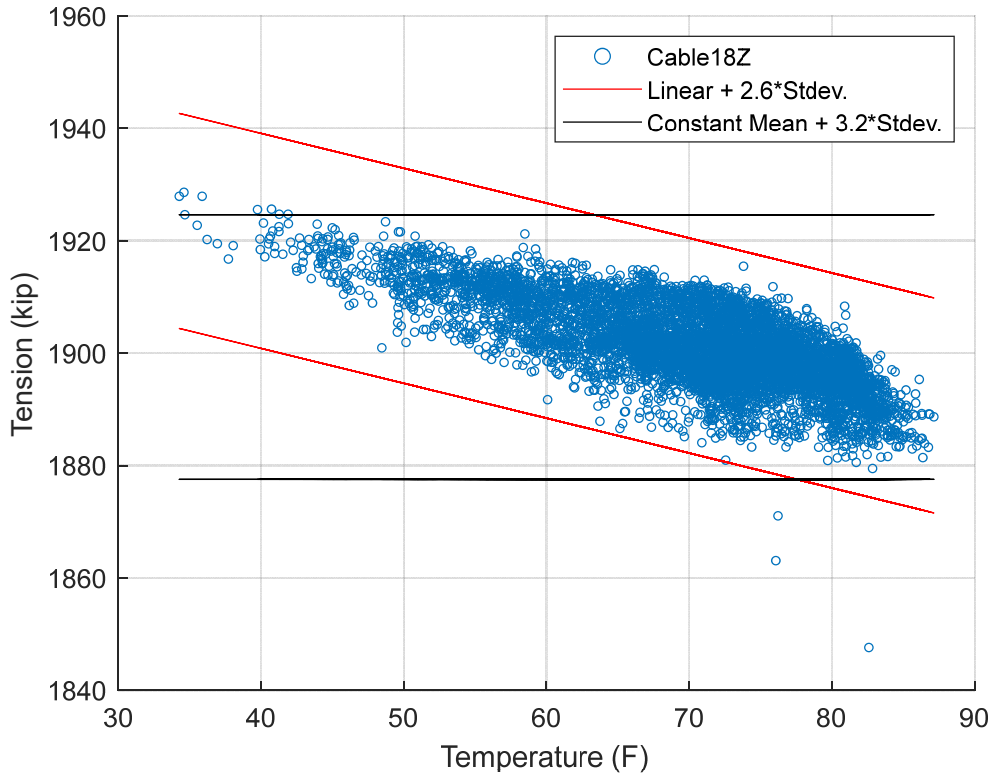


Figure 50. Tensions estimated in Cable 18 from Z-axis acceleration measurements.

Table 11. Percent of cable force estimates within the two types of bounds: temperature-dependent linear and constant.

	<b>Cable 13Y</b>	<b>Cable 13Z</b>	<b>Cable 18Y</b>	<b>Cable 18Z</b>
Temperature-dependent linear	99.51%	99.99%	99.08%	99.95%
Constant	99.55%	99.50%	99.74%	99.86%

There was no observed impact wind speed on cable forces; cable force estimates show no correlation with wind speed.

## 6.4 High-Wind Events and Bridge Closures

### 6.4.1 Bridge Closures

The bridge was closed three times during 2020 due to high wind events making it unsafe for traffic. On February 6, mean wind speeds increased from 20 mph around 12am to 40 mph around 6pm. The mean wind speeds were sustained around 40 mph until 8pm. Figure 51 shows the wind speeds from February 4 to 8, 2020. The maximum wind speed recorded was 63.8 mph at 8pm, at which point the mean wind speed dropped rapidly (see Figure 52), reaching a mean value of 12 mph around 11pm. During this period, cable accelerations peaked to ~0.2g as shown in Figure 53 for Cable 13. While higher than the typical response values, they are not of concern for the safety of the structure, especially given their short duration. Figure 54 shows the hourly RMS acceleration variation between February 4 and 8, showing that the drop in the Y-axis acceleration levels around

noon. This drop is likely due to the closure of bridge to traffic as traffic loading has the most impact on lateral cable acceleration. A similar drop in tower accelerations was observed when the bridge was closed to traffic. In contrast, the Z-axis acceleration has sustained high values until the wind speed drops around 8pm.

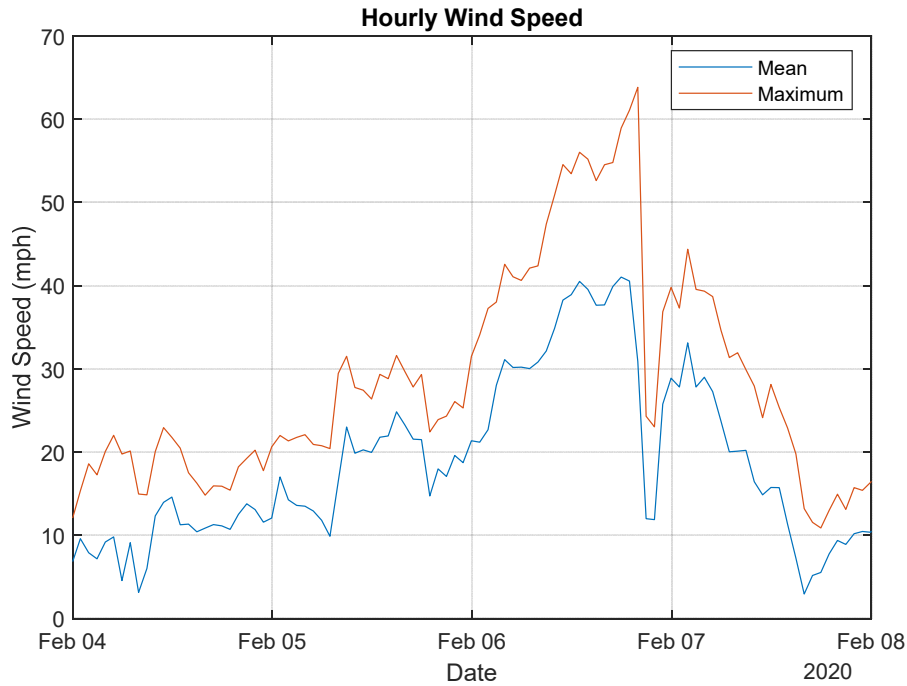


Figure 51. Hourly mean and maximum wind speed from February 4-8, 2020.

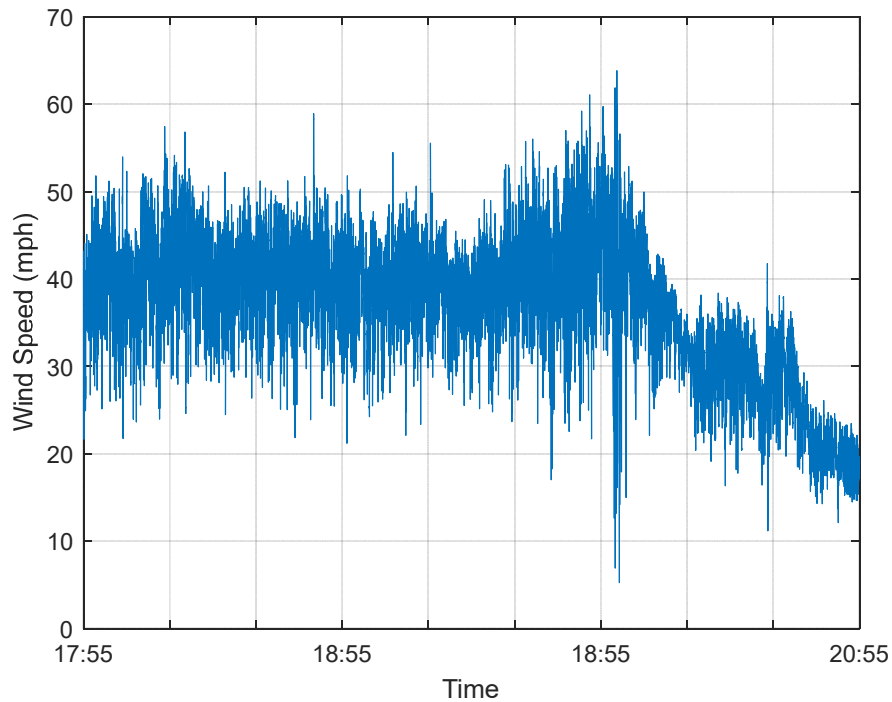


Figure 52. Wind speed measured on February 6 from approximately 6 to 9pm

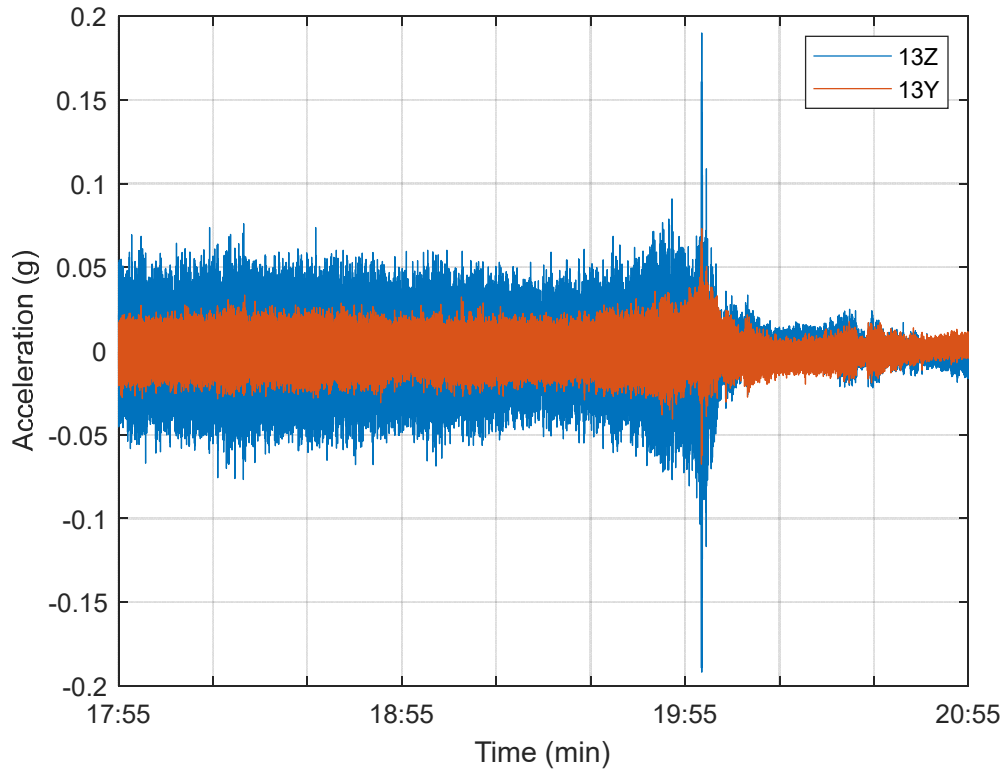


Figure 53. Cable 13 acceleration measured on February 6 from approximately 6pm to 9pm.

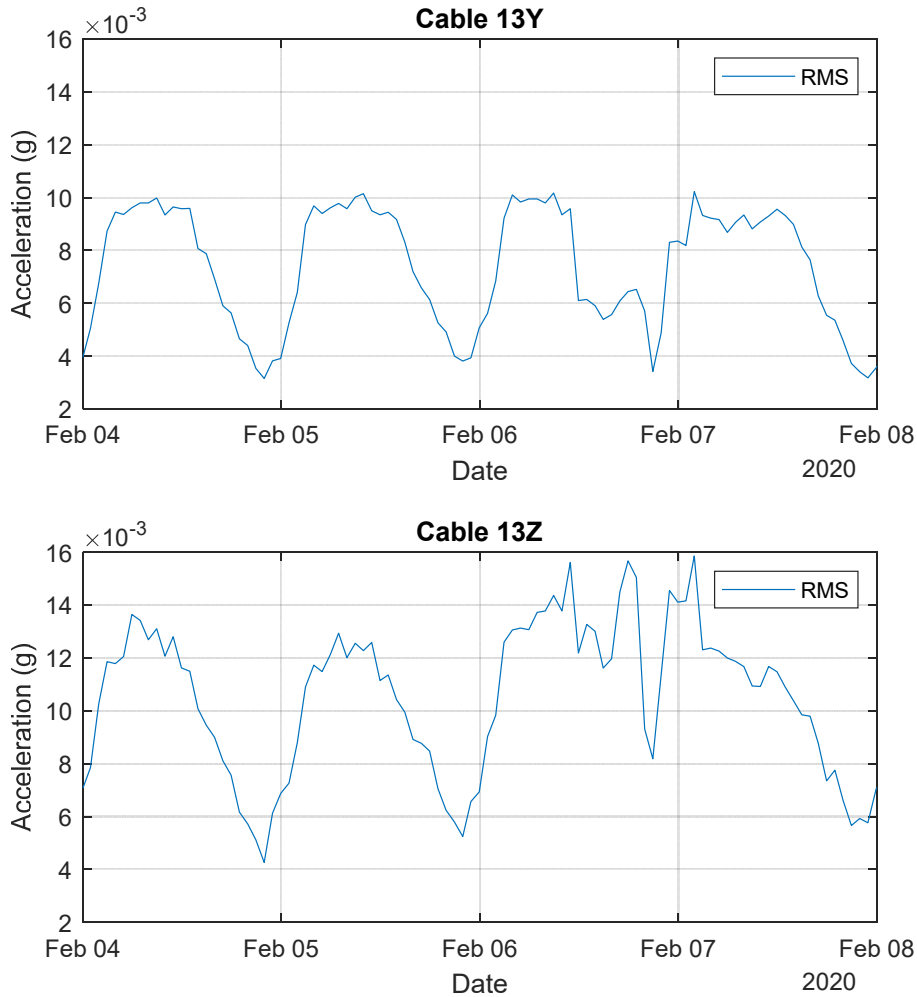


Figure 54. Hourly Cable 13 RMS acceleration values from February 4-8, 2020.

Other Bridge closures were associated with the nearby passage of Tropical Storm Eta in the second week of November. These closures occurred on November 9 when the maximum wind speed reached 61.9 mph and again on November 11 with high winds between 3pm and midnight with a maximum value of 71.9 mph around 8pm, as shown in Figure 55. The wind direction also shifted 360 degrees from November 10 to 13 (starting and ending from the NE). Figure 56 to Figure 61 show the hourly RMS and maximum accelerations recorded on Cables 13 and 18 and on the North Tower from November 7 to November 13, 2020. The cable vibrations were highest on November 8 and 9, while the Y-axis of the tower saw higher levels on November 11. The accelerations were higher than typical response values but did not reach a concerning level.



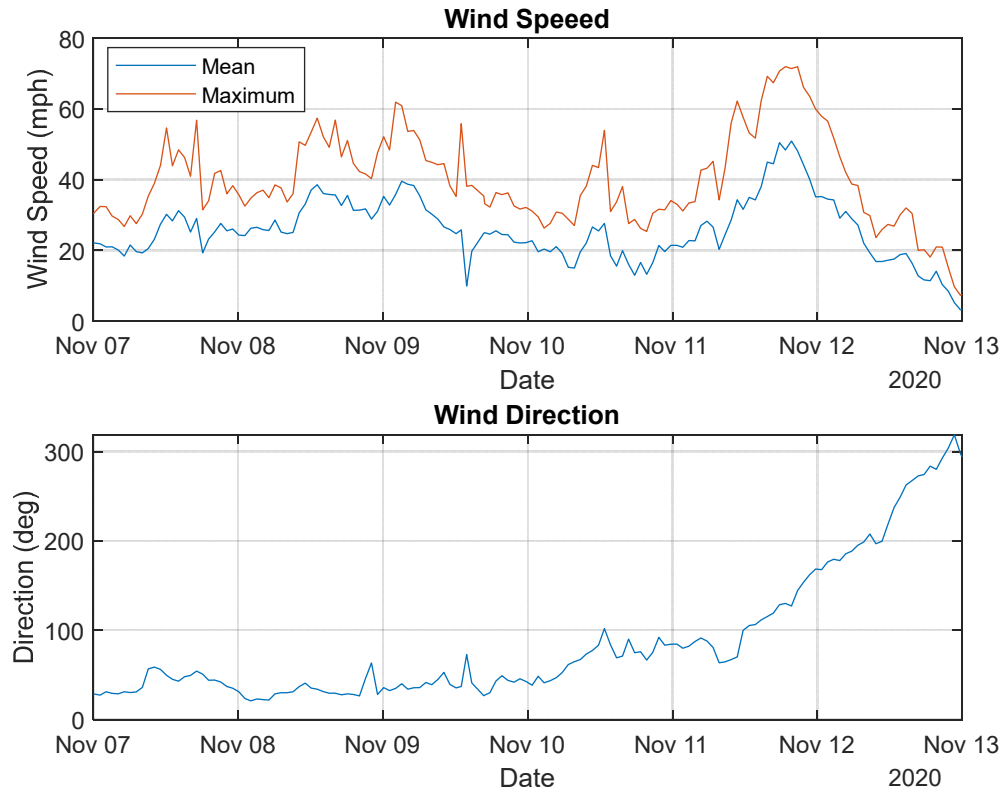


Figure 55. Wind speed hourly mean and maximum (top) and hourly direction (bottom) recorded between November 7 and 13, 2020, as Tropical Storm Eta passed nearby.

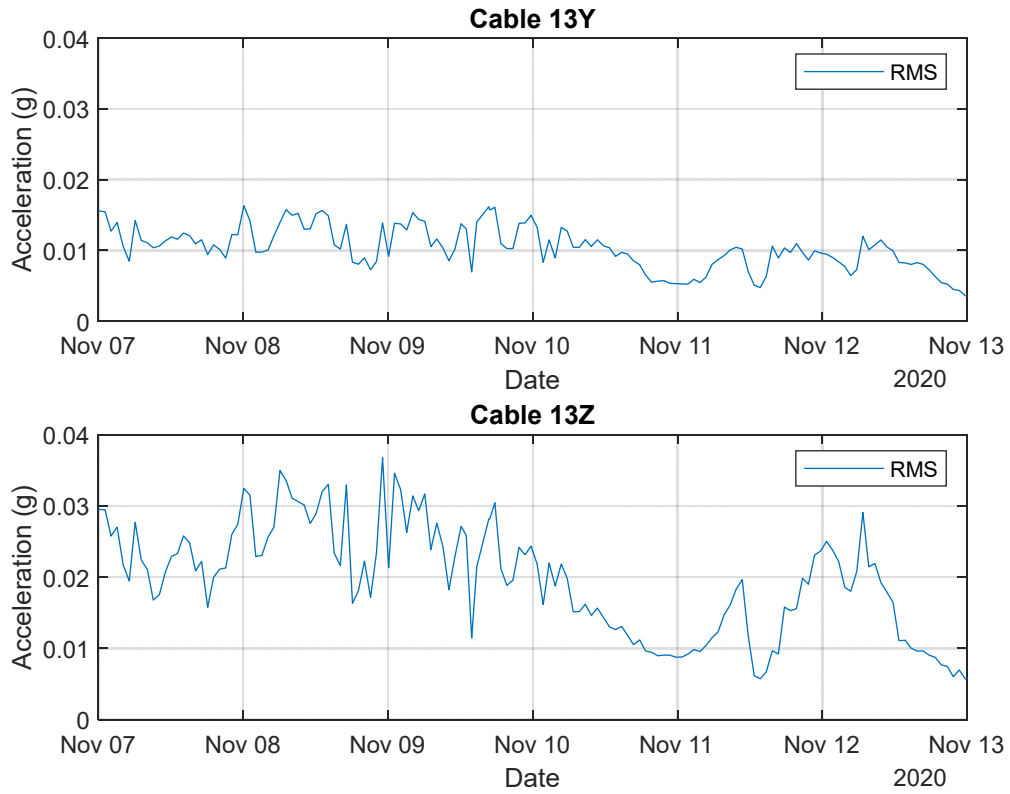


Figure 56. Cable 13 hourly RMS acceleration recorded between November 7 and 13, 2020, as Tropical Storm Eta passed nearby.

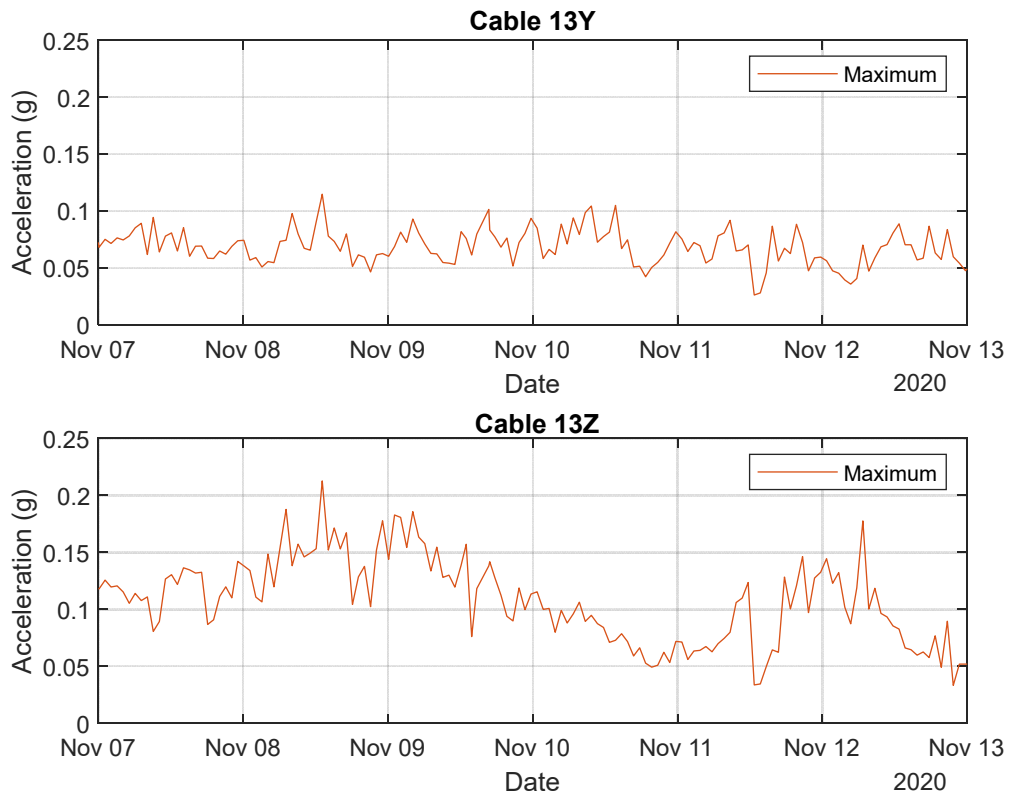


Figure 57. Cable 13 hourly maximum acceleration recorded between November 7 and 13, 2020, as Tropical Storm Eta passed nearby.

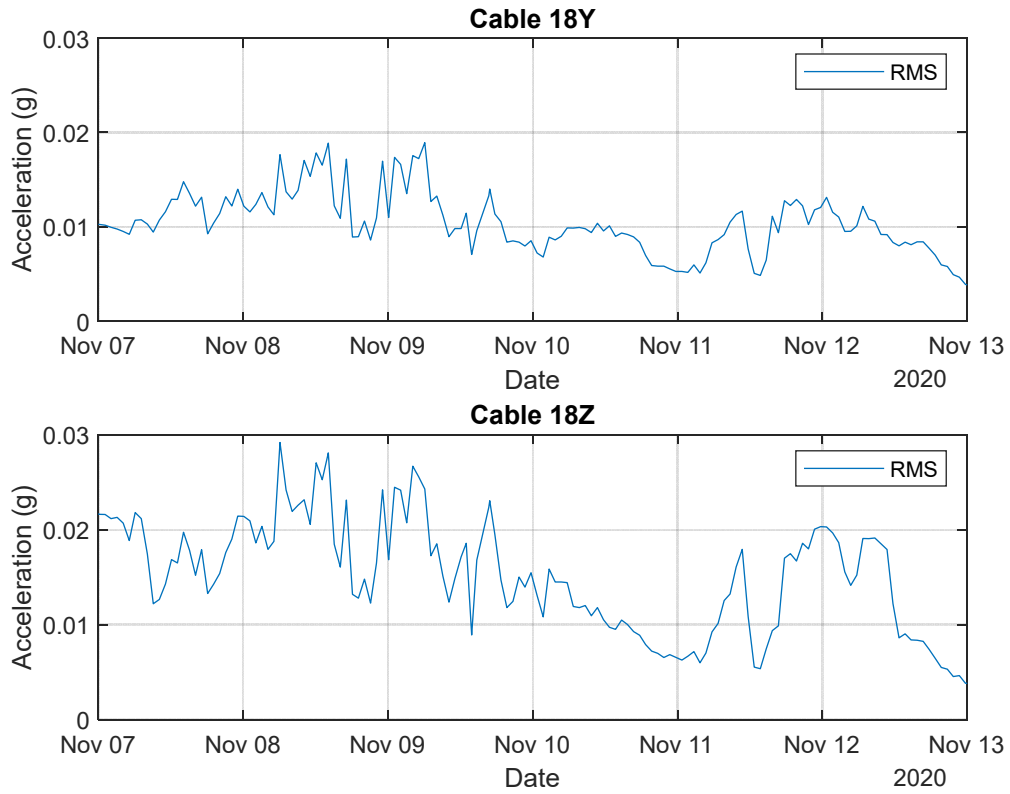


Figure 58. Cable 18 hourly RMS acceleration recorded between November 7 and 13, 2020, as Tropical Storm Eta passed nearby.

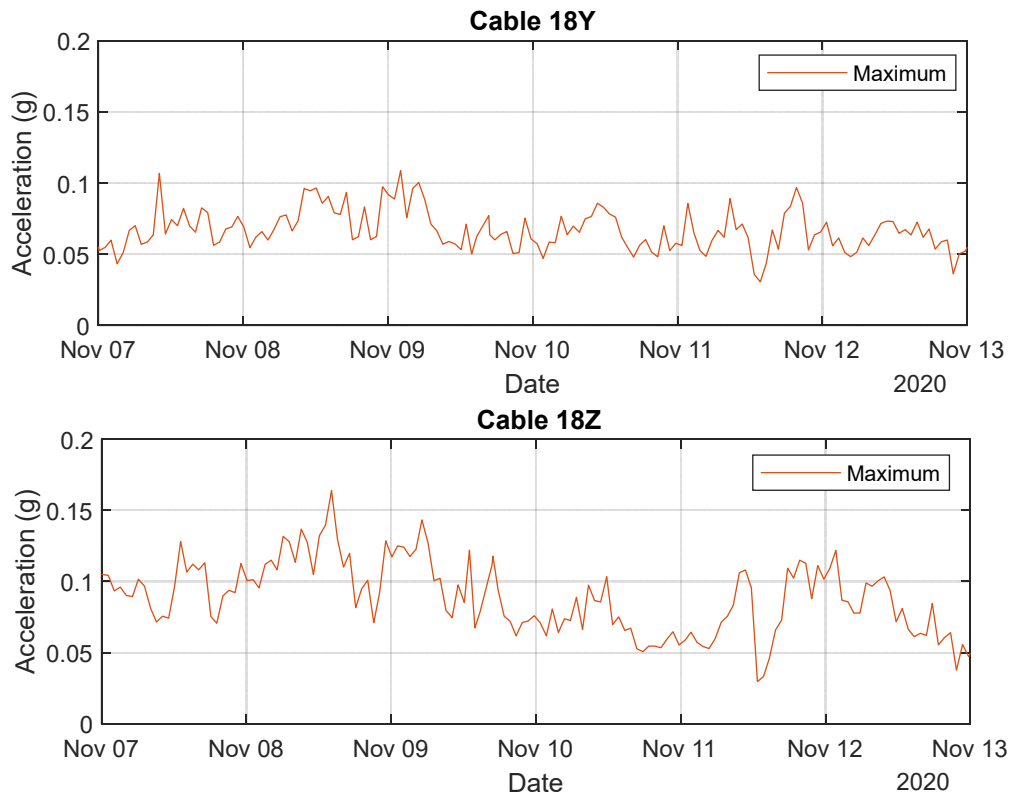


Figure 59. Cable 18 hourly maximum acceleration recorded between November 7 and 13, 2020, as Tropical Storm Eta passed nearby.

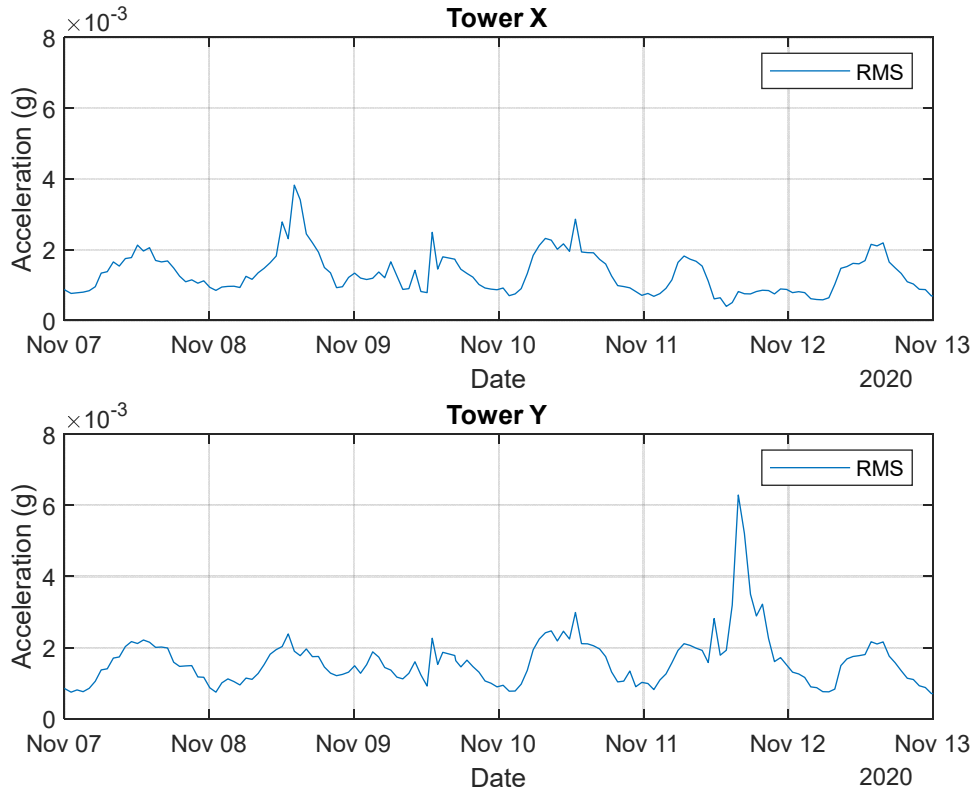


Figure 60. Tower hourly RMS acceleration recorded between November 7 and 13, 2020, as Tropical Storm Eta passed nearby.

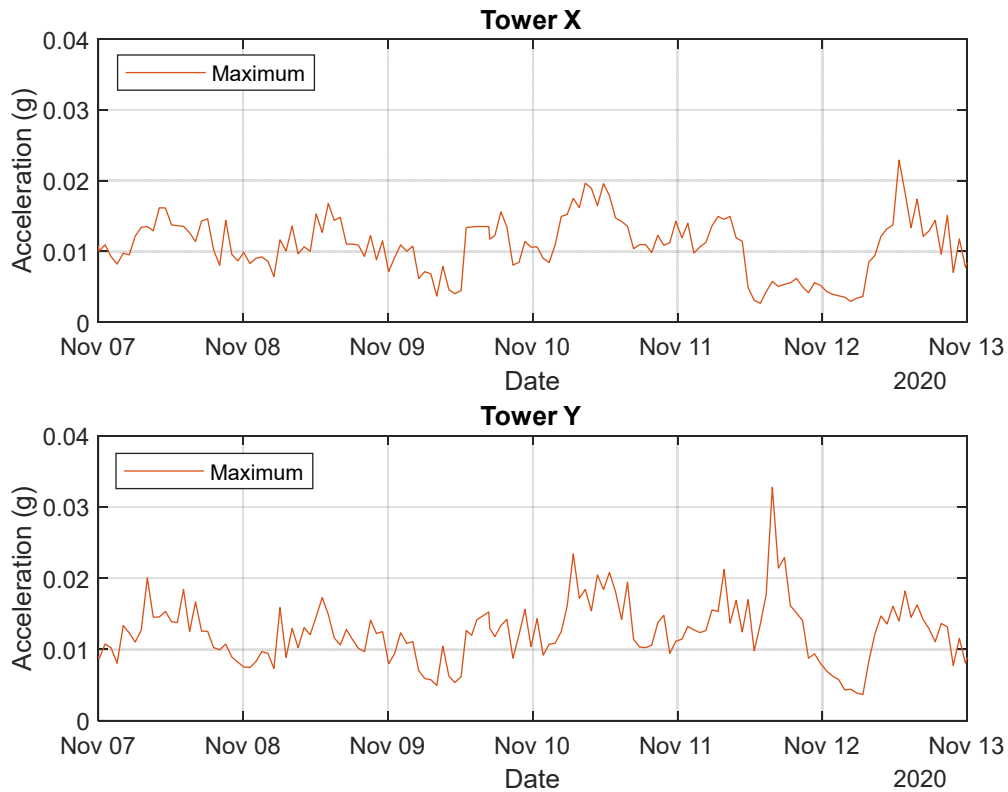


Figure 61. Tower hourly maximum acceleration recorded between November 7 and 13, 2020, as Tropical Storm Eta passed nearby.

#### 6.4.2 High Winds, No Closure

The bridge was not closed for the highest recorded wind gust of 76mph on December 24 at 7:26pm. The wind speed rapidly increased over a short time (~2 minutes) as shown in Figure 62, and then decreased to normal levels over the following 30 minutes. The rapid increase in wind speed and change in wind direction resulted in increased accelerations in the cables that subsided after the peak wind speed was reached. The Z-axis acceleration in both cables 13 and 18 reached approximately 0.17 g (Figure 63 and Figure 64).

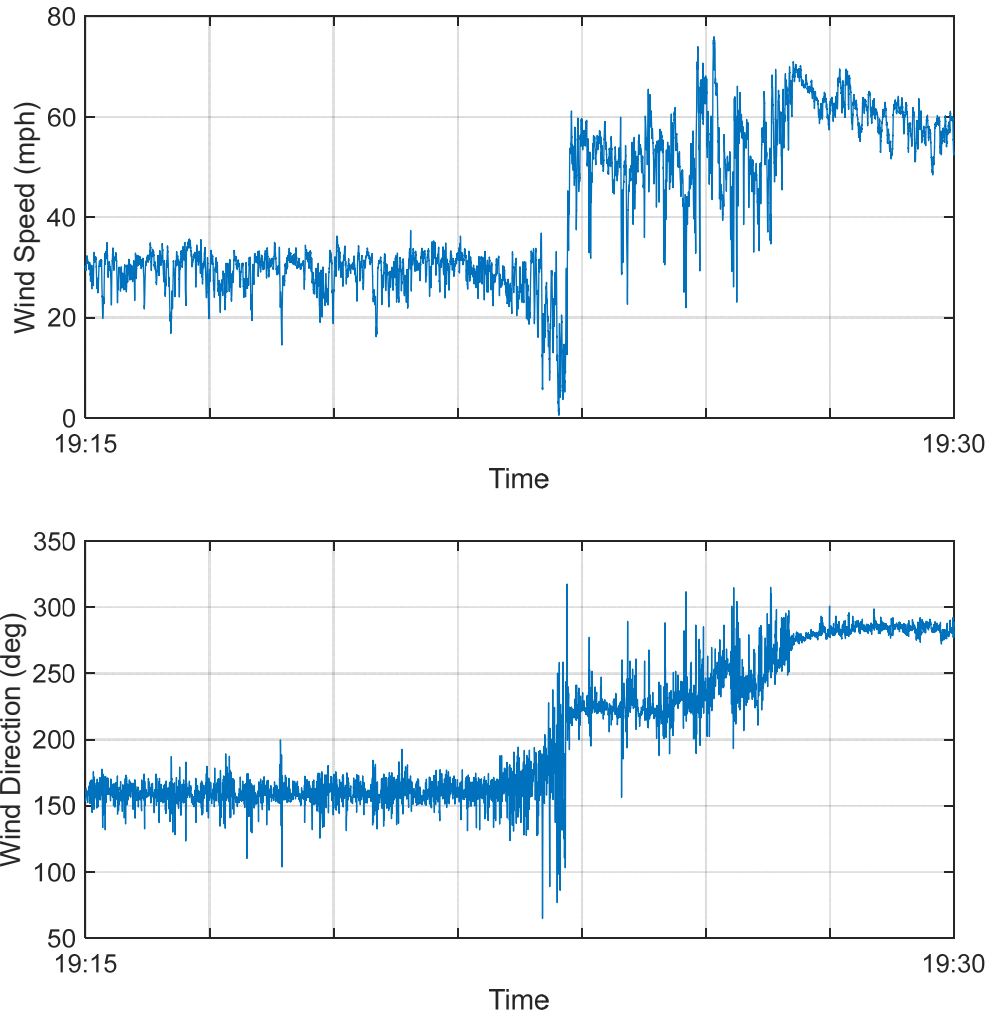


Figure 62. Wind speed (top) and wind direction (bottom) recorded from 7:15 to 7:30pm on December 24, 2020.



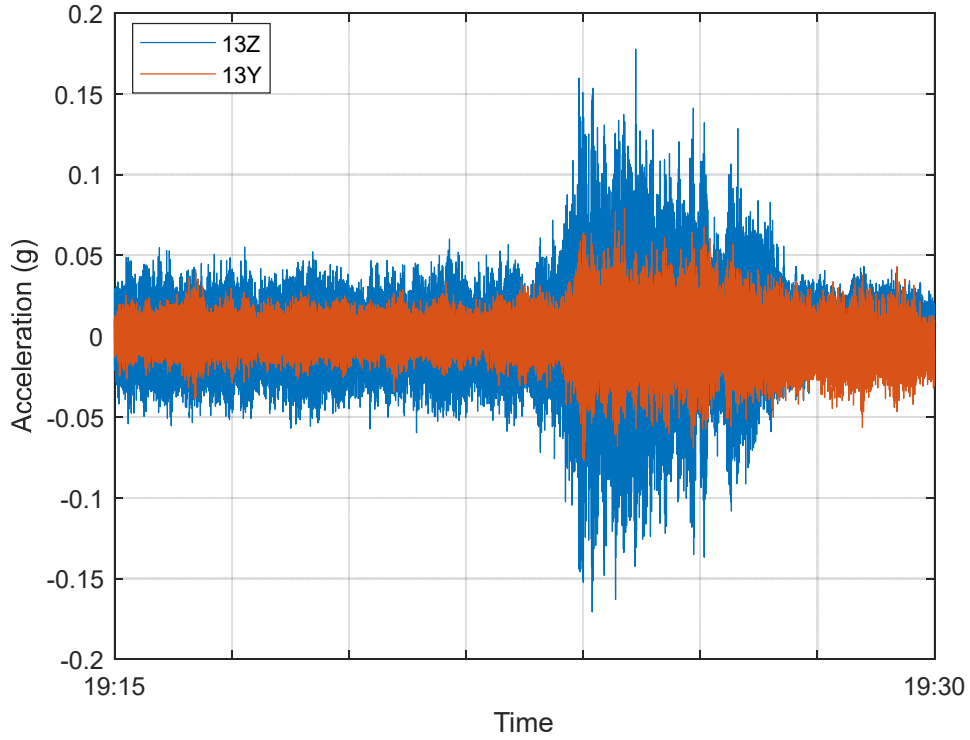


Figure 63. Cable 13 acceleration recorded from 7:15 to 7:30pm on December 24, 2020.

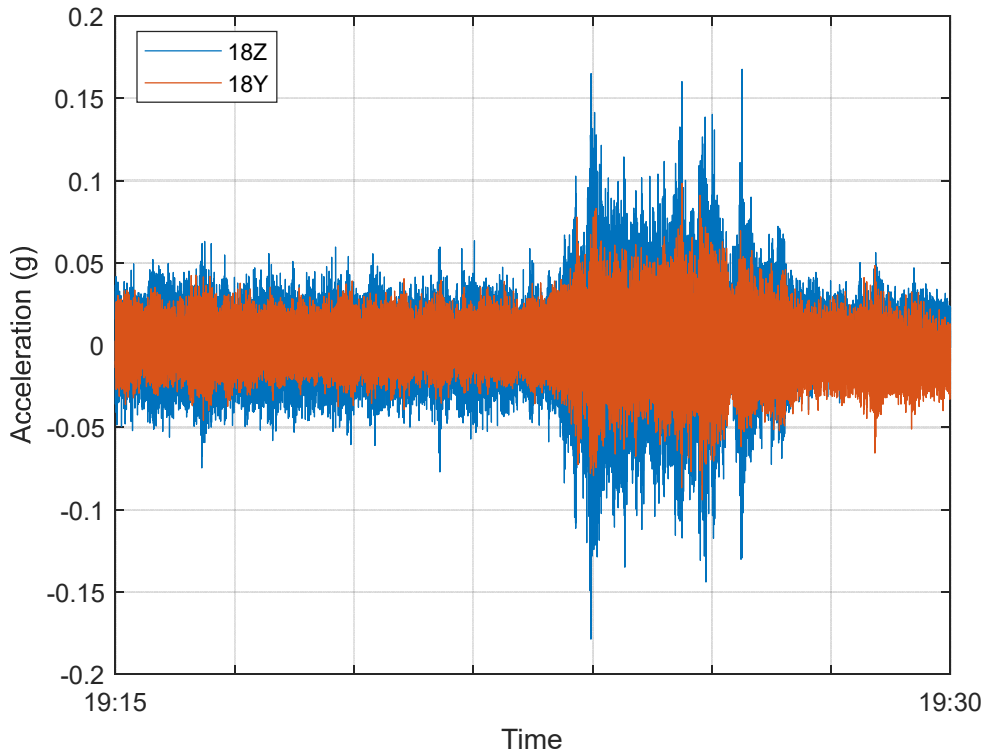


Figure 64. Cable 18 acceleration recorded from 7:15 to 7:30pm on December 24, 2020.

### 6.4.3 Skyway 10k with Partial Closure

On March 1, 2020, the northbound lanes of the bridge were closed from 3 to 11 am to accommodate the Skyway 10k race. There were no observed differences in cable accelerations or estimated cable forces. There were some high frequency acceleration spikes in the North Tower measurements starting at 6am, as shown in Figure 37 and Figure 38. These accelerations are short in duration and typical of localized excitation that is not a concern to the structure.

## 7 Bridge Alert Response Plan

This section proposes a procedure for responding to alerts generated from the Sunshine Skyway Bridge monitoring system, including the identification of roles and personnel.

### 7.1 Event Types

The monitoring system is limited to reporting response information resulting from measurements taken at the locations that are instrumented. The current system provides vibration data for Cables 13 and 18 and the North Tower. With the repair/replacement of current nonworking sensors, it will also provide vibration data for Cable 16 and 21, the deck at the base of Cable 8 and movement at the south end of the main span, north end of the main span, and the middle of the main span. For any of the cable sensors, a virtual channel can also be added to provide an estimate of cable force once per hour (or more often, if desired). In addition, the system currently provides temperature, wind speed, and wind direction near the base of the North Tower.

In general, the types of information that can be established with the current monitoring system, assuming existing sensors are repaired and/or replaced and cable force virtual channels are added are:

- Excessive vibrations of Cables 13, 16, 18, and 21, the deck at the base of Cable 8, and at the top of the North Tower due to dynamic loads such as wind, traffic, blast, or impact loading (acceleration, every minute or so as the live web interface updates data)
- Loss of force in Cables 13, 16, 18, and 21 (force from acceleration, every 60 minutes)
- Slowly evolving changes in main span movement due to temperature or settlement (GPS, 1 – 2 times per day)
- Permanent changes in main span position due an extreme loading event such as impact or blast (GPS, 1 – 2 times per day).

Some bridge measurements will indicate changes that occur slowly, such as support settlement or redistribution of cable forces due to cable deterioration. In these cases, daily and weekly trends should be observed and correlated with environmental measurements, specifically temperature. Other measurements may be used to capture the response to acute or extreme events, such as:

- An intense weather event
- An impact by an air/sea vessel
- A severe vehicular accident/explosion
- A targeted malicious attack

The accelerometers on the cables, deck, and tower can capture such events if they occur close to the sensor location. In addition, such events are likely result in significant measurements in more than one sensor, depending on their location and severity.

### 7.2 Alert Levels

Four levels of alerts ranging from 1 (low severity) to 4 (high severity), are proposed for the system provided by the monitoring system.

### 7.2.1 Level 1

A Level 1 alert will indicate that the output of one or more monitoring channels is either unavailable (not updating) or reading erroneous results (noise or other non-physical response). In the case of unavailable data, the monitoring system will generate the alert automatically. In some cases, a Level 1 alert will be initiated manually by either BDI, the ESC, or the DSMO Skyway Project Manager overseeing the monitoring system.

### 7.2.2 Level 2

A Level 2 alert will be generated automatically by the monitoring system when one or more data channels records a reading that is out of the bounds of the established threshold. This may be due to erroneous channel readings or indicate a physical event that requires additional investigation.

### 7.2.3 Level 3

A Level 3 alert will be generated manually if the review of a Level 2 alert by BDI indicates that a true threshold exceedance has occurred that requires additional review. Some of the key methods for determining if a threshold exceedance represents a true physical response include:

- The value must be physically possible. An unreasonably high/low response likely indicates a sensor reading or channel anomaly.
- The high/low value should not be a single data point. A single data point sampled at 100 Hz indicates a sensor reading anomaly and not a physical response.
- The data should maintain a reasonable variation. If the data points are reading consistently unreasonably high, unreasonably low, or bouncing between very high and very low values, it indicates a problem with the sensor reading.

Once the data is determined to represent a physical response, the severity of the event must be further evaluated as described in the Level 4 alert. If the alert is not escalated to a Level 4 alert, BDI and ESC will communicate at least every thirty minutes as the data is closely monitored and relevant CCTV footage (provided by ITS) is reviewed. This level of monitoring and observation will continue until the cause of the threshold exceedance is established and eliminated and the data returns to normal levels.

### 7.2.4 Level 4

A Level 4 alert is issued when it is determined that the response of the bridge has risen to emergency level. This occurs when the severity and/or duration the excessive response is determined to pose a risk to the safety of the bridge and its motorists as determined by ESC, along with any additional information from observations onsite or via CCTV. The response to a Level 4 alert is to be carried out in accordance with the Emergency Response Plan (ERP, see Section 7.4).

## 7.3 Alert Communication and Response

Figure 65. illustrates the procedure for response to the four alert levels. The relevant offices or personnel are indicated in square brackets for each response. Level 1 and some Level 2 alerts will be automatically generated by the monitoring system and communicated via text message and email to those in the appropriate distribution lists (see Table 1). Level 3 and 4 alerts, and some

Level 2 alerts will be initiated by BDI, ESC or DSMO upon review of data. These alerts will also be sent to pre-established text/email distribution lists as outlined below. The same distribution lists will be used to communicate when an alert level has been resolved.

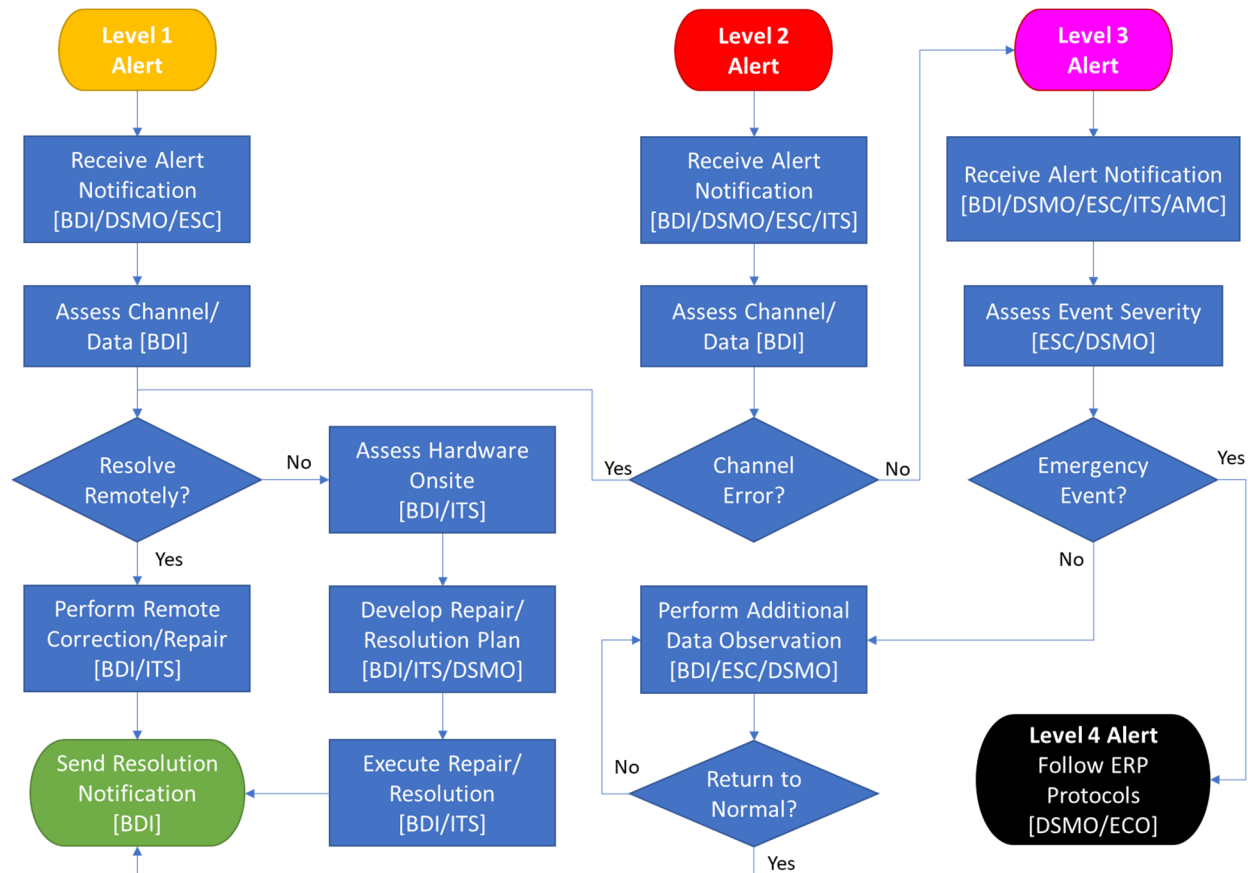


Figure 65. Procedure for communication of different alert levels. The responsible entity is shown in square brackets.

Table 12 provides a draft of the distribution lists that will receive each alert level. BDI will work with the ESC (currently TY Lin) and the DSMO to finalize the distribution lists and implement them in PI. The lists should be maintained by the Skyway Project Manager in the DSMO office and audited annually.

Table 12. Alert Distribution List

Name	Organization [Abbreviation]	Title/Role	Alert Levels			
			1	2	3	4
Jim Jacobsen	FDOT Districts 1 and 7 [DSMO]	Structures Maintenance Engineer	•	•	•	•
Daniel Buidens	FDOT Districts 1 and 7 [DSMO]	Skyway Project Manager	•	•	•	•
Jesse Sipple	BDI, Inc. [BDI]	Engineering Program Manager	•	•	•	•
Ivan Gualtero	Engineering Services Contractor, TY Lin [ESC]	Senior Structural Engineer	•	•	•	•
Atiq Alvi	Engineering Services Contractor, TY Lin [ESC]	Vice President	•	•	•	•
Jared Roso	FDOT District 7 [ITS]	IT Manager		•	•	•
Andrew Young	TransCore [ITS]	Senior Associate		•	•	•
Peter Martin	Asset Maintenance Contractor, DBi Services [AMC]	Point of Contact			•	•
Angela Aborizk	FDOT District 7 Emergency Coordination Officer [ECO]	Emergency Coordination Officer				•

#### 7.4 Response to Emergency Alerts (Level 4)

When a Level 4 alert is issued, the response will be coordinated according to the FDOT D7 “Bob Graham Sunshine Skyway Bridge Emergency Response Plan” (ERP), most recently updated in 2017. The ERP ensures timely and coordinated responses by the various state agencies and contractors responsible for aspects of the Skyway operation, safety, and maintenance and it references the District Seven Comprehensive Emergency Management Plan (CEMP). The contents of the ERP are confidential and, therefore, not provided in this report. The D7 Emergency Coordination Officer (ECO) oversees the emergency management as outlined in the ERP.

#### 7.5 Reporting

In addition to monitoring event thresholds, the routine monitoring system operation requires the generation of reports on a weekly, monthly, and yearly basis. These reports will provide data plots of the mean, minimum, and maximum measured value recorded each hour for environmental and acceleration-based channels and daily for GPS channels. The reports will also provide the mean, minimum and maximum values for each channel for the reporting period and note the percent change from the previous reporting period. The reports will also contain the status of each installed sensor and incident reports associated with alerts generated during the reporting period. The plots for the reports will be automatically generated by PI; however, the D7 Skyway Project Manager is responsible for compiling, checking, and transmitting the reports to the ESC for review.

## 8 Recommended Alert Thresholds

The statistical analysis of the data recorded during 2020 provides the basis of the thresholds recommended for generating alerts from the web interface. The procedure for establishing these thresholds is:

- Collect data for several months (in this case a year)
- Eliminate non-physical outliers
- Calculate the mean and standard deviation response values
- Determine the bounds as a number of standard deviations from the mean that encompass at least 99% of all measurement points
- Continue to refine the bounds as more response data becomes available (e.g., annually)

As existing sensors are repaired, and additional sensors are added to the system, a similar procedure may be used to establish alert thresholds.

It is important to note that these thresholds are not the same as an assessment of structural capacity; complementary finite element and structural analysis are required to establish capacity. However, it can be reasonably assumed that the structural capacity of the Skyway bridge elements was not exceeded in 2020 since no excessive (above design) loading events occurred and the structure did not experience any failures or damage.

The recommended cable acceleration alert thresholds are given in Table 13. These values are the mean hourly maximum accelerations recorded in 2020 plus 3.2 standard deviations, rounded to the next whole mg. These values can be input directly into the web interface by BDI.

Approximately 80 events during 2020 (primarily on the cables) would have exceeded these thresholds, mostly due to high winds. As a practical matter, the person evaluating the threshold exceedance alert will assess the conditions causing the excessive vibration and the duration of the high vibrations to determine if further action is required; in many cases no action will be required beyond monitoring of subsequent measurements. The recommended response plan outlined in Section 7 provides additional detail on response to system alerts.

Table 13. Recommended maximum acceleration thresholds for currently working sensors (mg).

<b>Cable 13Y</b>	<b>Cable 13Z</b>	<b>Cable 18Y</b>	<b>Cable 18Z</b>	<b>Tower X</b>	<b>Tower Y</b>
131	147	116	152	32	31

For simplicity, the constant threshold approach is recommended for setting cable tension bounds. While a temperature-based approach may provide more accuracy, it is not likely to result in better safety outcomes. The recommended thresholds for cable forces are the 2020 mean +/- 3.2 standard deviations, rounded to the nearest whole kip, as shown in Table 14. The application of these thresholds in the web interface first requires the establishment of a Cable Force virtual channels that provides cable force estimates once per hour. The thresholds can then be applied to the virtual channels to generate alerts if the channel results are outside of the bounds.

Table 14. Recommended cable force thresholds (kips).

	<b>Cable 13Y</b>	<b>Cable 13Z</b>	<b>Cable 18Y</b>	<b>Cable 18Z</b>
Low Threshold	1672	1695	1848	1878
High Threshold	1722	1727	1905	1925

## **9 System Security Plan**

Chapter 60GG-2 of the Florida Administrative Code (FAC) describes a set of cybersecurity standards for information technology (IT) resources. State Agencies must comply with these standards in the management and operation of state IT resources. As such, the Sunshine Skyway Monitoring System (SSMS) must adhere to these standards as well. To this end, a System Security Plan (SSP) was developed for the SSMS which outlines the security configuration of a system, identifies risks and vulnerabilities, and addresses how the risks will be mitigated. Security Plans are considered confidential and exempt from Section 119.07(1), F.S., pursuant to Sections 282.318, F.S. SSPs shall only be made available to those individuals with a business need to view, process, or maintain the plan. As such, the SSP itself cannot be provided herein.

The SSP was developed using a template (Version 8.1) provided by the FDOT Information Security (InfoSec) Administration Office. Use of this template ensures that the requirements from Chapter 60GG-2, F.A.C., are addressed. During development, the document was shared between stakeholders internally (InfoSec, DSMO, etc.) through a secure SharePoint site and externally (UF, BDI, etc.) through the use of a secure File Transfer Appliance (FTA). An updated draft system security plan (SSP) for the SSMS has been prepared by the research team based on input from DSMO, InfoSec, and BDI. The SSP (Version 1.8) is currently under review by InfoSec. Finally, it is noted that the SSP is considered a “living” document that gets updated to incorporate new and/or modified security controls any time the system goes through a major modification. As such it is expected that additional updates to the plan will be made when the contract with BDI is resumed and the re-branding effort between PI and II is completed.

## **10 Conclusions**

This project has resulted in a Sunshine Skyway Monitoring System (SSMS) framework that provides remote access to the sensors on the bridge through a web portal, a web map and interactive inventory database for all monitoring components installed on the bridge, data processing algorithms for cleaning the data and generating critical response information (cable vibration, North Tower vibration, and cable force), thresholds of typical response values, an alert response plan for when typical response values are exceeded, and user manuals for accessing and updating the system components.

BDI was selected as the contractor to develop the web portal and created a flexible system for the visualization of the data being measured by the sensors installed on the bridge. The system currently displays triaxial accelerometer data from four cables and the North Tower as well as wind speed, wind direction, and temperature. The system is also setup to display GPS data; however this data is not currently available. Virtual channels may be added in the future to display



hourly cable force estimates. Threshold values can be set so that the system can generate and send alerts when the thresholds are exceeded.

Detailed description of the methods and approaches for the analysis of one year of environmental and vibration data collected from the Sunshine Skyway Bridge have been presented. Overall, the quality of the data is good, exhibiting consistent results and reasonable variations in response to environmental and traffic loading conditions. Outliers in the data (both non-physical and other outliers) represent a less than 0.03% of the recorded data; the notable exception to this is the wind direction, which had 1.3% of values out of the expected 0-360° range. The reason for some high measurement values in some of the data channels is unknown but their occurrence is rare and not correlated to any known extreme loading event.

Year-long hourly response data and statistics have been presented, showing clear traffic- and temperature-dependent response amplitudes. The amplitude of cable and tower vibration is primarily driven by traffic loading on a day-to-day basis, exhibiting higher amplitudes during the day and lower amplitudes overnight. The exception to this pattern is high wind events, which induce higher cable vibrations, especially in the Z-direction.

The method for estimating cable forces from vibration measurements has been presented, including the conditions for eliminating an hourly cable force estimate based on poor regression analysis results. Cable forces are inversely proportional to ambient temperature, which is evident in daily and seasonal variation in estimated force values. Wind loading does not appear to impact cable forces. Forces estimated from Cable 13 Y acceleration measurements are not as consistent as Cable 13 Z or the either axis of Cable 18; however, the results are still reasonable.

The statistical analysis of the hourly response values provides the basis for establishing bounds of typical bridge behavior. These bounds are used to set recommended alert thresholds for implementation in the SSMS web interface. The current bounds have been set to encompass at least 99% of all the data recorded per measurement channel in 2020, after the removal of non-physical outliers, and are expected to be well below any structural capacity limits. Wind and traffic loading patterns are not used in setting alert thresholds but are useful in the manual review of data. Responses that do not follow the typical patterns are likely the result of high wind events.

Alert levels have been defined and personnel roles have been established for responding to them. D7 has the ultimate responsibility to determine and adopt the Skyway alert response protocols to meet their operational needs. Dedicated staff within the D7 DSMO (e.g. the Skyway Project Manager) will be required to ensure that the response plans and reporting are carried out as required.

Some of the desired web portal functionality has yet to be fully realized as the result of budget and contracting constraints during the project. The information provided in this report has laid a clear foundation for finalizing the remaining outstanding items, including the addition of cable force virtual channels, data alert thresholds, and an alert response plan. Future efforts will require an ongoing contract with BDI and dedicated DSMO staff to manage the project.

The appendices of this report provide guidance on the usage of the web portal, procedures for modifying the web map and inventory database, instructions for downloading raw data, and MATLAB code for processing the data to generate cable forces and other data statistics.

## 11 References

Bridge Engineering Solutions (2010). “Stay Cable Force and Damping Measurements for the Sunshine Skyway Bridge, St. Petersburg, Florida,” Lewiston, NY.

Bridge Engineering Solutions (2012). “Limited Cable Stay Monitoring of the Sunshine Skyway Bridge,” Lewiston, NY.

Bridge Engineering Solutions (2015). “Stay Cable Force and Damping Measurements for the Sunshine Skyway Bridge, St. Petersburg, Florida,” Youngstown, NY.

Figg Engineering Group (1988). “Manual for Inspection and Maintenance of the Sunshine Skyway Bridge Segmental Concrete Approaches and Main Span”, Tallahassee, FL.

Kim, B. H. and Park, T. (2007). “Estimation of cable tension force using the frequency-based system identification method,” *Journal of Sound and Vibration*, 304(3–5), 660-676.

PB Americas, Inc. (2010). “Sunshine Skyway Bridge Manual 2 for Inspection and Maintenance.”

VSL Corp. (1987). “Stay Cable Tensioning Data.”

## 12 Appendix A. Editing the Inventory Database and Interactive Web Map

To identify and assess the condition and challenges of the existing monitoring hardware installed on the Sunshine Skyway Bridge by the FDOT and other organizations, a comprehensive inventory database and interactive web map were developed as part of Phase I. This system has since been upgraded as part of Task 2 of Phase II. This appendix provides a user's guide to the Phase II version of the inventory database and web map. A similar guide for the Phase I version can be found in a previous report.

The inventory database consists of a simple Excel spreadsheet. The interactive web map was constructed using Leaflet, an open-source JavaScript library. Links to both the database and web map, as well as the main directory, have been provided to the SSMS stakeholders listed in Table 1 of this report. From the main directory, zip files containing the inventory database, web map, mapping tiles, and the necessary html and JavaScript libraries necessary to view/edit both the database and web map locally on any computer, using only a web browser, can be downloaded. Alternatively, the content of these two zip files could be placed on an intranet/internet-facing web server to allow multiple people the ability to view the same data simultaneously. The method by which additional information and items are added to the web map has been made easier since Phase I, in that the data can be read directly from the database. This is significant, as it provides a medium for researchers and the FDOT to more easily expand or modify the inventory database and web map in accordance with their needs.

To illustrate how to add additional data to the database and web map, a simple example follows which leverages the high-resolution base map of the bridge to identify and mark northbound and southbound cars near the North tower. While marking cars is not something that will be done in the web map, this example is representative of other more useful information that could be added to the database and web map such as the locations of new sensors, pavement test sections, previous/future maintenance work, etc. To begin, the two zip files are downloaded and copied to a folder and then unzipped in place. With this local copy, it is possible to edit the map to one's preference, as any changes will take place locally on the user's personal computer. To mark the cars on the web map, changes will be made to the "Inventory.xlsx" file within the "Database-v2" which is found in the unzipped file.

The local web map can be opened by opening the "index-v2.html" file and then selecting "Web Map". From this page, the user must manually select the CSV file, which can be found in the "Database-v2" file, in the top left corner of the web page. This software was designed to be run on a local computer, so the manual selection of the CSV file was added to address a security issue that most browsers had with reading an HTML file locally. In the future, the software will be hosted on a private/public webserver, at which point the web map will be altered to automatically select the appropriate CSV file from the webserver. The browsers in Table 15 are all compatible with the web map and inventory database.

Table 15. Compatible browsers.

<b>Internet Explorer</b>
<b>Microsoft Edge</b>
<b>Google Chrome</b>
<b>Firefox</b>
<b>Safari</b>

### 12.1 Excel Sheet Organization

The Excel sheet for the inventory database from Phase I was organized using tabs, which pertained to each office, as well as a tab for general points of interest and a collection of all manuals in the database. The data pertaining to the different offices and general points of interest has since been condensed into a single tab, and the collection of manuals is still located in a separate datasheet tab. Figure 66 below shows a view of the inventory database excel file, which includes the columns used to describe the item marked as well as its location.

	Group	Category	Item	Type	Location	Identifier	Manufacturer	Manufacturer_Number
497	Points of Interest	Dolphin	Main Dolphin		NE Dolphin	102		
498	Points of Interest	Dolphin	Main Dolphin		NW Dolphin	101		
499	Points of Interest	Dolphin	Main Dolphin		SE Dolphin	104		
500	Points of Interest	Dolphin	Main Dolphin		SW Dolphin	103		
501	Points of Interest	Dolphin	Supplemental Dolphin		Northeast Quadrant	6N-2		
502	Points of Interest	Dolphin	Supplemental Dolphin		Northeast Quadrant	5N-2		
503	Points of Interest	Dolphin	Supplemental Dolphin		Northeast Quadrant	4N-2		
504	Points of Interest	Dolphin	Supplemental Dolphin		Northeast Quadrant	3N-4		
505	Points of Interest	Dolphin	Supplemental Dolphin		Northeast Quadrant	3N-3		
506	Points of Interest	Dolphin	Supplemental Dolphin		Northeast Quadrant	2N-6		
507	Points of Interest	Dolphin	Supplemental Dolphin		Northeast Quadrant	2N-5		
508	Points of Interest	Dolphin	Supplemental Dolphin		Northeast Quadrant	2N-4		
509	Points of Interest	Dolphin	Supplemental Dolphin		Northwest Quadrant	6N-1		
510	Points of Interest	Dolphin	Supplemental Dolphin		Northwest Quadrant	5N-1		
511	Points of Interest	Dolphin	Supplemental Dolphin		Northwest Quadrant	4N-1		
512	Points of Interest	Dolphin	Supplemental Dolphin		Northwest Quadrant	3N-2		
513	Points of Interest	Dolphin	Supplemental Dolphin		Northwest Quadrant	3N-1		
514	Points of Interest	Dolphin	Supplemental Dolphin		Northwest Quadrant	2N-3		

Figure 66. Sensor information in Excel worksheet

The purpose of each column shown in Figure 66 is explained in Table 16.

Table 16. Title and description of each column shown in Figure 66.

<b>Group</b>	<b>Identifies the office the marked item belongs to, or whether it is a general point of interest</b>
<b>Category</b>	General description of the item marked
<b>Item</b>	Exact description of the marked item
<b>Type</b>	Additional descriptive information about the item
<b>Location</b>	Description of the location of the item
<b>Identifier</b>	Further description of the location of the item or a specific way to point out the marker
<b>Manufacturer/ Manufacturer number</b>	Information about the maker of the item as well as the model number

Figure 67 shows a view of the inventory database excel file, which including the columns used to include images of the item marked as well as information about the image.

Pic1_Descript	Pic1_Filename	Pic1_Hyperlink	Pic1_Date	Pic2_Descri	Pic2_Filename	Pic2_Hyperlink	Pic2_Date
Container	20150921_140550_MM_	<a href="#">Link</a>	9/21/15	Device	20150921_140528_	<a href="#">Link</a>	9/21/15
Container	20151104_104711_MM_	<a href="#">Link</a>	11/4/15	Device	20150921_111726_	<a href="#">Link</a>	9/21/15
Container	20151104_102712_MM_	<a href="#">Link</a>	11/4/15	Device	20150921_105351_	<a href="#">Link</a>	9/21/15
Container	20151104_101917_MM_	<a href="#">Link</a>	11/4/15	Device	20150921_145008_	<a href="#">Link</a>	9/21/15
Container	20150921_143435_MM_	<a href="#">Link</a>	9/21/15	Device	20150921_143538_	<a href="#">Link</a>	9/21/15
Cabinet							
Cabinet							
Cabinet							
Cabinet							
Cabinet	20150921_140550_MM_	<a href="#">Link</a>	9/21/15				
Cabinet	20151104_104711_MM_	<a href="#">Link</a>	11/4/15				
Cabinet	20151104_102712_MM_	<a href="#">Link</a>	11/4/15				
Cabinet (Unm:	20151104_101917_MM_	<a href="#">Link</a>	11/4/15				
Cabinet	20150921_143435_MM_	<a href="#">Link</a>	9/21/15				
Cabinet							
Cabinet							
Cabinet							
Cabinet							

Figure 67. Image information in Excel worksheet.

Each image is described through a “Description”, “Filename”, “Hyperlink”, and “Date Taken” column. The purpose of each column shown in Figure 67 is explained in Table 17.

Table 17. Title and description of each column shown in Figure 67.

<b>Description</b>	<b>Broad description of what is seen in the image</b>
<b>Filename</b>	The exact filename of the image from the database
<b>Hyperlink</b>	The link to the image
<b>Date</b>	The date that the image was taken

Figure 68 shows a view of the inventory database excel file, which including the columns used to assign a location and properties to the item marker.

Feature_Type	Feature_Color	Feature_Coord_X	Feature_Coord_Y
line	red	55939	79567
line	red	56259	79812
point	green	49704	110950
point	blue	50117	110950
point	blue	51207	74135
point	blue	51862	74544
point	blue	52332	75579
point	blue	49704	76176
line	red	50117	76595
line	red	51207	76963
line	red	51862	77283
line	red	52332	110950
line	red	56937	110950

Figure 68. Marker type and location information

The purpose of each column shown in Figure 68 is explained in Table 18.

Table 18. Title and description of each column shown in Figure 68.

<b>Feature_Type</b>	<b>Indicates whether the marker is a point or line marker</b>
<b>Feature_Color</b>	Assigns a color to the marker
<b>Feature_Coord_X</b>	Assigns the X-axis pixel location on the basemap image
<b>Feature_Coord_Y</b>	Assigns the Y-axis pixel location on the basemap image

## 12.2 Datasheets Tab

When the Inventory file is downloaded from the web server, it includes a file that contains manuals and specification sheets for certain devices that are on the bridge. This allows for quick access to specific information on each device. If the user wishes to add a manual to their inventory, they should add certain information to this tab. The tab is separated into columns that are different than the ones used for the “Database” tab. The first column, “Device”, is used to describe the device by its Manufacturer and Model. The following column, “Description”, allows for the user to elaborate on the office and general location of the device. The “Internet Link” column contains direct web links for each manual, while the “Local Hyperlink” column directly refers to the inventory located on the personal computer. The “Filename” refers to the filename of the document located in the inventory, while “Download Date” allows the user to state when each manual was downloaded. Subsequently, “Rev. Date” contains information pertaining to when each manual was revised by each manufacturer. To ensure that the manual is referring to the correct device, one may add a picture of the object. “Picture Filename”, “Picture Hyperlink”, and “Picture Date” all follow similar formats to the office tabs.

## 12.3 Establishing Points to Place Markers

The markers that show up on the map when a category is chosen from the control panel in the upper right-hand corner of the web map are placed based on map coordinates of the basemap (and its associated tiles). The coordinates reflect a specific position that is unique to a certain point on the photograph, and are placed on points of interest that the user wishes to identify and elaborate on. For example, on the initial map, when the user clicks on the control panel icon, a list of offices is displayed that have different devices on the bridge. For the FDOT ITS (Florida Department of Transportation Intelligent Transportation System), one may click the “Roadway Camera” option, and a marker will appear at the location where every roadway camera (that is operated by that specific office) is located. The ultimate goal of a user is to place markers exactly where one wishes to identify their points of interest. In the case of the example that will be used in this report, the points of interest are the cars that are photographed near the north tower. To begin editing, go to the same control panel that houses the offices and click the last category labeled “Edit Mode.” Choose the “Mouse Click Event” option, as seen in Figure 69. This will allow the user to place a temporary marker anywhere on the map by initially clicking on any point. By clicking the dropped marker, the pop-up will display the exact map coordinates of its location. It is helpful to copy/paste these locations for future reference. Additionally, if the marker does not appear exactly where

desired, it can be dragged by holding down a click on the marker and moving it around with the mouse.

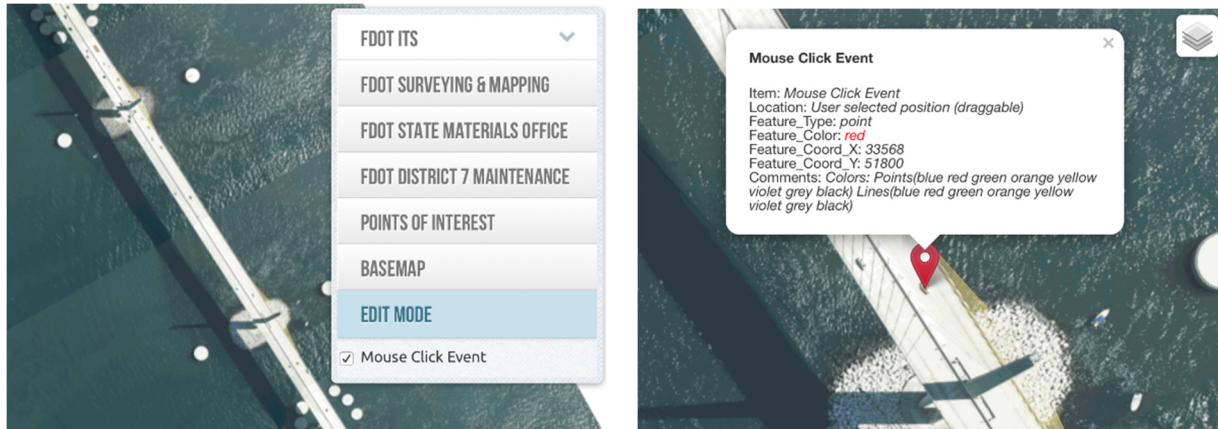


Figure 69. Screen shot of “Mouse Click Event” selection from the control panel (left) and screen shot of example resulting pop-up (right).

## 12.4 Adding Items to the Web Map and Inventory database

Using the exact coordinates of each prospective marker, which we obtained previously, one can now edit the map by modifying the Excel spreadsheet. Items can be added to the map by going into the appropriate tab within the Excel spreadsheet and adding a new row for the desired item, as seen in Figure 70.

Group	Category	Item	Type	Location	Identifier	Feature_Type	Feature_Color	Feature_Coord_X	Feature_Coord_Y
Car	Other	Vehicle	NB	North Tower		point	blue	31973	49309
Car	Other	Vehicle	NB	North Tower		point	blue	31888	49170
Car	Other	Vehicle	NB	North Tower		point	blue	31935	49172
Car	Other	Vehicle	SB	North Tower		point	red	31786	49206
Car	Other	Vehicle	SB	North Tower		point	red	31896	49436
Car	Other	Vehicle	SB	North Tower		point	red	31906	49380
Car	Other	Vehicle		North Tower		point	red		
Car	Other	Vehicle		North Tower		point	red		
Car	Other	Vehicle		North Tower		point	red		
Car	Other	Vehicle		North Tower		point	red		

Figure 70. Modifications to the Excel Inventory showing how the Car Example would be added.

Once a row containing the necessary information about the new item has been added, the excel file must be saved as an XLSX file, and then saved again as a CSV file in the “Database-v2” folder, as seen in Figure 71. The CSV file is what will be read by the web map; the XLSX file is used for editing purposes simply because it is more user friendly.



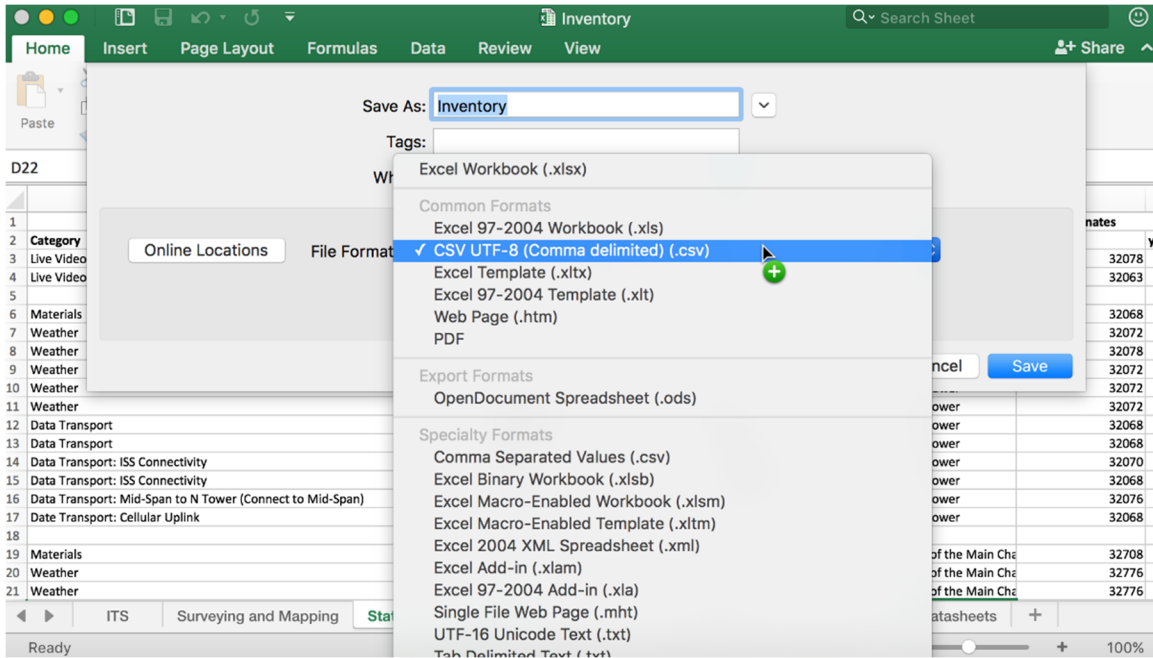


Figure 71. Saving spreadsheet as a CSV file

At this point, the new marker should be visible on the web map, in the desired location and the appropriate information should be displayed in the pop-up, as seen in Figure 71.

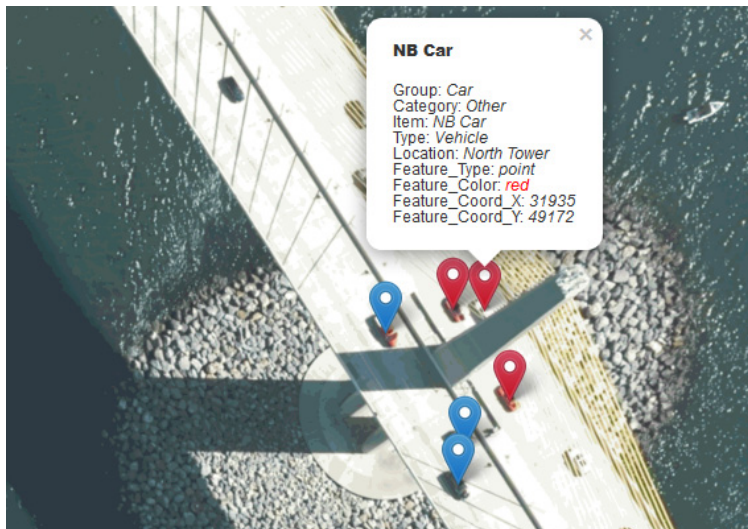


Figure 72. Cars marked on the web map.

## 13 Appendix B. BDI PI User Manual



RAW DATA. REFINED RESULTS.



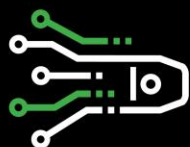
**Platform**Interactive

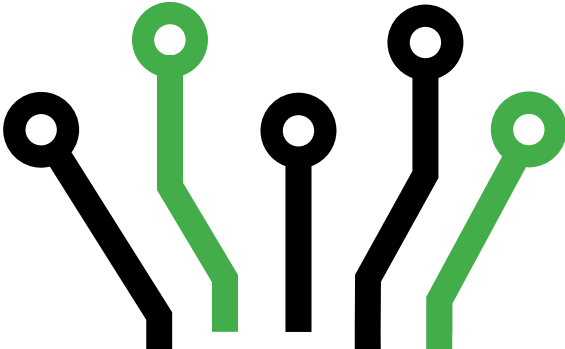
ONLINE SENSOR MANAGEMENT

APPLICATIONS

**DATA.BDITEST.COM**

# USER MANUAL





Document Revision History

<b>Version</b>	<b>Date</b>	<b>Changes</b>
1.0	2/18/2020	Initial release document
1.1	3/10/2020	Updated cover branding

No part of this operations manual may be reproduced, by any means, without the written consent of BDI.

The information contained within this manual is believed to be accurate and reliable. However, BDI assumes no responsibility for errors, omissions or misinterpretations. The information herein is subject to change without notification.

Copyright © 1989 – 2018

Bridge Diagnostics, Inc. (dba BDI)



# TABLE OF CONTENTS

1. Overview .....	5
2. User Access .....	5
3. Site Navigation .....	6
3.1 Projects Screen .....	6
3.2 Layouts .....	7
3.2.1 Image Layout .....	7
3.2.2 Map Layout.....	8
3.2.3 Graph Layout.....	9
3.2.4 Events Layout.....	10
4. Data Download .....	11

## 1. OVERVIEW

Platform Interactive is a cloud-based data management and presentation software suite that provides clients with remote access to data from deployed monitoring equipment. Users can view current and historic data, receive email or SMS notifications if data is out of range, and download selected data sets as needed.

## 2. USER ACCESS

All users must have a login and password in order to access data.bditest.com.

New users can be requested by emailing [monitoring@bditest.com](mailto:monitoring@bditest.com) with the following information:

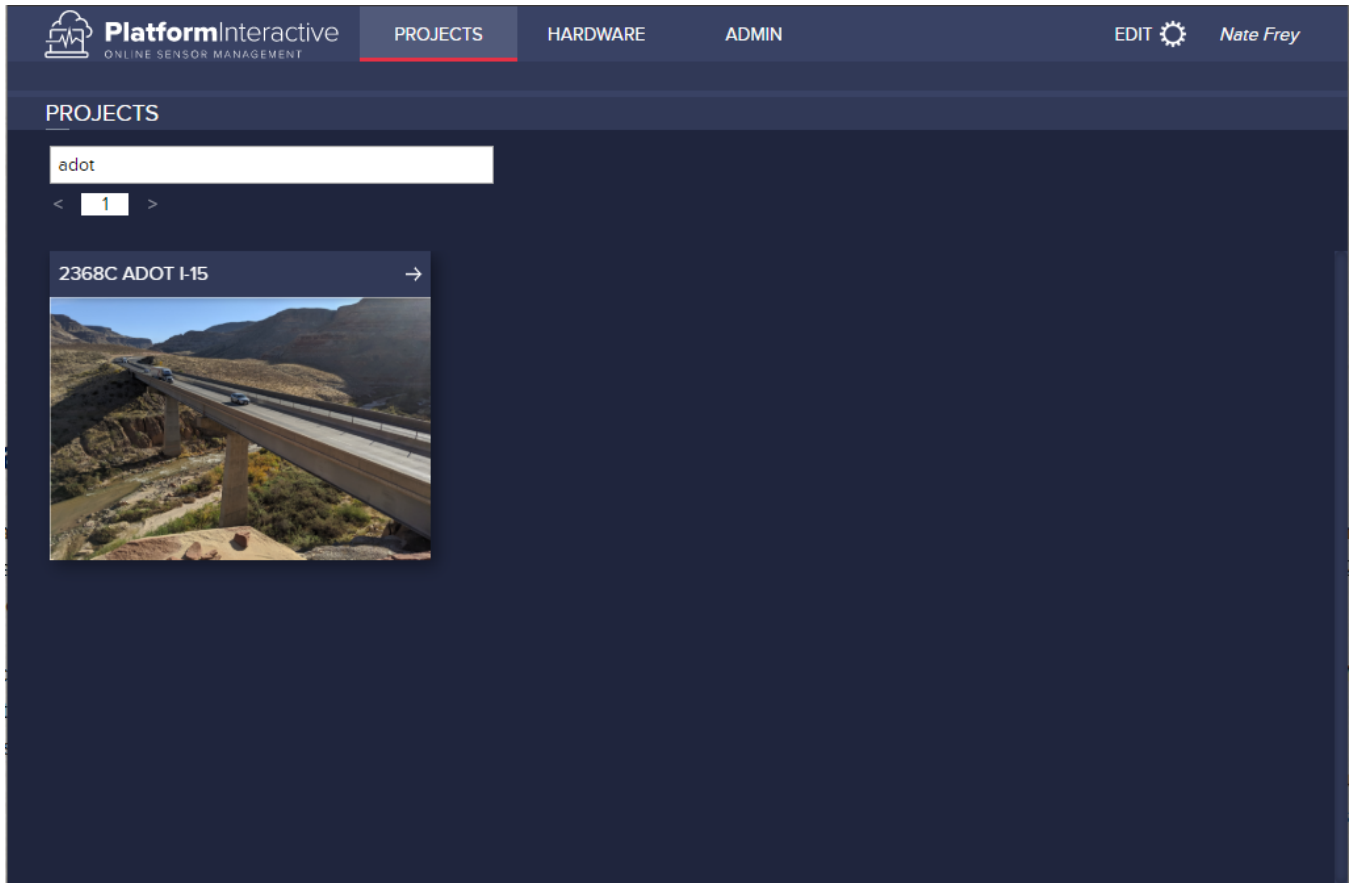
- Users first and last name
- Email address (if email notifications are desired)
- Cell phone number (if SMS notifications are desired)

Password reset requests and updates to notification settings should also be sent to [monitoring@bditest.com](mailto:monitoring@bditest.com).

## 3. SITE NAVIGATION

### 3.1 PROJECTS SCREEN

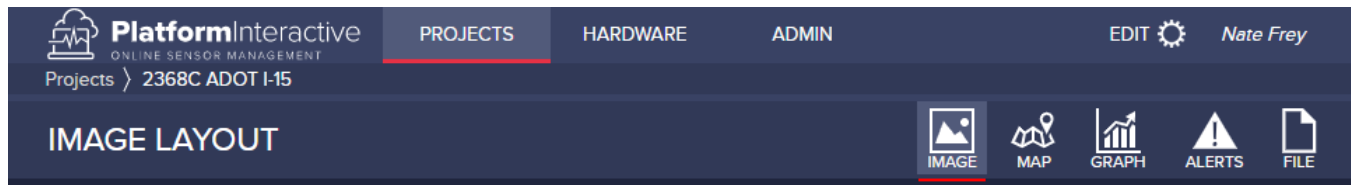
After logging in, users will first see the Projects screen. This allows the user to search for and select any projects associated with their account. Selecting the right arrow for a project will open the default layout for that project





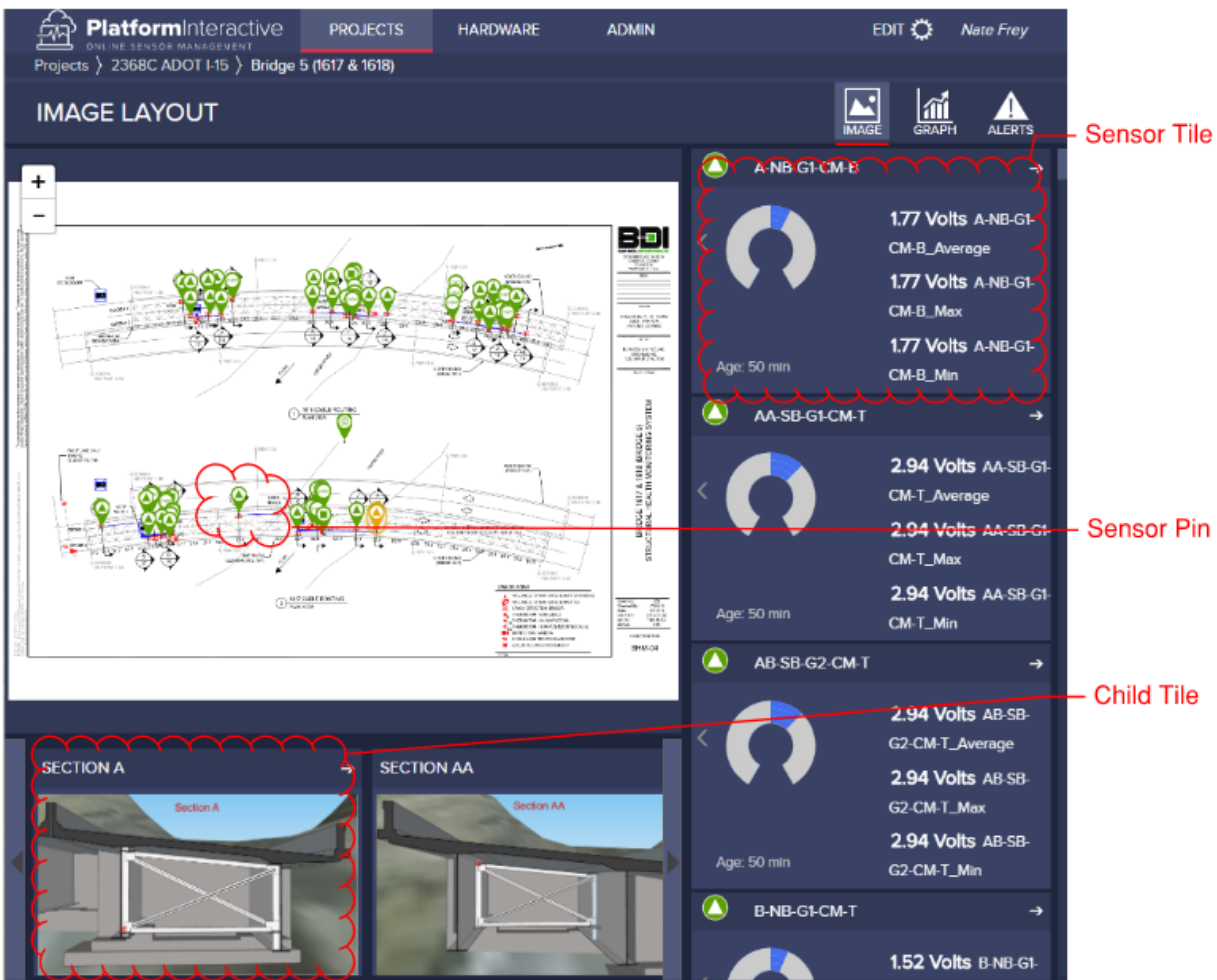
### 3.2 LAYOUTS

Content on the site is presented in one of several layouts. There is a top navigation bar to allow users to select the layout of interest.



#### 3.2.1 Image Layout

The Image Layout presents an image in the top left portion of the viewing window. Along the right column of the screen, there may be zero to many **sensor tiles** for individual sensors. Sensor tiles may have associated **Sensor Pins** identifying the location of the sensor on the image. Along the bottom row of the screen are **child tiles** leading to additional layouts.



### 3.2.2 Map Layout

The Map Layout will display a map in the top left portion of the window and will place sensor pins on the map for any sensor tiles that are included in the layout.

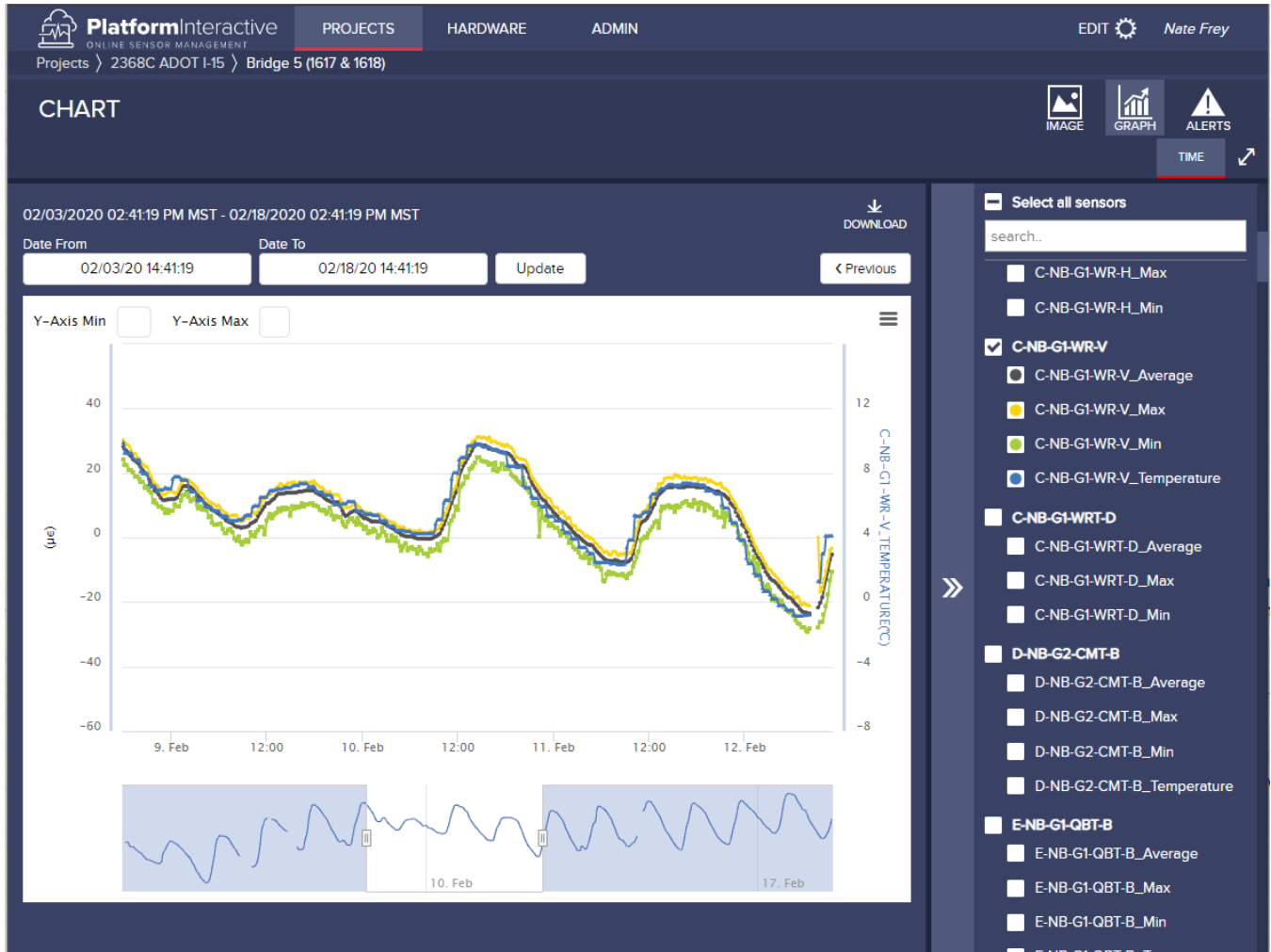
The screenshot displays the PlatformInteractive software interface. At the top, the navigation bar includes 'PROJECTS', 'HARDWARE', and 'ADMIN', with the user 'Nate Frey' logged in. The main title is 'MAP LAYOUT'. Below this, a map shows a street layout with a yellow sensor pin on 'Ponte Dom Pedro II'. To the right of the map is a sidebar with several panels:

- Camera 1:** Shows a night-time video feed from a camera. The timestamp is '02/17/2020 11:58:24 PM -03'.
- Camera 2:** Shows a night-time video feed from another camera. The timestamp is '02/18/2020 05:23:29 AM -03'.
- Events:** Shows the latest event occurred on '02/18/2020 05:21:25 AM -03'.
- Weather Station:** Displays current weather data:
  - Temperature: 28.53 °C (Age: 50 min)
  - Relative Humidity: 70.34 RH
  - Wind Speed: 2.01 m/s
  - Precipitation: 0 mm/h

At the bottom of the interface, there are two panels labeled 'Cabinet Group 1' and 'Cabinet Group 2', each showing a live video feed of a bridge structure with a large red number '1' and '2' overlaid on the bottom right of each feed.

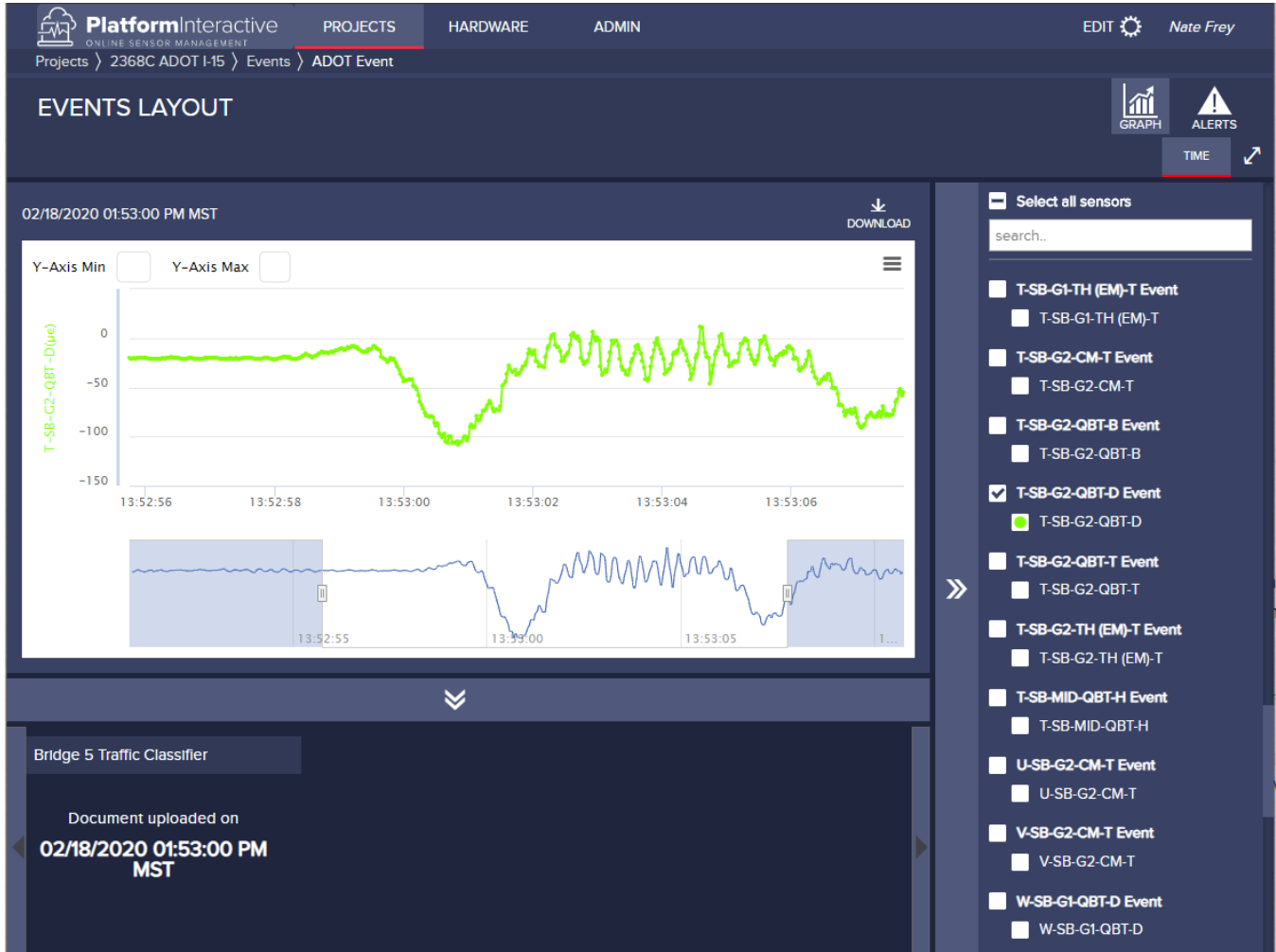
### 3.2.3 Graph Layout

The Graph Layout allows for visualization of selected sensors from the right column over selected time periods using the date picker in the top left. The graph can be zoomed to specific time windows using the handles on the lower preview graph.



### 3.2.4 Events Layout

The events layout will include a graph layout consisting of all sensor data for the duration of the event. It will also provide a lower menu of related documents and/or images to view or download related to the event.

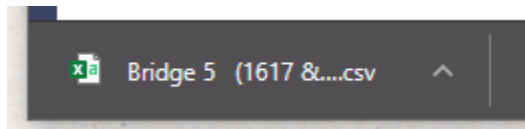


## 4. DATA DOWNLOAD

From the graph layout, the selected sensors over the selected time range can be downloaded using the download link in the top right of the graph.



Downloaded data will be available in .csv format.

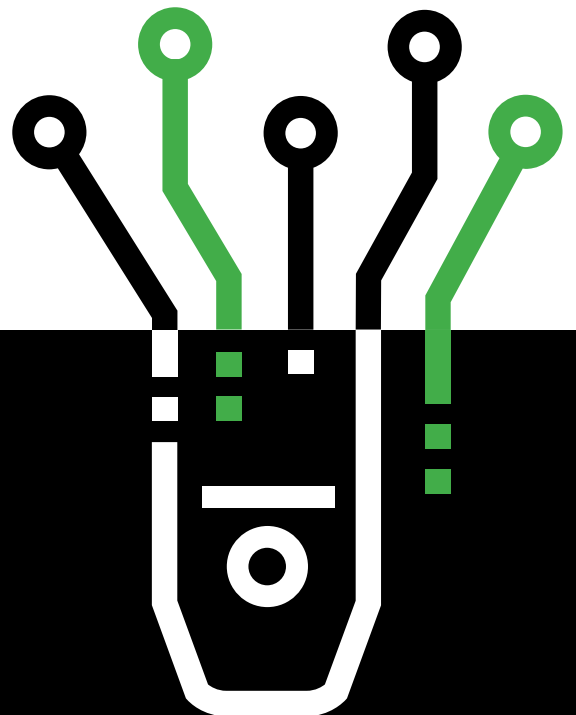






RAW DATA. REFINED RESULTS.

**DATA YOU CAN TRUST.**  
**RESULTS YOU CAN BUILD ON.**



P +1.303.494.3230 740 S PIERCE AVE UNIT 15  
F +1.303.494.5027 LOUISVILLE CO 80027

BDITEST.COM  
sales@bditest.com

## 14 Appendix C. Alternate Approaches to Downloading Data

Although the primary mechanism for users to obtain raw data is through the download capabilities in the web interface, several low- and medium-level methods exist should II become unavailable for some reason.

It is possible to directly access the data acquisition computer through TeamViewer (or via the legacy approach based on RDP). During the data collection process, data from the BDI sensors on the bridge (accelerometers, weather station, etc.) is first stored on this computer before it is uploaded to II through the Internet. Based on the disk capacity of this system and through the use of compression tools (e.g. 7-Zip), several months of data is kept on this computer before being eventually purged. If II is unavailable, a direct connection to this computer can be used to download the recent historical data (Figure 73). Downloading of files through TeamViewer can be achieved using Drag and Drop in Windows (would also work for RDP connections) or via TeamViewer “File Transfer” which appears in the Windows context menu. Further details on the file transfer process can be found at the TeamViewer website (<https://www.teamviewer.com>) under Resources/Documents. Additional tips and tricks can be found in the TeamViewer Community Blog.

Similarly, it is also possible to directly access the GPS receivers and download recent data. Storage on these systems is relatively small and thus only a few hours- to days-worth of data would be available for download depending on their configuration. The methods by which data would be obtained are technically complex and would require the knowledge and direct use of Leica software. As such, it is not anticipated that DSMO would ever access data in this way; thus, documentation on required steps for obtaining data in this manner is not described herein. Should there ever result a situation in which obtaining GPS data directly from the receivers would be beneficial, it is recommended that DSMO consult with the Surveying and Mapping Office as their experience in using these systems and the required software is significant.



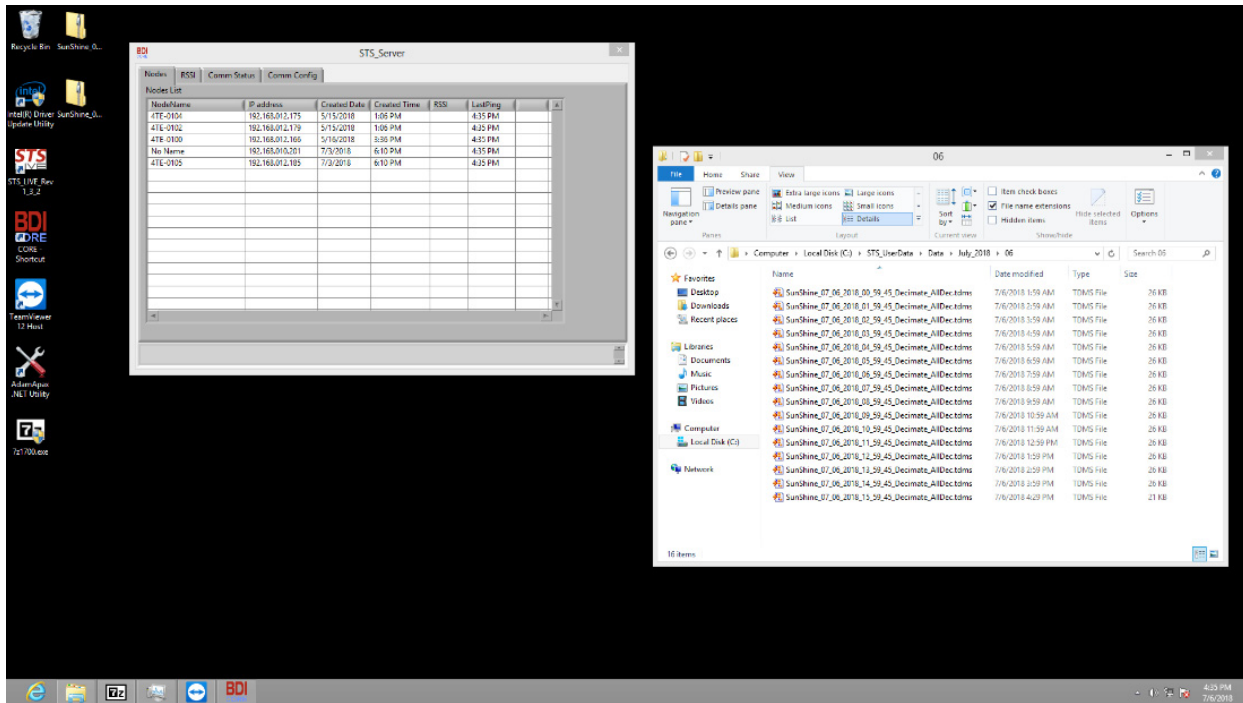


Figure 73. Screenshot of the data acquisition computer via a remote TeamViewer connection showing raw data files which can be downloaded.

Although the primary endpoint of system data is II, BDI also makes the raw data available at a medium-level through a BDI-branded FileCloud account. Access to this system is controlled by BDI with each use requiring access being authorized by DSMO. Each week, BDI packages the collective data files together manually into a single Zip file and then makes it available on FileCloud. As the II system was under development during the project, this approach was used by UF whenever data needed to be obtained for analysis. Depending on how the system was configured at the time (e.g., raw data or post-processed summary/analyzed data), different types of data was made available (Figure 74). However, for purposes of the UF analysis, only the high-speed data was downloaded (Figure 75). After FileCloud account creation by BDI, a web link and credentials will be provided to the user. The user simply clicks on the link opening up a website in an Internet browser, enters the credentials, and then files can be selected. Once selected, files are downloaded when the “Download” button is clicked (Figure 76).

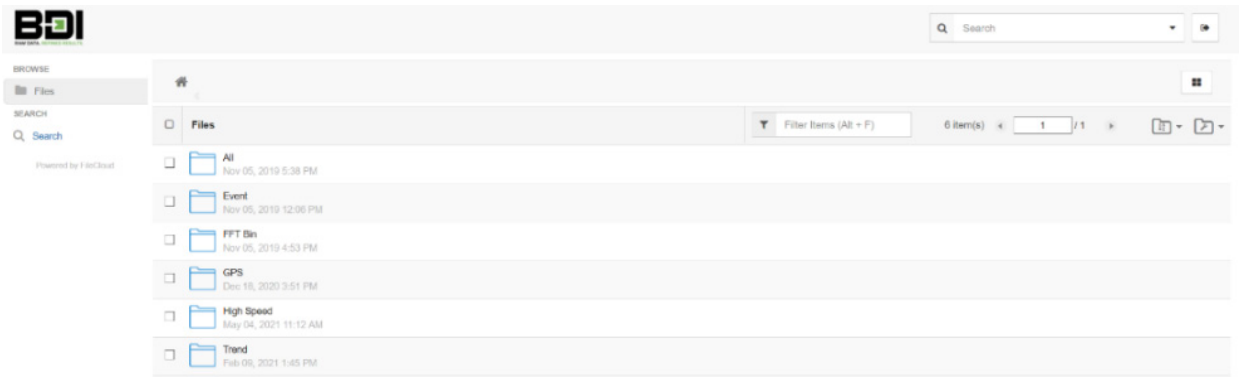


Figure 74. Types of data available for download through the BDI-branded FileCloud web application.

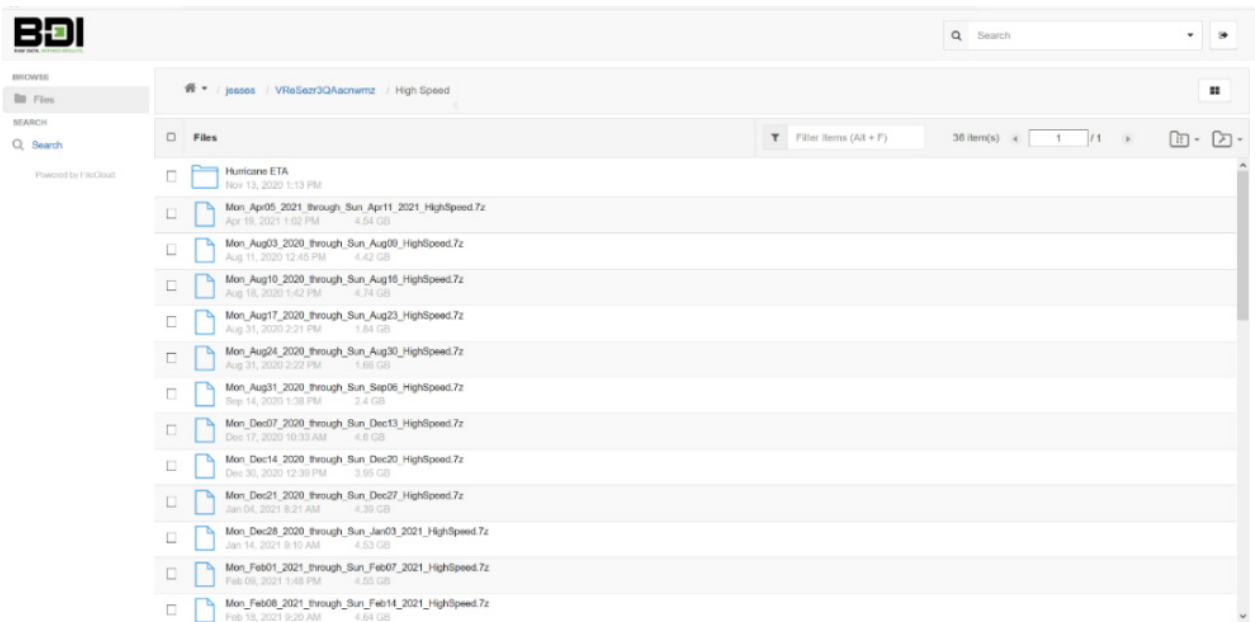


Figure 75. High speed (200 Hz) data files available for download through the BDI-branded FileCloud web application.

BROWSE

Files

SEARCH

Search

Powered by FileCloud

Home / jesses / VReSez3QAacnmz / High Speed

Download 3 items selected

Filter Items (Alt + F) 36 item(s) 1 / 1







<input type="checkbox"/>	 Hurricane ETA Nov 13, 2020 1:13 PM
<input checked="" type="checkbox"/>	 Mon_Apr05_2021_through_Sun_Apr11_2021_HighSpeed.7z Apr 19, 2021 1:02 PM 4.54 GB
<input checked="" type="checkbox"/>	 Mon_Aug03_2020_through_Sun_Aug09_HighSpeed.7z Aug 11, 2020 12:45 PM 4.42 GB
<input checked="" type="checkbox"/>	 Mon_Aug10_2020_through_Sun_Aug16_HighSpeed.7z Aug 18, 2020 1:42 PM 4.74 GB
<input type="checkbox"/>	 Mon_Aug17_2020_through_Sun_Aug23_HighSpeed.7z Aug 31, 2020 2:21 PM 1.84 GB
<input type="checkbox"/>	 Mon_Aug24_2020_through_Sun_Aug30_HighSpeed.7z Aug 31, 2020 2:22 PM 1.66 GB

Figure 76. After files to be downloaded have been selected, a “Download” button appears.

## 15 Appendix D. Data Analysis Code (MATLAB)

### 15.1 unzip\_process\_writetofile.m

```
% MATLAB script which unzips (via 7z) a file and then processes the
% individual files extracted and writes to summary .mat files.
% Unzipped data files are removed after processing but zipped files are not.

% Justin R. Davis, Qiheng Fan, and Jennifer Bridge
% 6/28/2021
% v 2.0

% Clear out variables
clear all; close all; clc;
addpath(genpath('.\Version_2p5_Final'));

% Unzip
% Locations of 7z executable
Exec7z="C:\Program Files\7-Zip\7z.exe";

%Locations/extensions of zip files and the extension of the file to process

%ZipFileDir="..\Data\zipdata";
ZipFileDir="C:\Users\jenarice\OneDrive - University of Florida\Phase
II\Data\Data\DataFromWeb\weekly 7z Files";
ZipFileExt=".7z";
FileExt=".tdms";

% temporary directory where files will be extracted to
TempDir = "C:\Users\jenarice\Desktop\Temp";

% make sure 7z installed
if isfile(Exec7z)
    fprintf("7z exists\n")
else
    fprintf("7z (https://www.7-zip.org/) is not installed, exiting...\n")
    return
end

% Make sure temp dir exists
if isdir(TempDir)
    fprintf("Temp directory exists: %s\n", TempDir)
else
    fprintf("Temp directory does not exist, creating: %s\n", TempDir)
    mkdir(TempDir)
end
%

Dir=sprintf("%s\\*%s", ZipFileDir, ZipFileExt);
ZippedFiles=dir(Dir);
for cellZippedFile = {ZippedFiles.name}

    f_zip=sprintf("%s\\%s",ZipFileDir,cellZippedFile{:});
    fprintf("Extracting: %s\n", f_zip);

    Command=sprintf("%s" e "%s" -aos -o"%s", Exec7z, f_zip, TempDir );
    fprintf("    Command: %s\n", Command);
    [status,cmdout] = system(Command);
    if status
        fprintf("    Error: %s\n",cmdout)
        return
    else
        fprintf("    Success\n");
    end
end
```

Process each unzipped file

Loop through the files in the temp directory

```
fprintf("%s\\*%s",TempDir,FileExt);
TdmsFiles=dir(sprintf("%s\\*%s",TempDir,FileExt));
for cellTdmsFile = {TdmsFiles.name}
```

```

f_to_proc=sprintf("%s\\%s",TempDir,cellTdmsFile{:});
fprintf(" Processing: %s\n", f_to_proc)

% Do individual processing of individual files (f_to_proc) here

warning('off', 'signal:findpeaks:largeMinPeakHeight')

file_proc=char(f_to_proc);

file_split=strsplit(file_proc,'_');
month=file_split(3);
day=file_split(4);
year=file_split(5);
hour=file_split(6);
minute=file_split(7);
sec=file_split(8);

% output files

% Make sure SummaryFiles dir exists
SummDir=".\SummaryFiles";
%SummDir=".\SummaryFilesTest";
if isdir(SummDir)
else
    fprintf("SummaryFiles directory does not exist, creating: %s\n", SummDir)
    mkdir(SummDir)
end

file_out=strcat("SummaryFiles/SummaryOutput",'_',month,"_",day,"_",year,"_",hour,"_",minute,"_",s
ec, '.txt');

try
my_tdms_struct = TDMS_getStruct(file_proc);
catch ME
    fprintf('tdms file read error: %s, moving on\n', ME.message);
    fprintf(" Removing: %s\n", f_to_proc)
    delete(f_to_proc)
    continue; % Jump to next iteration of: for i
end

my_tdms_struct = TDMS_getStruct(file_proc);
time=(my_tdms_struct.AllNormal.Time.data)';
if isfield(my_tdms_struct.AllNormal,'TEMP')&& ~isempty(my_tdms_struct.AllNormal.TEMP.data)
temp=(my_tdms_struct.AllNormal.TEMP.data)';
else
temp=zeros(length(time),1);
end
if isfield(my_tdms_struct.AllNormal,'WIND_SPEED')&&
~isempty(my_tdms_struct.AllNormal.WIND_SPEED.data)
WS=(my_tdms_struct.AllNormal.WIND_SPEED.data)';
else
WS=zeros(length(time),1);
end
if isfield(my_tdms_struct.AllNormal,'WIND_DIRECTION')&&
~isempty(my_tdms_struct.AllNormal.WIND_DIRECTION.data)
WD=(my_tdms_struct.AllNormal.WIND_DIRECTION.data)';
else
WD=zeros(length(time),1);
end
lengths=[length(time),length(temp),length(WS),length(WD)];
datalength=min(lengths);

dt=time(2)-time(1); %timestep
fs=1/dt; %sampling rate

cables={'13','16','18','21'};
num_cables=length(cables);
ax={'_X','_Y','_Z'};
for i=1:num_cables
    for j=1:3
        heading=['Cable_',cables{i},ax{j}];
        vib_headings{j+3*(i-1)}=heading;
    end
end

for k=1:3
    vib_headings{i*j+k}=['Tower',ax{k}];

```

```

end
% Determine minimum data length to truncate all data to same length
num_vib=length(vib_headings);
for i=1:num_vib
    struct_name= ['my_tdms_struct.AllNormal.',vib_headings{i},'.data'];
    if isfield(my_tdms_struct.AllNormal,vib_headings{i})
        datalengthtest=length(eval(struct_name));
    else
        datalengthtest=0;
    end
    if datalengthtest == 0
        elseif datalengthtest>0&&datalengthtest<datalength
            datalength=datalengthtest;
        end
    end

% truncate data already pulled out:
time=time(1:datalength);
WS=WS(1:datalength);
temp=temp(1:datalength);
WD=WD(1:datalength);

% Pull out vibration data
vib_data=zeros(datalength,num_vib);
data=vib_data;
for i=1:num_vib
    struct_name= ['my_tdms_struct.AllNormal.',vib_headings{i},'.data'];
    if ~isfield(my_tdms_struct.AllNormal,vib_headings{i})
        D=zeros(datalength,1);
    else
        D=eval(struct_name);
    end
    if isempty(D)
        D=zeros(datalength,1);
    else
        D=D(1:datalength);
        data(:,i)=D;
        vib_data(:,i)=detrend(D');
    end
end

Data_d=[temp,WD,WS,vib_data ];
DataNames={'Temp','WD','WS'};

for i = 4:size(Data_d,2)
    DataNames(i) = vib_headings(i-3);
end

%Determine averages in time domain after detrending
mu_d=zeros(1,size(Data_d,2));
for i=1:size(Data_d,2)
    mu_d(i)=mean(Data_d(:,i));
end

%Determine standard deviations in time domain after detrending
sigma_d=zeros(1,size(Data_d,2));
for i = 1:size(Data_d,2)
    sigma_d(i)=std(Data_d(:,i));
end

%Determine RMS in time domain after detrending
RMS_d=zeros(1,size(Data_d,2));
for i=1:size(Data_d,2)
    RMS_d(i)=rms(Data_d(:,i));
end

%Determine the max accerlation amplitude
maxi = zeros(1,size(Data_d,2));
for i=1:size(Data_d,2)
    maxi(i)= max(abs(Data_d(:,i)));
end

```

Get Rid of cable data pertain to axial direction (X-direction)

vib\_headings\_e and vib\_data\_e means eliminate data in x-direction only for cables

```

for i=1:num_cables
    for j=2:3
        heading=['Cable_', cables{i}, ax{j}];
        vib_headings_e{2*i+j-3}=heading;
    end
end
for k=1:3
    vib_headings_e{i*(j-1)+k}=['Tower', ax{k}];
end
for i=1:length(vib_headings_e)
    struct_name_e= ['my_tdms_struct.AllNormal.',vib_headings_e{i},'.data'];
%     D=eval(struct_name_e);
    if ~isfield(my_tdms_struct.AllNormal,vib_headings_e{i})
        D=zeros(dataLength,1);
    else
        D=eval(struct_name_e);
    end
    if isempty(D)
        D=zeros(dataLength,1);
    else
        D=D(1:dataLength);
        data(:,i)=D;
        vib_data_e(:,i)=detrend(D');
    end

%     if isempty(D)
%         D=zeros(dataLength,1);
%         data(:,i)=D;
%         vib_data_e(:,i)=detrend(D');
%     else
%         D=D(1:dataLength);
%         data(:,i)=D;
%         vib_data_e(:,i)=detrend(D');
%     end
end
end

```

## Peaks finding algorithm

```

PeakNumber=20;
CableNumber=length(vib_headings_e);
mat_frqc=zeros(PeakNumber,length(vib_headings_e));
NFFT = 2^16; % 2^14 = 16384

for i=1:2 %cable_13_y and cable_13_z
    [p,f]=cpsd(vib_data_e(:,i),vib_data_e(:,i),[],[],NFFT,fs);
    indices = find(f>=0.7);
    f = f(indices);
    p = p(indices);
    [pks,locs] = findpeaks(abs(p),f,'MinPeakProminence',1.0*10^-7,'MinPeakDistance', 0.7);
    if length(locs)<PeakNumber
        continue
    end
    mat_frqc(:,i) = locs(1:PeakNumber);
end

for i=3:4 %cable_16_y and cable_16_z
    [p,f]=cpsd(vib_data_e(:,i),vib_data_e(:,i),[],[],NFFT,fs);
    indices = find(f>=0.7);
    f = f(indices);
    p = p(indices);
    [pks,locs] = findpeaks(abs(p),f,'MinPeakProminence',1.0*10^-7,'MinPeakDistance', 0.7);
    if length(locs)<PeakNumber
        continue
    end
    mat_frqc(:,i) = locs(1:PeakNumber);
end

for i=5:6 %cable_18_y and cable_18_z
    [p,f]=cpsd(vib_data_e(:,i),vib_data_e(:,i),[],[],NFFT,fs);
    indices = find(f>=0.66);
    f = f(indices);
    p = p(indices);
    [pks,locs] = findpeaks(abs(p),f,'MinPeakDistance',0.6,'MinPeakProminence',1*10^-8);
    if length(locs)<PeakNumber
        continue
    end
end

```

```

end
mat_frqc(:,i) = locs(1:PeakNumber);
end
for i=8 %cable_21_y and cable_21_z
[p,f]=cpsd(vib_data_e(:,i),vib_data_e(:,i),[],[],NFFT,fs);
indices = find(f>=0.5);
f = f(indices);
p = p(indices);
[pks,locs] = findpeaks(abs(p),f,'MinPeakDistance', 0.5,'MinPeakProminence',1*10^-10);
if length(locs)<PeakNumber
    continue
end
mat_frqc(:,i) = locs(1:PeakNumber);
end
for i=9:10 %tower_x and tower_y
[p,f]=cpsd(vib_data_e(:,i),vib_data_e(:,i),[],[],NFFT,fs);
indices = find(f>=0.5);
f = f(indices);
p = p(indices);
[pks,locs] = findpeaks(abs(p),f,'MinPeakDistance',0.4,'MinPeakHeight',1*10^-7);
if length(locs)<PeakNumber
    continue
end
mat_frqc(:,i) = locs(1:PeakNumber);
end
for i=11 %tower_z
[p,f]=cpsd(vib_data_e(:,i),vib_data_e(:,i),[],[],NFFT,fs);
indices = find(f>=0.5);
f = f(indices);
p = p(indices);
[pks,locs] = findpeaks(abs(p),f,'MinPeakDistance', 0.4,'MinPeakHeight',1*10^-8);
if length(locs)<PeakNumber
    continue
end
mat_frqc(:,i) = locs(1:PeakNumber);
end
end

```

## Subtracting frequencies from tower

```

mat_m=zeros(PeakNumber,length(vib_headings_e));
mat_m=mat_frqc;
for i=find(contains(vib_headings_e,'Tower_X')),find(contains(vib_headings_e,'Tower_Z'))]
    for j=1:PeakNumber
        for m=[find(contains(vib_headings_e,'Cable_13_Z')),...
                find(contains(vib_headings_e,'Cable_16_Z')),...
                find(contains(vib_headings_e,'Cable_18_Z')),...
                find(contains(vib_headings_e,'Cable_21_Z'))]
            for n=1:PeakNumber
                if mat_frqc(n,m)==mat_frqc(j,i)||mat_m(n,m)==0
                    mat_m(n,m)=0;
                else
                    mat_m(n,m)=mat_frqc(n,m);
                end
            end
        end
    end
end
mat = mat_m;
for i=find(contains(vib_headings_e,'Tower_Y'))
    for j=1:PeakNumber
        for m=[find(contains(vib_headings_e,'Cable_13_Y')),...
                find(contains(vib_headings_e,'Cable_16_Y')),...
                find(contains(vib_headings_e,'Cable_18_Y')),...
                find(contains(vib_headings_e,'Cable_21_Y'))]
            for n=1:PeakNumber
                if mat_m(n,m)==mat_m(j,i)||mat(n,m)==0
                    mat(n,m)=0;
                else
                    mat(n,m)=mat_m(n,m);
                end
            end
        end
    end
end

```



```

end
end

```

## Subtracting frequencies from deck.

```

mat_1=zeros(PeakNumber,length(vib_headings_e));
mat_1=mat;
A = 1:find(contains(vib_headings_e,'cable_21_z'));
% for i=1:8
%     for j=1:PeakNumber
%         for m=setdiff(A,i)
%             for n=1:PeakNumber
%                 if mat(n,m)==mat(j,i)||mat_1(n,m)==0
%                     mat_1(n,m)=0;
%                 else
%                     mat_1(n,m)=mat(n,m);
%                 end
%             end
%         end
%     end
% end

for i = 1:length(vib_headings_e)
    mat_1(:,i)=move_me(mat_1(:,i),0);
end

nf = 12; %number of frequency desired
ms = [145.631 145.162 146.229 143.651]; %masses per meter of cable 13 16 18 21, unit:kg/m
mass = [ms(1) ms(1) ms(1) ms(1) ms(3) ms(3) ms(4) ms(4)];
ls = [128.661 152.349 167.530 190.398]; %lengths of cable 13 16 18 21, unit:m
lgth = [ls(1) ls(1) ls(1) ls(1) ls(3) ls(3) ls(4) ls(4)];
nc = size(mat_1,2)-3; % the number of cable in y and z direction

for i = 1:nc %columns
    for j = 1:nf %rows
        X(j,i) = j^2;
        Y(j,i) = mat_1(j,i).^2/j.^2;
    end
end

%linear regression
for i = 1:nc %columns
    format long
    xx = [ones(length(X(:,i)),1) X(:,i)];
    b = xx\Y(:,i);

    %built-in function liner regression
    p = polyfit(X(:,i),Y(:,i),1);
    f = polyval(p,X(:,i));
    Rsq1(:,i) = 1 - sum((Y(:,i) - f).^2)/sum((Y(:,i) - mean(Y(:,i))).^2);

    slope(:,i) = b(2);
    intercept(:,i) =b(1);
    Ycalc1 = b(2)*X(:,i)+b(1);
    Rsq2(:,i) = 1 - sum((Y(:,i) - Ycalc1).^2)/sum((Y(:,i) - mean(Y(:,i))).^2);
end

% RMS preparation
rms_m = RMS_d(find(contains(DataNames,vib_headings_e)));%non-normalized RMS cable and tower
rms_v = mat2gray(rms_m(1:nc));%normalized RMS value between 0 and 1;for cable
rms_c = rms_m(1:nc);%non-normalized value for cable

%R2 check and Rms check
a_x = (1+2):1:(nc-2);

% Tension
for i = 1:nc
    T(i)=4*mass(i)*lgth(i)^2*intercept(i)/1000; %units:kN
    T1(i)=T(i)/4.448;%units:kip
    fprintf('Tension from %s is ',char(txt(i)));
    fprintf('\t%.2fkN\tor %.2fkip\n',T(i),T1(i));
end

%output preparation
R2 = zeros(18,1);
Tension = zeros(18,1);

```

```

Slope = zeros(18,1);
f1 = zeros(18,1);
txt = vib_headings_e(1:nc);
for i = 1:nc
    R2(find(contains(DataNames,txt(i))))= Rsq1(i);
    Tension(find(contains(DataNames,txt(i))))= T1(i);
    Slope(find(contains(DataNames,txt(i)))) = slope(i);
    f1(find(contains(DataNames,txt(i)))) = mat_frqc(1,i);
end
txt = vib_headings_e(1:11);
for i=9:11
    f1(find(contains(DataNames,txt(i)))) = mat_frqc(1,i);
end

```

## Output time domain and tensions

```

Heading = {'DataName', 'MEAN', 'STDEV', 'RMS', ...
           'MAX', 'TENSION', 'RSQUARE', 'SLOPE', 'fn'};

fileID = fopen(file_out, 'w');
fprintf(fileID, ...
        '%-15s\t%15s \t %15s \t %15s \t %15s \t %15s \t %15s \t %15s\n', ...
        char(Heading(1)),char(Heading(2)),char(Heading(3)),char(Heading(4)), ...
        char(Heading(5)),char(Heading(6)),char(Heading(7)), ...
        char(Heading(8)),char(Heading(9)));
table=[mu_d',sigma_d',RMS_d',max_i',Tension,R2,Slope,f1];
summ={DataNames,table};
for i= 1:size(table,1)
    fprintf(fileID, ...
           '%-15s\t %15.6f\t %15.6f\t %15.6f\t %15.6f\t %15.6f\t %15.2f\t %15.4f\t %15.6f \t
%15.6f\n', ...
           char(summ{1}(i),summ{2}(i,:)));
end
fclose(fileID);

```

## Done processing

```

clear D data Data_d vib_data_e temp WD WS

fprintf("      Removing: %s\n", f_to_proc)
delete(f_to_proc)

end

end

```

*Published with MATLAB® R2020b*

## 15.2 SummaryPlots.m

```
% MATLAB script that processes summary data files
% - removes outliers and bad data
% - plots time histories and correlation plots
% - generates statistics

% Jennifer Bridge
% 6/28/2021
% v 2.0

clear all; close all;
load results_test4.mat; %all hourly summary data from January - Dec, 2020

% Sort time and data
[t,idx]=sort(time,'ascend');
data=summarydata;
for i=1:length(DataNames)
    data(:,i)=summarydata(idx,i);
end

% Select relevant data to plot
PlotList={'Temp_mean'; 'WD_mean'; 'WS_mean'; 'WS_std'; 'WS_max';
'Cable_13_Y_rms'; 'Cable_13_Y_max'; 'Cable_13_Y_tension'; 'Cable_13_Y_r_2'; 'Cable_13_Y_fn';
'Cable_13_Z_rms'; 'Cable_13_Z_max'; 'Cable_13_Z_tension'; 'Cable_13_Z_r_2'; 'Cable_13_Z_fn';
'Cable_16_Y_rms'; 'Cable_16_Y_max'; 'Cable_16_Y_tension'; 'Cable_16_Y_r_2'; 'Cable_16_Y_fn';
'Cable_16_Z_rms'; 'Cable_16_Z_max'; 'Cable_16_Z_tension'; 'Cable_16_Z_r_2'; 'Cable_16_Z_fn';
'Cable_18_Y_rms'; 'Cable_18_Y_max'; 'Cable_18_Y_tension'; 'Cable_18_Y_r_2'; 'Cable_18_Y_fn';
'Cable_18_Z_rms'; 'Cable_18_Z_max'; 'Cable_18_Z_tension'; 'Cable_18_Z_r_2'; 'Cable_18_Z_fn';
'Cable_21_Y_rms'; 'Cable_21_Y_max'; 'Cable_21_Y_tension'; 'Cable_21_Y_r_2'; 'Cable_21_Y_fn';
'Cable_21_Z_rms'; 'Cable_21_Z_max'; 'Cable_21_Z_tension'; 'Cable_21_Z_r_2'; 'Cable_21_Z_fn';
'Tower_X_rms'; 'Tower_X_max'; 'Tower_X_fn';
'Tower_Y_rms'; 'Tower_Y_max'; 'Tower_Y_fn'};
ix=find(contains(DataNames,PlotList)); %indices of data to plot
datared=zeros(length(data),length(ix));

%extract only releveant data
for i=1:length(ix)
    datared(:,i)=data(:,ix(i));
end
```

Fix known errors

Fix cable 13/16 labelling errors Prior to 7/9/2020 (index 4512) 21:00:

-Cable labelled as 16 is actually Cable 13

-Cable labelled as 13 is not good - patterns reasonable but values too low

After 7/9/2020 21:00

-Cable 13 is labelled as 13

-Cable 16 data no longer available

```
% Swap accelerations
chg_idx=4512; %Index when labels were corrected
i16=find(contains(PlotList,'16'));
i13=find(contains(PlotList,'13'));
for i=1:length(i13)
    data13(1:chg_idx,i)=datared(1:chg_idx,i16(i));
    data16(1:chg_idx,i)=datared(1:chg_idx,i13(i));
end

for i=1:length(i13)
    datared(1:chg_idx,i13(i))=data13(1:chg_idx,i);
    datared(1:chg_idx,i16(i))=data16(1:chg_idx,i);
end
```

```

end

% Correct WS (mean and max) data prior to April 15 (index 2463)
% invert sign and convert from m/s to mph
datared(1:2463,3)=-2.23694*datared(1:2463,3);
datared(1:2463,5)=2.23694*datared(1:2463,5);
% Remove bad WS data from April 15 to July 9
datared(2464:4500,3)=0;
datared(2464:4500,5)=0;
% Define units of relevant data
UnitList={'deg F'; 'deg'; 'mph'; 'mph'; 'mph'
'g'; 'g'; 'kip'; 'kip'; 'kip';
'g'; 'g'; 'kip'; 'kip'; 'kip';
'g'; 'g'; 'kip'; 'kip'; 'kip';
'g'; 'g'; 'kip'; 'kip'; 'kip';
'g'; 'g'; 'kip'; 'kip'; 'kip';
'g'; 'g'; 'kip'; 'kip'; 'kip';
'g'; 'g'; 'kip'; 'kip'; 'kip';
'g'; 'g'; 'kip'; 'kip'; 'kip';
'g'; 'g'; 'Hz'; 'g'; 'g'; 'Hz'};

```

Setup channels to analyze

Acceleration to analyze

```

cables={'13'; '18'};
tower={'Tower'};
tow_ax={'X'; 'Y'};
cab_ax={'Y'; 'Z'};
num_ax=2; % number of axes of interest per location
num_cables=length(cables);
num_cab_ch=num_cables*num_ax;
% Determine indexes of acceleration data to analyze
iaccrms=zeros(1,num_cab_ch+length(tow_ax)); ifn=iaccrms;
for i=1:num_cables
    for j=1:num_ax
        datlab=strcat(cables{i}, '_ ', cab_ax{j}, '_rms');
        iaccrms((i-1)*(num_ax)+j)=find(contains(PlotList, datlab));
        datlab=strcat(cables{i}, '_ ', cab_ax{j}, '_fn');
        ifn((i-1)*(num_ax)+j)=find(contains(PlotList, datlab));
    end
end
for i=num_cables+1:num_cables+length(tow_ax)-1
    for j=1:num_ax
        datlab=strcat(tower, '_ ', tow_ax{j}, '_rms');
        iaccrms((i-1)*(num_ax)+j)=find(contains(PlotList, datlab));
        datlab=strcat(tower, '_ ', tow_ax{j}, '_fn');
        ifn((i-1)*(num_ax)+j)=find(contains(PlotList, datlab));
    end
end

iaccmax=iaccrms+1;
itens=iaccmax+1; itens=itens(1:num_cab_ch);
ir2=itens+1;

```

Impose thresholds for physically possible values

This process removes obviously bad data, not high/low physical measurements

```

minrmsaccel=0;
maxrmsaccel=1;
minmaxaccel=0;
maxaccel=1;
mintension=0;
maxtension=5000;
minr2=0;
maxr2=1;
minfn=0;
maxfn=100;

```

```

% Create matrix of threshold values
Thvals=zeros(length(ix),2);
Thvals(1,:)= [15 120]; %Mean temperature (F)
Thvals(2,:)= [0 360]; %Mean wind direction (deg)
Thvals(3,:)= [0 250]; %Mean wind speed (mph)
Thvals(4,:)= [0 50]; %Wind speed std. dev. (mph)
Thvals(5,:)= [0 200]; %Wind speed max (mph)
for i=1:8
    Thvals(i*5+1:i*5+5,1:2)=[minrmsaccl maxrmsaccl; minmaxaccl maxaccl;
        mintension maxtension; minr2 maxr2; minfn maxfn];
end
Thvals(46:48,1:2)=[minrmsaccl maxrmsaccl; minmaxaccl maxaccl;minfn maxfn];
Thvals(49:51,1:2)=[minrmsaccl maxrmsaccl; minmaxaccl maxaccl;minfn maxfn];

% remove zeros since they were put in when raw data had missing value,
% replace with NaN
missingdata=zeros(size(dated));
for i=1:length(ix)
    for j=1:length(idcx)
        if dated(j,i)==0
            missingdata(j,i)=1;
            dated(j,i)=NaN;
        end
    end
end

% remove data outside of thresholds and put NaNs in
thr_rem=zeros(size(dated));
for i=1:length(ix)
    for j=1:length(idcx)
        if dated(j,i)>Thvals(i,2) || dated(j,i)<Thvals(i,1)
            dated(j,i)=NaN;
            thr_rem(j,i)=1;
        end
    end
end

% count percent of missing or thresholded out data per channel
missingcount=zeros(1,length(ix)); %count of data missing
thr_exc_count=zeros(1,length(ix)); %count of data exceeding thresholds
for i=1:length(ix)
    imissing=find(missingdata(:,i));
    missingcount(i)=length(imissing);
    ithr_rem=find(thr_rem(:,i));
    thr_exc_count(i)=length(ithr_rem);
end

% percent of data removed outside bounds
thr_pct=[thr_exc_count./length(idcx)]'*100;

% Determine amount of remaining data per channel
gooddata=zeros(1,length(ix));
for i=1:length(ix)
    gooddata(i)=length(idcx)-missingcount(i);
end

missingcount=missingcount'+309; %309 is the number of missing overall files
mcpct=missingcount./8904;

% Remove cable tension estimates for low r2 values
r2th=[0.89 0.89 0.79 0.79]; %Set r2 thresholds (add for more cables if needed)
remcnt=zeros(1,num_cab_ch);
for j=1:length(idcx)
    for i=1:num_cab_ch
        if dated(j,ir2(i))<r2th(i)
            dated(j,itens(i))=NaN;
            remcnt(i)=remcnt(i)+1;
        end
    end
end

% Percent of tensions removed due to low r2
pctrem=zeros(1,num_cab_ch);
for i=1:num_cab_ch
    pctrem(i)=remcnt(i)/gooddata(itens(i)); %percent removed
end

```

Remove NaNs and create corresponding time vectors for each dataset

NaNs must be removed for statistics

```
for i=1:length(ix)
    d=datared(:,i);
    index=find(~isnan(d));
    data_clean=d(index);
    time_clean=t(index);
    structnamedat=strcat('CleanData.',PlotList{i,1},'.data');
    structnametime=strcat('CleanData.',PlotList{i,1},'.time');
    stringeval=sprintf('%s = data_clean;',structnamedat);
    eval(stringeval);
    stringeval=sprintf('%s = time_clean;',structnametime);
    eval(stringeval);
end
```

Statistics:

```
% Tension
TensStats=zeros(4,length(itens));
for i=1:length(itens)
    structname=strcat('CleanData.',PlotList{itens(i),1},'.data');
    TensStats(1,i)=mean(eval(structname));
    TensStats(2,i)=min(eval(structname));
    TensStats(3,i)=max(eval(structname));
    TensStats(4,i)=std(eval(structname));
end

% Max Acceleration
MaxAccelStats=zeros(4,length(iaccmax));
for i=1:length(iaccmax)
    structname=strcat('CleanData.',PlotList{iaccmax(i),1},'.data');
    MaxAccelStats(1,i)=mean(eval(structname));
    MaxAccelStats(2,i)=min(eval(structname));
    MaxAccelStats(3,i)=max(eval(structname));
    MaxAccelStats(4,i)=std(eval(structname));
end

% RMS Acceleration
RMSAccelStats=zeros(4,length(iaccrms));
for i=1:length(iaccrms)
    structname=strcat('CleanData.',PlotList{iaccrms(i),1},'.data');
    RMSAccelStats(1,i)=mean(eval(structname));
    RMSAccelStats(2,i)=min(eval(structname));
    RMSAccelStats(3,i)=max(eval(structname));
    RMSAccelStats(4,i)=std(eval(structname));
end

% Natural Frequencies
fnStats=zeros(4,length(ifn));
for i=1:length(ifn)
    structname=strcat('CleanData.',PlotList{ifn(i),1},'.data');
    fnStats(1,i)=mean(eval(structname));
    fnStats(2,i)=min(eval(structname));
    fnStats(3,i)=max(eval(structname));
    fnStats(4,i)=std(eval(structname));
end

% Determene acceleration percent in bounds
accstd=3.5;
for i=1:length(iaccrms)
    accth(i)=MaxAccelStats(1,i)+MaxAccelStats(4,i)*accstd;
    obaccnt=0;
    structname=strcat('CleanData.',PlotList{iaccmax(i),1},'.data');
    accdat=eval(structname);
    for j=1:length(accdat)
        % Count outside linear fit
        if accdat(j)>accth(i)
            obaccnt=obaccnt+1;
        end
    end
    obaccpct=obaccnt/length(accdat);
```

```

        ibpctacc(i)=1-obaccpct; %percent in bounds
    end

```

## Correlation plots

```

% Temp vs tension: linear regression
% Fill in NaNs to allow regression analysis
Temp_mean=datared(:,1);
Tempfilled=fillmissing(Temp_mean,'linear','SamplePoints',t);
Tens=zeros(length(idx),num_cab_ch);Tensfilled=Tens;f=Tens;d=Tens;
Tensplus=Tens;Tensminus=Tens;Tenslimconstplus=Tens;Tenslimconstminus=Tens;
p1=zeros(1,num_cab_ch);p2=p1;ibpcttemp=p1;ibpctconst=p1;
for i=1:length(itens)
    Tens(:,i)=datared(:,itens(i));
    Tensfilled(:,i)=fillmissing(Tens(:,i),'linear','SamplePoints',t);
    [p,S]=polyfit(Tempfilled,Tensfilled(:,i),1); %linear regression func.
    [f(:,i),d(:,i)]=polyval(p,Tempfilled,S);
    p1(i)=p(1);p2(i)=p(2);
    f(:,i)=p(1)*Tempfilled+p(2);
    numtempstd=2.6; %number of standard deviations from linear fit
    numconststd=3.2; %number of standard deviations from constant mean
    %Linear bounds
    Tensplus(:,i)=f(:,i)+numtempstd*TensStats(4,i);
    Tensminus(:,i)=f(:,i)-numtempstd*TensStats(4,i);
    %Constant bounds
    Tenslimconstplus(:,i)=(TensStats(1,i)+numconststd*TensStats(4,i))*ones(1,length(idx));
    Tenslimconstminus(:,i)=(TensStats(1,i)-numconststd*TensStats(4,i))*ones(1,length(idx));

    % Determine percent of data inside bounds
    obtempcnt=0;obconstcnt=0;
    for j=1:length(idx)
        % Count outside linear fit
        if Tensfilled(j,i)>Tensplus(j,i)||Tensfilled(j,i)<Tensminus(j,i)
            obtempcnt=obtempcnt+1;
        end
        % Count outside constant bound
        if Tensfilled(j,i)>Tenslimconstplus(j,i)||Tensfilled(j,i)<Tenslimconstminus(j,i)
            obconstcnt=obconstcnt+1;
        end
    end
    obtemppct=obtempcnt/length(idx);
    obconstpct=obconstcnt/length(idx);
    ibpcttemp(i)=1-obtemppct; %percent in linear fit bounds
    ibpctconst(i)=1-obconstpct; %percent in constant bounds

    figure;scatter(Temp_mean,Tens(:,i),'SizeData',10');hold all;
    plot(Tempfilled,f(:,i),'k',datared(:,1),Tensplus(:,i),'r',Temp_mean,Tensminus(:,i),'r',...
        Temp_mean, Tenslimconstplus(:,i),'--m',Temp_mean, Tenslimconstminus(:,i),'--m');

    namesplit=strsplit(PlotList{itens(i),1},'_');legname=strcat('Cable',namesplit{2},namesplit{3});
    std1leg=['Linear + ',num2str(numtempstd),'*Stdev.'];
    std1leg2=['Constant Mean + ',num2str(numconststd),'*Stdev.'];
    legend(legname,'Linear',std1leg,std1leg2);grid('on');
    xlabel('Temperature (F)');ylabel('Tension (kip)');
end
%
% Perpendicular WS vs RMS acceleration
WS_mean=datared(:,3);
WD_mean=datared(:,2);
WS_perp=zeros(1,length(idx));
for i=1:length(idx)
    WS_perp(i)=abs(WS_mean(i)*cos(pi*WD_mean(i)/180));
end
figure;
for i=1:num_cables+2
    subplot(num_cables+1,num_ax,i);scatter(WS_perp,datared(:,iaccrms(i)),'SizeData',10')
    namesplit=strsplit(PlotList{iaccrms(i),1},'_');legname=strcat(namesplit{2},namesplit{3});
    legend(legname);
    grid('on');xlabel('Wind Speed (mph)');ylabel('Acceleration RMS (g)');
end
% Time of Day vs RMS Acceleration
tod=hour(time)+minute(time)/60;
figure;
for i=1:num_cables+2
    subplot(num_cables+1,num_ax,i);scatter(tod,datared(:,iaccrms(i)),'SizeData',10');
    namesplit=strsplit(PlotList{iaccrms(i),1},'_');legname=strcat(namesplit{2},namesplit{3});

```

```

legend(legname);grid('on');xlim([0 24]);
xlabel('Hour of the Day');ylabel('Acceleration RMS (g)');
end

```

## Time history plots with NaNs

```

% beginning and end dates for plotting (xlim)
bdate=datetime(2020,1,1,0,0,0);
edate=datetime(2021,1,1,0,0,0);

% bdate=datetime(2020,7,27,0,0,0);
% edate=datetime(2020,8,2,0,0,0);

% Plot mean and max WS and WD
figure;
datatoplot='WS_mean';
WS_max=datared(:,5);
ind=find(contains(PlotList,datatoplot));
subplot(2,1,1);plot(t,datared(:,ind),t,WS_max);hold all
xlim([bdate edate]);title('wind Speed');xlabel('Date');
ylabel('Wind Speed (mph)');grid('on');legend('Mean','Maximum');
datatoplot='WD_mean';
ind=find(contains(PlotList,datatoplot));
subplot(2,1,2);plot(t,datared(:,ind));
xlim([bdate edate]);title('Wind Direction');xlabel('Date');
ylabel('Direction (deg)');grid('on');

% Plot Temperature
figure;
datatoplot='Temp_mean';
ind=find(contains(PlotList,datatoplot));
plot(t,datared(:,ind));
xlim([bdate edate]);title('Mean Temperature');xlabel('Date');
ylabel('Temperature (F)');grid('on');

% Plot Accelerations
% RMS
% Cables
for i=1:num_cables
figure;
for j=1:num_ax
subplot(num_ax,1,j);plot(t,datared(:,iaccrms(2*(i-1)+j)),t,datared(:,iaccmax(2*(i-1)+j)));
namesplit=split(PlotList{iaccrms(2*(i-1)+j)},1,'-');
titlename=strcat('Cable ',namesplit{2},namesplit{3});
xlim([bdate edate]);
title(titlename);xlabel('Date');
ylabel('Acceleration (g)');grid('on');legend('RMS','Maximum');
end
end
% Tower
i=i+1;
figure;
for j=1:num_ax
subplot(num_ax,1,j);plot(t,datared(:,iaccrms(2*(i-1)+j)),t,datared(:,iaccmax(2*(i-1)+j)));
namesplit=split(PlotList{iaccrms(2*(i-1)+j)},1,'-');
titlename=strcat(namesplit{1},namesplit{2});
xlim([bdate edate]);
title(titlename);xlabel('Date');
ylabel('Acceleration (g)');grid('on');legend('RMS','Maximum');
end
end
% Max accels
% Cables
for i=1:num_cables
figure;
for j=1:num_ax
subplot(num_ax,1,j);plot(t,datared(:,iaccmax(2*(i-1)+j)),t,datared(:,iaccmax(2*(i-1)+j)));
namesplit=split(PlotList{iaccmax(2*(i-1)+j)},1,'-');
titlename=strcat('Cable ',namesplit{2},namesplit{3});
xlim([bdate edate]);
title(titlename);xlabel('Date');
ylabel('Acceleration (g)');grid('on');legend('Maximum');
end
end
% Tower
i=i+1;
figure;
for j=1:num_ax

```



```

subplot(num_ax,1,j);plot(t,dated(:,iaccmax(2*(i-1)+j)),'color',[0.8500 0.3250 0.0980]);
namesplit=split(PlotList{iaccrms(2*(i-1)+j),1},'_');
titlename=strcat(namesplit{1},namesplit{2});
xlim([bdate edate]);
title(titlename);xlabel('Date');
ylabel('Acceleration (g)');grid('on');legend('Maximum');
end

% Tension Plots
figure;
for i=1:num_cables
subplot(num_cables,1,i);plot(t,dated(:,itens(2*i-1)),t,dated(:,itens(2*i)));
namesplit=split(PlotList{iaccrms(2*i-1),1},'_');
titlename=strcat('Cable',namesplit{2});
xlim([bdate edate]);title(titlename);xlabel('Date');
ylabel('Tension (kip)');grid('on');legend('Y','Z');
end

```

*Published with MATLAB® R2020b*